

1-1-2015

The Relationship Between Axonal Injury, Biomarker Expression And Mechanical Response In A Rodent Head Impact Acceleration Model

Yan Li

Wayne State University,

Follow this and additional works at: http://digitalcommons.wayne.edu/oa_dissertations

Recommended Citation

Li, Yan, "The Relationship Between Axonal Injury, Biomarker Expression And Mechanical Response In A Rodent Head Impact Acceleration Model" (2015). *Wayne State University Dissertations*. Paper 1150.

This Open Access Dissertation is brought to you for free and open access by DigitalCommons@WayneState. It has been accepted for inclusion in Wayne State University Dissertations by an authorized administrator of DigitalCommons@WayneState.

**AN INVESTIGATION OF THE RELATIONSHIP BETWEEN
AXONAL INJURY, BIOMARKER EXPRESSION
AND MECHANICAL RESPONSE
IN A RODENT HEAD IMPACT ACCELERATION MODEL**

by

YAN LI

DISSERTATION

Submitted to the Graduate School

of Wayne State University,

Detroit, Michigan

in partial fulfilment of the requirements

for the degree of

DOCTOR OF PHILOSOPHY

2015

MAJOR: BIOMEDICAL ENGINEERING

Approved by:

Advisor Date

Co-advisor

© COPYRIGHT BY

YAN LI

2015

ALL Rights Reserved

ACKNOWLEDGMENTS

"Teamwork is the ability to work together toward a common vision, the ability to direct individual accomplishments toward organizational objectives. It is the fuel that allows common people to attain uncommon results."

- Andrew Carnegie

This dissertation could not have been completed without the great support and serious contribution that I have received from so many people over the years. I am indebted to them for making the time working on my PhD an unforgettable experience.

First and foremost I want to thank my advisor Dr. John M. Cavanaugh. He is the nicest advisor and one of the smartest people I know. It has been an honor to be his PhD student. His great guidance and enormous support always encourage me, even during tough times in my PhD pursuit, and allow me to grow as a good researcher. His advice on both research as well as on my career have been invaluable. I would like to express my special appreciation and thanks to my co-advisor Dr. Liying Zhang. Her distinguished expertise helped improve and significantly expedite the process of this dissertation work. I appreciate all her contributions of time, ideas, and funding to make my PhD experience productive and stimulating.

I would also like to convey my sincere thanks to Dr. Kevin K. Wang, Dr. Pamela J. Vandevord, and Dr. Yuchuan Ding for kindly accepting to serve on my doctoral dissertation committee. Their insightful suggestions for my research during the course of this dissertation work are greatly appreciated. I learned a lot from them about research, how to tackle new problems and how to develop techniques to solve them. I gratefully

acknowledge the funding received towards my PhD from the National Health Institute grants No. 5R01 EB006508.

My colleagues at the Spine Research Lab ensured I was constantly engaged and entertained along the way. I thank Dr. Srinivasu Kallakuri for training me in performing surgery and histological staining with patience. Thanks to Dr. Chaoyang Chen for his great advices on research and career pursuit. Thanks to Mr. Runzhou Zhou for sharing his extensive knowledge of finite element modeling. Thanks to Ms. Ke Feng for her valuable technical assistance. The assistance of Mr. Alok Desai and Ms. Abigail Cohen in various parts of this dissertation work is gratefully acknowledged.

Finally, a special thanks to my family. I owe heartfelt appreciation to my mother-in-law, father-in-law, my mother, and father for steadily supporting and encouraging me through the ups and downs during my PhD study. Words cannot express how grateful I am to my beloved wife Shuo Zhang for her faithful support and understanding. To my beloved daughter Chenxuan Li, I would like to express my thanks for being such a good girl always cheering me up.

FOREWORD

In the United States 1.4 million people sustain traumatic brain injury (TBI) each year, resulting in 235,000 hospitalizations and 50,000 fatalities annually. Traumatic axonal injury (TAI) is a serious outcome of TBI that accounts for 40-50% of hospitalizations due to head injury and one third of the mortality due to TBI, and it is difficult to diagnose and evaluate using current imaging modalities. Pathologically, TAI comprises diffuse and extensive lesions of the white matter tracts. TAI is produced by rapid head acceleration / deceleration during a traumatic event with consequent shear / tension on axons. The Marmarou impact acceleration model has been extensively used to study the pathomechanisms of TAI. However, there is a paucity of published work on the mechanical responses induced by this model and their correlation to TAI. Hence, a modified version of this model will be developed to elucidate the relationship between the mechanical responses induced by head impact and the consequent expression of TAI and other pathobiological outcomes.

The goal of this research is 1) to characterize the kinematics of the rat head during dynamic impact of various severities using the modified Marmarou model; 2) to quantify the intensity and distribution of the axonal changes throughout corpus callosum and brainstem using histopathologic techniques; 3) to determine correlation between head impact response and TAI, and identify potential injury predictors for TAI; 4) to establish a panel of biomarkers to evaluate traumatic axonal injury; and 5) to investigate the predictive value of multiple biomarkers compared to a single biomarker.

TABLE OF CONTENTS

<u>CHAPTER</u>	<u>PAGE</u>
ACKNOWLEDGMENTS	ii
FOREWORD	iv
LIST OF TABLES	ix
LIST OF FIGURES	x
CHAPTER 1 – INTRODUCTION	1
1.1 Epidemiology of TBI and TAI	1
1.2 Pathobiology of TAI and Related Cellular Mechanisms of TBI	3
1.3 Clinical Assessment of TAI	6
CHAPTER 2 – BIOMECHANICS OF TRAUMATIC AXONAL INJURY	10
2.1 Brain Injury Kinematics	10
2.2 Biomechanism of TAI	12
2.3 Current Animal Models for TBI study	14
2.3.1 Animal Models for TBI	14
2.3.2 Marmarou Impact Acceleration Model	17
CHAPTER 3 – BIOMARKERS FOR TRAUMATIC AXONAL INJURY	21
3.1 Background of Biomarkers for TBI	21
3.2 Challenge of Biomarker Studies	26
CHAPTER 4 – SIGNIFICANCE OF THIS STUDY	29
4.1 Modified Marmarou Impact Acceleration Model	29
4.2 Quantified Immunohistochemical Technique	30
4.3 A Panel of Biomarkers	32

4.4	Hypotheses and Specific Aims	33
CHAPTER 5 – AN IMPROVED RODENT HEAD IMPACT ACCELERATION DEVICE		
35		
5.1	Introduction	35
5.2	Materials and Methods	37
5.2.1	Design of the Head Impact Device	37
5.2.2	Comparison of Impact Velocities between Existing and New Devices	38
5.2.3	Impact Velocity as a Function of Drop Height Using New Device	41
5.2.4	Rat Head Kinematics Measurements	42
5.2.5	Statistical Analysis	43
5.3	Results	43
5.3.1	Pre-impact Velocity	43
5.3.2	Drop Height and Impact Velocity Relationship	44
5.3.3	Measurements of rat head kinematics	45
5.4	Discussion	48
CHAPTER 6 – CORRELATION BETWEEN IMPACT BIOMECHANICS AND TRAUMATIC AXONAL INJURY		
53		
6.1	Introduction	53
6.2	Methods	55
6.2.1	Animal Handling and Preparation	55
6.2.2	Instrumentation and Experimental Preparation	55
6.2.3	Induction of Traumatic Brain Injury	57
6.2.4	Head Impact Data Processing and Analysis	57
6.2.5	β -amyloid precursor protein (β -APP) immunostaining	60

6.2.6	Quantitative Analysis of TAI	62
6.2.7	Statistical Analysis	64
6.3	Results	65
6.3.1	Head Kinematics	65
6.3.2	TAI Assessment and Quantification	67
6.3.3	Injury Predictor for Severe TAI	69
6.3.4	Injury Tolerance for Severe TAI	75
6.4	Discussion	76
6.4.1	Model Development	76
6.4.2	Injury Mechanics in Different Brain Regions	79
6.4.3	Head Kinematics-based Predictors for Severe TAI	82
CHAPTER 7 – CORRELATION BETWEEN BIOMARKERS AND TRAUMATIC AXONAL INJURY		85
7.1	Introduction	85
7.2	Methods	92
7.2.1	Animal Handling and Preparation	92
7.2.2	Instrumentation and Experimental Preparation	92
7.2.3	Induction of Traumatic Brain Injury	93
7.2.4	Head Impact Data Processing and Analysis	94
7.2.5	TAI Quantification	95
7.2.6	Biomarker Quantification	95
7.2.7	Statistical Analysis	96
7.3	Results	98
7.3.1	Head Kinematics	98

7.3.2	TAI Quantification in CC and Py	98
7.3.3	Biomarker Assessment in CSF and Serum	99
7.3.4	Comparison of CSF and Serum Biomarker Levels	100
7.3.5	Biomarker for Severe TAI	101
7.3.6	Correlation between Biomarker Levels and Mechanical Response	103
7.4	Discussion	103
CHAPTER 8 – CONCLUSIONS		110
CHAPTER 9 – FUTURE WORK		112
9.1	Scaling: Animal to Human	112
9.2	Combined Biomechanical and Computational Approach	113
9.3	Temporal Changes of Biomarker Levels	114
APPENDIX		117
REFERENCES		120
ABSTRACT		151
AUTOBIOGRAPHICAL STATEMENT		154

LIST OF TABLES

<u>TABLE</u>	<u>PAGE</u>
Table 3-1: Attributes of ideal TBI biomarkers	31
Table 5-1: Comparison of pre-impact velocity from 2 m drop height between various devices and release mechanisms	44
Table 6-1: Mechanical responses of rat head in 1.25m & 2.25m weight drop	66
Table 6-2: Critical values of all potential predictors to predict 25%, 50%, and 80% probability of severe TAI in global brain	74
Table 7-1: Experiment matrix	93
Table 7-2: Mechanical and behavioral responses of rat head in weight-drop experiments	98
Table A-1: Significance test for univariate and multivariate logistic regression models of biomechanical response to predict TAI in CC	116
Table A-2: Significance test for univariate and multivariate logistic regression models of biomechanical response to predict TAI in Py	117
Table A-3: Significance test for univariate and multivariate logistic regression models of biomechanical response to predict to predict TAI in combined CC and Py region	118
Table A-4: Significance test for univariate and multivariate logistic regression models for biomarkers to predict TAI	119

LIST OF FIGURES

<u>FIGURE</u>	<u>PAGE</u>
Figure 1-1: Leading causes of TBI	1
Figure 1-2: The major pathways associated with the progression of secondary injury after a traumatic brain injury	3
Figure 1-3: Flow chart representing the consequences of TAI	5
Figure 1-4: Histology evidence of TAI	6
Figure 2-1: The Wayne State Tolerance Curve	10
Figure 2-2: Biomechanics of an oblique impact	11
Figure 2-3: TAI threshold developed for lateral rotation	13
Figure 2-4: Animal models of TBI	15
Figure 2-5: Original Marmarou impact acceleration injury model	18
Figure 3-1: Biomarkers of TBI in CSF and Serum	23
Figure 5-1: Comparison of the original Marmarou device and the modified impact acceleration injury model with instrumentation	38
Figure 5-2: Impact velocity as a function of drop height determined for the new impact acceleration device	45
Figure 5-3: Rat head impact event	46
Figure 5-4: Rat head impact acceleration	47
Figure 5-5: Typical time-history traces of translational acceleration and rotational velocity	47
Figure 6-1: Diagrams of the modified impact-acceleration injury model and instrumentation setup	56
Figure 6-2: Diagrams illustrating data processing from accelerometer and velocity sensors	58
Figure 6-3: Illustration of CC and Py in rat brain	61

Figure 6-4: A representative panoramic view of corpus callosum used to quantify β -APP reactive (+) axonal (arrow) profiles	62
Figure 6-5: Correlation between linear component and angular component of head response in 2.25 m impact	66
Figure 6-6: Representative injury map showing TAI distribution in CC and Py	67
Figure 6-7: TAI distribution along the rostro-caudal direction in 2.25 m impacted rats	68
Figure 6-8: Logist plots of the predicted severe TAI probability in CC	69
Figure 6-9: Specificity and sensitivity for predicting severe TAI in CC	70
Figure 6-10: Logist plots of the predicted severe TAI probability in Py	71
Figure 6-11: Specificity and sensitivity for predicting severe TAI in Py	71
Figure 6-12: Logist plots of the predicted severe TAI probability in combined CC and Py brain regions	73
Figure 6-13: Specificity and sensitivity for predicting severe TAI in combined CC and Py brain regions	74
Figure 6-14: Severe TAI tolerance for rat head impact based on average linear acceleration and time duration	75
Figure 6-15: Severe TAI tolerance for rat based on average linear acceleration and average angular velocity	76
Figure 6-16: Logist plots of the predicted severe TAI probability in combined CC and Py brain regions based on Power and HIC	82
Figure 7-1: Origins of CSF and serum biomarkers	87
Figure 7-2: CSF collection from Cisterma Magna	96
Figure 7-3: TAI counts in CC and Py	99
Figure 7-4: Comparisons of biomarker levels between different impact heights in CSF and Serum	100
Figure 7-5: Correlation of biomarker levels in CSF and Serum	101

Figure 7-6: CSF GFAP to predict severe TAI	102
Figure 7-7: CSF NF-H to predict severe TAI	102
Figure 7-8: Serum GFAP to predict severe TAI	103
Figure 7-9: Serum NF-H to predict severe TAI	103
Figure 7-10: Correlation between biomarkers and biomechanics	104
Figure 9-1: Frame work of combined biomechanical and computational approach ...	114

CHAPTER 1

INTRODUCTION

1.1 EPIDEMIOLOGY OF TBI AND TAI

Traumatic brain injury (TBI) is a major public health problem in the United States, contributing to about 30% of all injury deaths (Faul et al., 2010). In 2010, about 2.5 million emergency department (ED) visits and hospitalizations were associated with TBI alone or other injuries in combination with TBI (CDC, 2010). Each year, TBI contribute to a large number of deaths and cases of permanent disability. Sport related TBI is also on the rise in the past decade. From 2001 to 2009, the rate of ED visits for sport concussion or other injuries in combination with sport concussion rose 57% among children age 19 or younger (CDC, 2011).

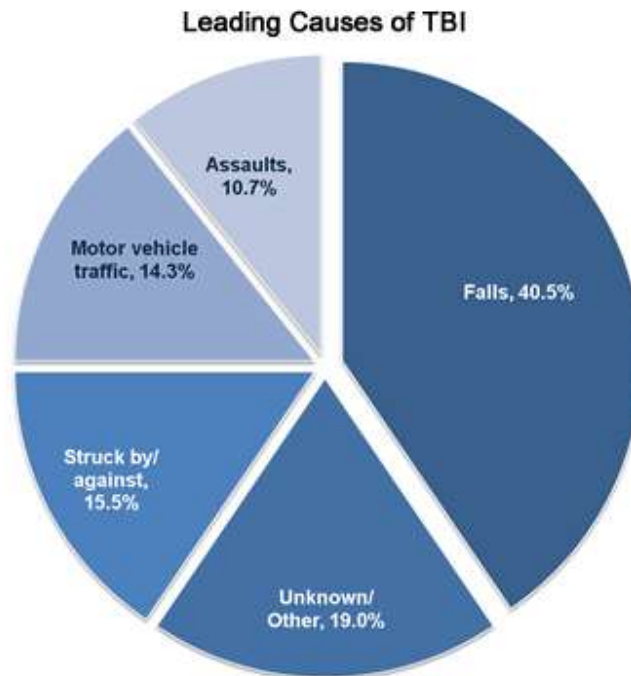


Figure 1-1: Leading causes of TBI (CDC, 2010).

The leading causes of TBI are falls, motor vehicle accidents (MVAs), unintentional blunt trauma (e.g., being hit by an object), and accidental impacts (CDC, 2010). While falls are the greatest cause of TBI, MVAs cause the most hospitalizations. Among TBI-related deaths, falls were the leading cause of death for persons 65 years or older, while MVAs were the leading cause for people ages 5-24 years. The direct and indirect costs of TBI are estimated to be \$60 billion annually (Finkelstein et al., 2006).

TBI typically result in either diffuse or focal injuries or a combination of both. Focal injuries, readily observed using standard imaging techniques, include cortical contusions and subdural, epidural and intracerebral hematomas. Diffuse injuries, on the other hand, are associated with more widespread disruption that is usually not observable with standard imaging. These injuries include concussions, diffuse axonal injury (DAI) and diffuse brain swelling (Gennarelli, Thibault et al. 1998).

DAI is a well-recognized consequence of blunt head injury (Adam et al., 1982) and was originally described by Strich (1956) as diffuse degeneration of cerebral white matter (WM). Smith and Meaney (2000) showed that the pattern of axonal damage in the white matter is more accurately described as 'multifocal' rather than diffuse in TBI case, thus suggested to refer it as traumatic axonal injury (TAI) instead of DAI. Pathologically, TAI comprises diffuse and extensive lesions of the white matter tracts (Blumbergs, 1997). TAI is produced by rapid head acceleration/deceleration during a traumatic event (Adams et al., 1982; Kelley et al., 2006) with consequent shear / tension on axons.

TAI is a predominant injury in 40-50% of TBI requiring hospitalization in the United States and is associated with one-third of deaths in severe TBI (Meythaler et al.

2001). The most common cause of TAI is car accidents, followed by falls, assault and other incidents involving strong inertial forces on the brain (Adams et al., 1984).

1.2 PATHOBIOLOGY OF TAI AND RELATED CELLULAR MECHANISMS OF TBI

TBI is characterized by a complex pathology. Acute TBI is characterised by two injury phases. The primary injury includes focal / multifocal injury, haematomas and contusions at the time of the initial impact. This results in a cascade of cellular processes which then leads to secondary brain injury. The major known pathways in secondary injuries have been summarized by Parker (2008) in Figure 1-2.

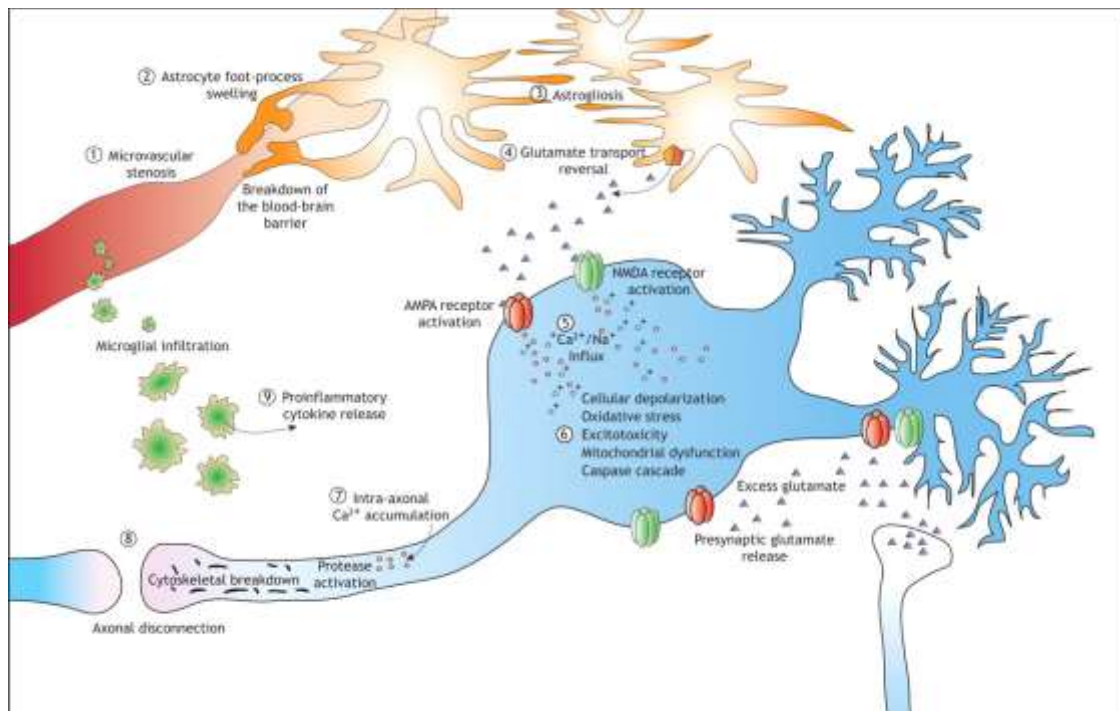


Figure 1-2: The major pathways associated with the progression of secondary injury after a traumatic brain injury (Parker et al., 2008).

Sudden head acceleration and deceleration causes tensile, shear, and compressive strains within the brain tissue, and leads to local Ca^{2+} influx due to altered neuron

membrane permeability by strains. Abnormal calcium homeostasis plays a major role in the progression of secondary brain injury in both grey and white matter. In neuronal cell injury, it is proved to lead to excitotoxic cell death, programmed cell death and postsynaptic modifications (Parker et al., 2008). Calcium overload is also linked to early mitochondrial swelling (Buki et al., 2006). Excessive influx of calcium into mitochondria causes its membrane to depolarize, open the membrane permeability transition pores and consequently release the proinflammatory cytokine and initiate the programmed cell death (Stefanis 2005). Proliferation of astrocytes (astrogliosis) is also a characteristic of injuries to the CNS, and their dysfunction results in a reversal of glutamate uptake and neuronal depolarization through excitotoxic mechanisms. In addition, astrocyte foot processes swelling can cause microcirculatory derangements, loss of microvasculature, and breakdown of blood–brain barrier (Parker et al., 2008).

In TAI, calcium initiates a cascade of events resulting in axonal disconnection (Fig. 1-3). First, influx of Ca^{2+} activates a cellular and molecular cascade ultimately leading to the activation of proteolytic enzymes such as cysteine proteases, calpain, and caspase (Pike et al. 1998; McCracken et al. 1999). Secondly, these enzymes degrade spectrin, an essential component of the axon cytoskeletal network, causing a buildup of axonal transport proteins within axonal varicosity swellings called “retraction balls” (Povlishock et al., 1983; Yaghmai et al., 1992). Other studies have shown that a traumatic event evokes focal alterations in axolemmal permeability which was also shown to be associated with significant neurofilament compaction (Povlishock, 1996).

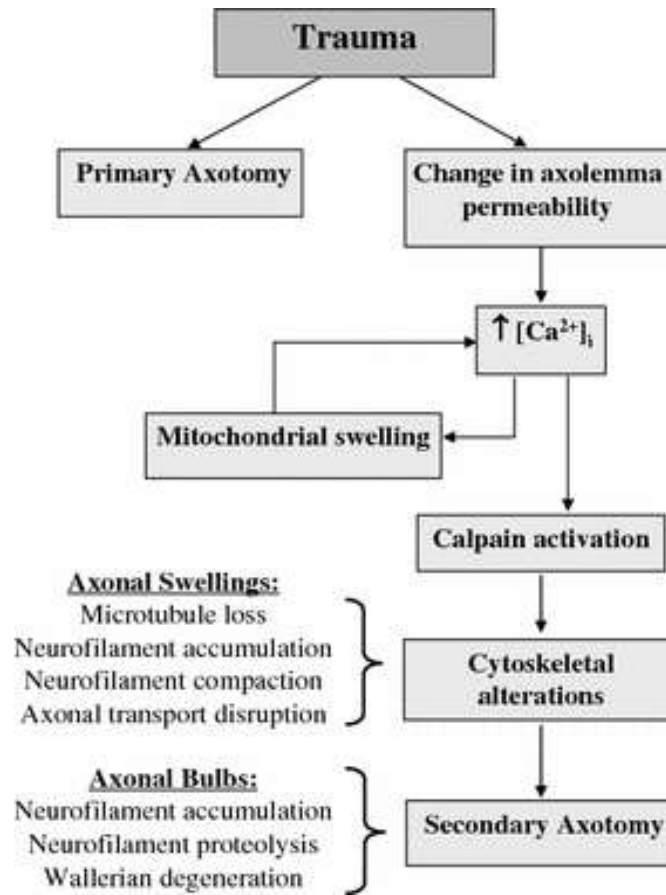


Figure 1-3: Flow chart representing the consequences of TAI (Serbest et al., 2007).

The proteolytic enzymes can also destroy the mitochondria and lead to release pro-apoptotic factors such as cytochrome c, and caspase enzymes, which promote apoptosis (Tang-Schomer et al. 2012). Widespread axonal degeneration associated with a traumatic event can lead to neuronal disconnection due to downstream synaptic degeneration and deafferentation of target postsynaptic cells and may be attributed to the underlying neurobehavioral changes (Rafols et al., 2007). These pathological changes are commonly found in the areas where have high white matter densities, such as the parasagittal white matter, corpus callosum, and the brainstem (Riddle et al. 2012).

Depending on the pattern, severity and location, TAI is categorized into grades I, II and III (Gennarelli, Thibault et al. 1998). Histology by silver staining reveals axonal

swellings within 15-18 h followed by reactive changes including migration of microglia, reactive astrocytosis and changes in capillary endothelium. Several weeks after TBI, microglial accumulation, axonal fragmentation and myelin sheath breakdown are observed. Figure 1-4 shows characteristic swellings and retraction balls of TAI pathology.

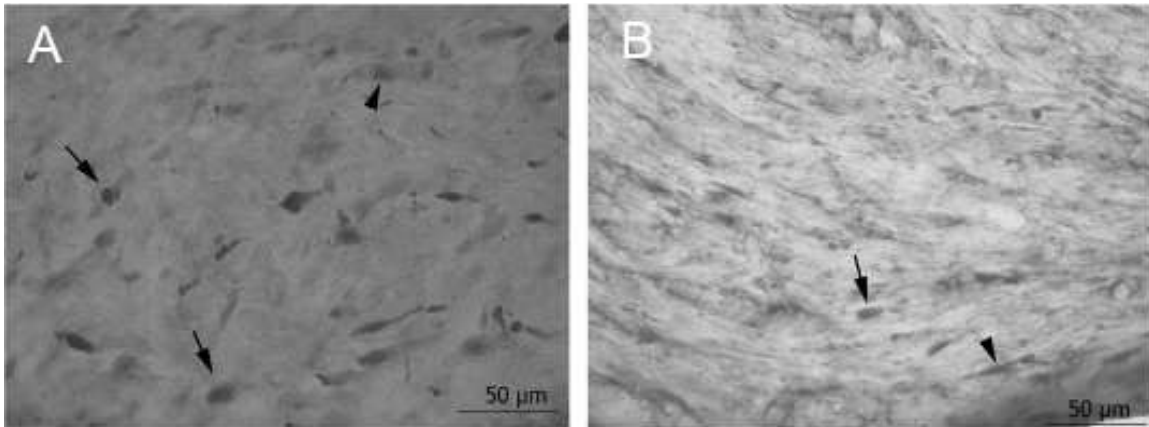


Figure 1-4: Histology evidence of TAI. An image of β -APP-IR retraction balls (arrows) and swollen axons (arrow head) in Py (A), and a sample image of RMO-IR swellings (arrow head) and retraction balls (arrow) in the most caudal Py (B) (Kallakuri et al. 2012).

TAI is increasingly recognized as a huge negative impact on the quality of patients' life with either severe or mild TBI. Although extensive studies aimed at understanding the cellular pathway, inflammatory initiation and apoptosis following TBI have been done, many areas regarding the pathobiology of TBI still need to be elucidated, and the effective translation of basic research findings into meaningful clinical therapy remains a challenge.

1.3 CLINICAL ASSESSMENT OF TAI

Both structural and ischaemic changes can be detected with recent advances in imaging techniques. CT scanning, which is now widely available in the emergency

departments of most hospitals, has the advantage of being able to rapidly image the patient, since time is important in evaluating the head trauma in the acute stage. Primary head injury lesions seen on CT include acute extradural haematoma, acute subdural haematoma, subarachnoid haemorrhage, contusions, intracerebral haematoma and diffuse axonal injury. However, initial CT scans is only able to detect TAI in 20%–50% of cases (Toyama et al., 2005). A study by Bigler et al. has indicated that there is poor correlation between acute CT and prognosis, apart from those patients with brainstem injury (Bigler et al, 2006).

MRI is not routinely used in the acute phase of traumatic brain injury due to availability. After the patient has been stabilized, MRI can be used to obtain a clearer picture of the extent of injury. MRI has a much higher sensitivity for detecting TAI (Bradley et al., 1993). Recently specialized MRI techniques have further improved the detection of TAI. Susceptibility weighted imaging (SWI) exploits the susceptibility differences between tissues (e.g., oxygenated vs. deoxygenated blood and iron) and uses the phase image to detect these differences (Ashwal et al., 2006). It has been shown to demonstrate superior image enhancement of primary lesion sites, micro-hemorrhage area and axonal damage sites compared to conventional MRI (Murai et al., 1996). Magnetic resonance spectroscopy (MRS) identifies individual brain chemicals or metabolites and measures its concentration by producing a spectrum. It provides neurophysiological data that is related to structural damage/changes, neuronal health, and other brain functions (Arslanoglu et al., 2004; Baker et al., 2008). MRS showed improved sensitivity for detection of TAI and axonal pathology in swine traumatic brain injuries (Mcgowan et al., 1999; Smith et al., 1998). The directionality of

diffusion is called anisotropy and is measured by diffusion tensor imaging (DTI). This technique relies upon the difference in isotropic diffusion of water molecules in normal and injured brain (Huisman 2003). DTI is now regarded as the best imaging technique for detecting white matter integrity/damage (Shenton et al, 2012). It is hoped that DTI will be able to visualize microscopic white matter injury at specific brain tracts (e.g., corpus callosum, superior longitudinal fasciculus, uncinated), which are not seen on conventional scans, and give some information regarding prognosis both in severe and mild TBI. Many of the manuscripts published are case reports, but show some promising results (Naganawa et al., 2004; Ducreux et al., 2005; Yen et al., 2006).

Another emerging field focuses on using biomarkers as an alternative non-invasive clinical approach for diagnosis of TAI. These markers could be detected in CSF or serum samples due to the breakdown products of neurons passing through the damaged blood brain barrier of TBI patients. Potential biomarkers generally include proteins related to primary structural damage or proteins involved in cellular and molecular cascade during the secondary axonomy, which we will discuss in detail in Chapter 3.

In TAI there may be a therapeutic window for treatment. For example, dopaminergic blockade may be contraindicated in the early stages of TBI but beneficial in TAI (Meythaler et al. 2001). While animal studies of new treatment modalities have been promising, clinical trials are often disappointing. This is likely related to the varying mechanisms of injury in clinical studies in contrast to animal studies, where the mechanism of injury has been very focused. Clinical studies are fraught with uncertainty, including the mechanisms of injury involved, the timing of various mechanisms, and

uncertainty regarding the therapeutic window of various treatments (Maas et al. 1999). More objective diagnostic testing is absolutely necessary to reduce this uncertainty. Advanced imaging procedures and protein biomarkers provide great promise in revealing these mechanisms in the clinical setting.

CHAPTER 2

BIOMECHANICS OF TRAUMATIC AXONAL INJURY

2.1 BRAIN INJURY KINEMATICS

Brain injury can occur through many different mechanisms. In vehicle accident, head impact may or may not occur, but the head will be decelerated (accelerated) in the process. In the absence of direct impact to the skull, the loading to the head is inertial. It is the movement of the skull that causes the brain to be subjected to various stresses and strains which leads to disruption of brain tissue and associated injury (King 2000).

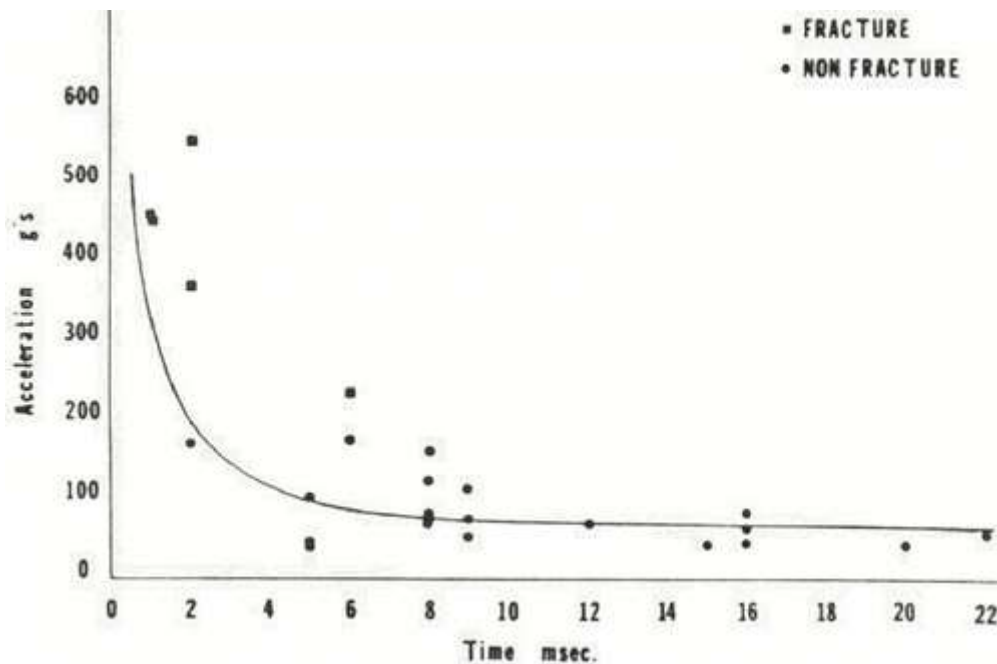


Figure 2-1: The Wayne State Tolerance Curve (McElhaney et al., 1976)

Several head injury assessment functions have been proposed in the past 40 years to establish the threshold of head injury during impact (Newman, 1998). The current standard for head injury protection is the Head Injury Criterion (HIC) (Versace, 1971). Another well-known head injury predictor is the Gadd Severity Index (GSI) (Gadd, 1966).

Both GSI and HIC were developed using the Wayne State tolerance curve (WSTC) (Figure 2-1, Lissner et al., 1960), which was derived from head acceleration data from animal concussion experiments and cadaveric forehead impact tests. The WSTC predicts that as the duration of the effective translational acceleration of the head increases, the magnitude of acceleration required to produce head injury decreases. This criterion is based solely on linear acceleration of the head, but in most head impacts both linear and angular acceleration are present. In a vehicle impact, it is more likely that both linear and rotational head kinematics occur during an oblique impact (Fig. 2-2).

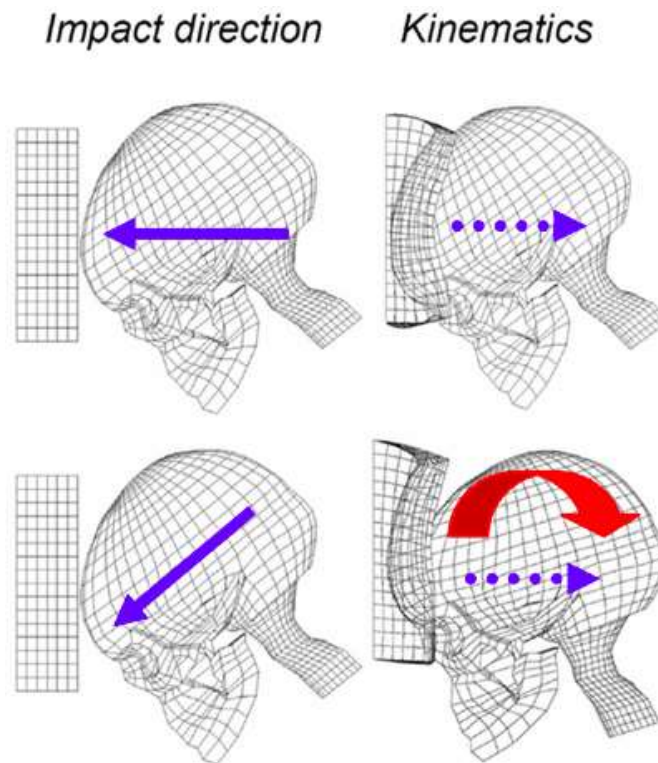


Figure 2-2: Biomechanics of an oblique impact (lower), compared to a corresponding perpendicular one (upper) (Kleiven 2013).

Ommaya et al. (1968) conducted experiments on monkeys to demonstrate that even without direct impact on the head, its rotational displacement may cause serious brain damage. In their pioneering primate study, Gennarelli et al. (1982) applied scaled

angular acceleration to the head of primates in different directions. They found that the majority of the animals that was enduring the coronal motion suffered coma lasting longer than 6 hours, while all animals that were accelerated in the sagittal plane had coma lasting less than 2 hours. It indicated the direction of rotation can affect the injury severity. Recently, other animal models such as miniature swine (Meaney et al., 1995; Smith et al., 1997) and sheep (Anderson et al., 1997) were used to study the effect of angular acceleration to the head in the different plane. Thresholds for brain injury have also been discussed in terms of rotational acceleration, rotational velocity, and pulse duration (Goldsmith and Ommaya, 1984; Margulies and Thibault, 1992; Pincemaille et al., 1989).

However, these criteria are not injury specific, nor do they provide information on injury location. Furthermore, they do not facilitate in any further understanding of the biomechanical factors that initiate the development of axonal pathology, which is responsible for most cases of poor neurological outcome after traumatic head injury (Gennarelli et al., 1982). Therefore, an injury predictor specific for TAI is of great importance in designing safety measures either in vehicles or in sports helmets.

2.2 BIOMECHANISM OF TAI

TAI occurs during sudden acceleration and deceleration of the brain. During the sudden motion, the brain is subject to forces that pull compress and shear the axon. Previously, strain has been proposed as an injury indicator for subarachnoid hematoma and diffuse axonal injury using finite-element (FE) head models (Ruan et al., 1993; Zhou et al., 1994). More recently, using a high resolution human head FE model to simulate

on-field accident data (Zhang et al., 2001a), both localized strain and strain rate were found to have significant correlations with memory, cognitive impairments, loss of consciousness and intervals required to return to plays sustained by concussed NFL players (Zhang et al., 2003; King et al., 2003; Zhang et al., 2004; Viano et al., 2005). In addition, secondary insults such as increased intracranial pressure, intracranial hemodynamic disorders, and hematoma formation, may also lead to TAI (Bruce, et al., 1973; Graham, et al., 1989; Zhang, et al. 2004; Manley, et al. 2006). Various in vitro stretch experiments using the squid giant axon (Galbraith et al., 1993), guinea pig optic nerve (Bain et al., 2001), rat spinal nerve roots (Singh et al., 2006) have been performed to develop a proposed threshold of axonal injury from mechanical damage.

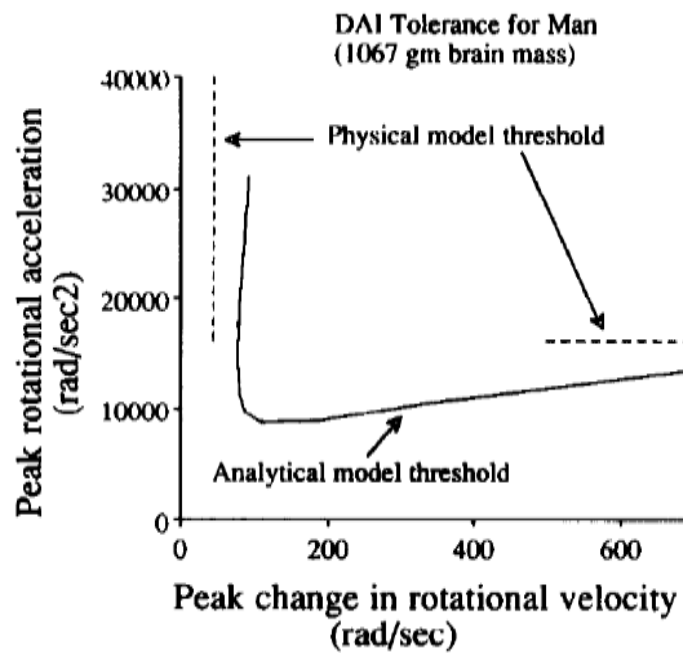


Figure 2-3: TAI threshold developed for lateral rotation (Margulies et al., 1992).

These studies, although capable of providing data related to damage in individual nerves or axons, cannot fully explain the complex mechanical input that the axons experience during an impact event, and do not consider the contribution of external forces,

both linear and angular acceleration, in predicting injury at different brain regions. Margulies et al. (1992) proposed a tolerance criterion for TAI specific to lateral rotational loads (Fig. 2-3). This curve shows that if changes in peak angular velocity are small, high peak angular acceleration is required to produce injury, while for high values of peak change in angular velocity, even low peak angular acceleration could lead to injury. However, the criterion does not include the contribution of the linear acceleration of the head to injury production. Therefore, a biomechanical model of traumatic brain injury that can relate mechanical parameters of head response to localized mechanical response at the axonal level is needed for a proper assessment of TAI.

2.3 CURRENT ANIMAL MODELS FOR TBI STUDY

2.3.1 Animal Models for TBI

Animal models are essential for studying the biomechanical, molecular and cellular aspects of TBI that cannot be addressed in clinical trial. An important application of the study of biomechanics in brain injury is the determination of accurate tissue tolerance. An improved understanding of injury biomechanics and the resulting brain response will facilitate the development of improved head protective equipment. Determination of tolerance criteria are largely based on cadaveric studies, which may not accurately represent the properties of living tissue. Animal studies, in which a defined mechanical insult can be applied and tissue response can be measured, therefore have an advantage for the determination of tissue level tolerance and then lead to improvement of human injury criteria. The choice of desirable experimental model depends on both the research goal and underlying objectives. A number of laboratory experimental models

have been developed to reproduce representative features of human TBI in an effort to identify cellular processes contributing to the neuropathophysiological outcomes, and has been reviewed by Xiong et al. (2013).

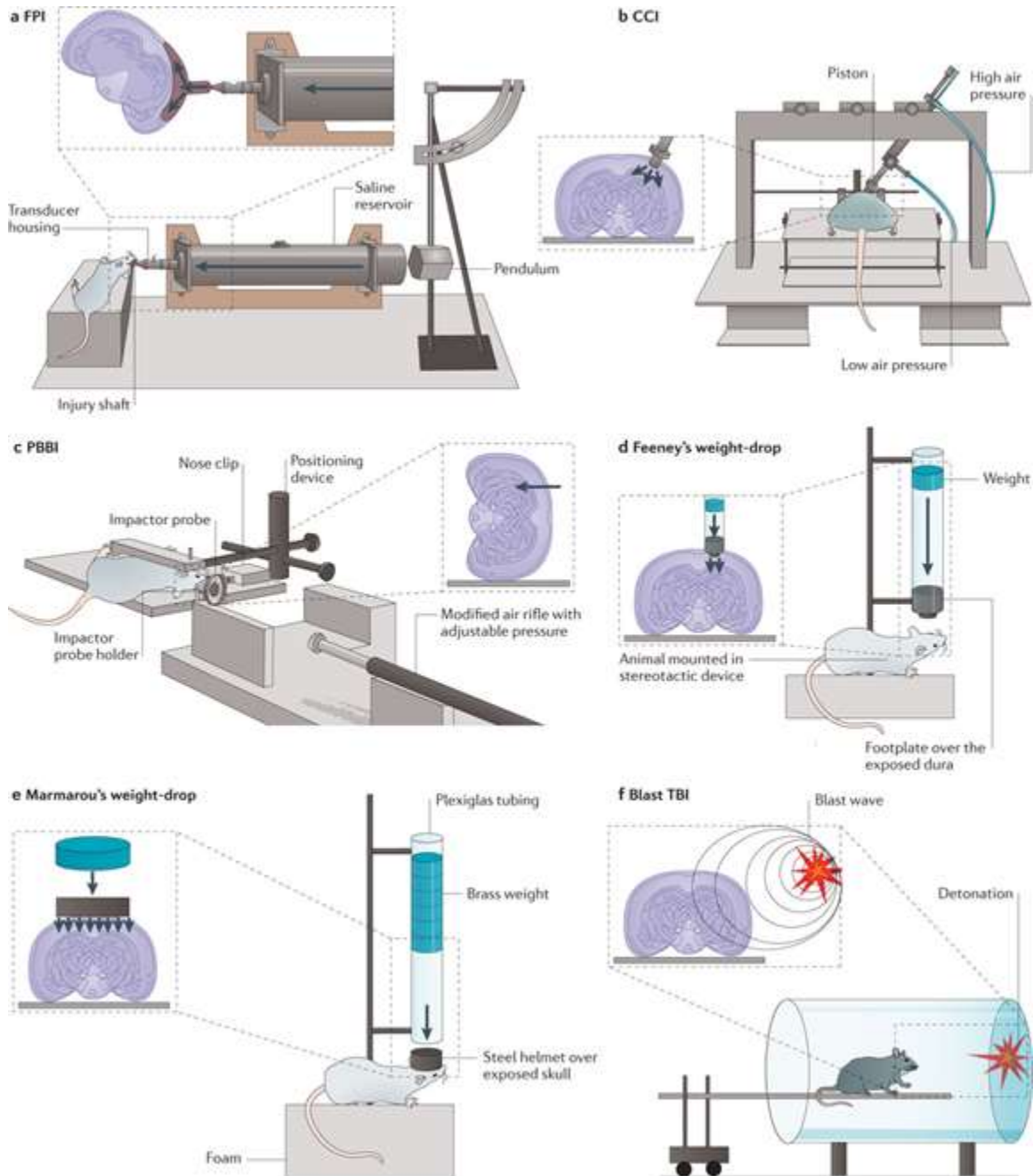


Figure 2-4: Animal models of TBI (Xiong et al., 2013).

The fluid percussion injury (FPI) device uses pendulum to strike the piston to generate a fluid pulse in to the epidural space (McIntosh et al., 1987, 1989). FPI can replicate pathophysiological hallmarks of human TBI, such as intracranial haemorrhage, brain swelling and progressive grey matter damage (Dixon et al., 1987; McIntosh et al. 1989; Povlishock, 1983). The controlled cortical impact (CCI) model applies an air driven piston to penetrate the brain at a known distance and velocity (Lighthall 1988). The advantage of this model over other TBI models is the mechanical factors, such as velocity and depth of impact, can be controlled. It can produce acute subdural haematoma, axonal injury, concussion, blood–brain barrier (BBB) dysfunction and cortical tissue loss (Dixon et al., 1991; Smith et al., 1995). The penetrating ballistic-like brain injury (PBBI) involves the transmission of high energy projectile (Williams et al., 2005), which produces a temporary cavity in the brain that is many times the size of the projectile itself and induces brain swelling, white and grey matter damage, cortical spreading depression and neuroinflammation (Williams et al., 2006, 2007). In the weight-drop models, a free weight is dropped directly onto the exposed dura (Feeney et al., 1981) or onto a metal disk over the skull to prevent bone fracture (Marmarou et al., 1994). Injury severity in these models can be controlled by adjusting the drop height of the weight. Marmarou’s impact acceleration model is discussed in detail in next section. Blast TBI model use a compression-driven shock tube to generate blast wave. Non-impact blast injury can cause diffuse cerebral brain oedema, extreme hyperaemia and neurological dysfunction (Cernak et al., 2010; Kuehn et al., 2011). TAI was also found in rat during the initial 2 weeks after exposure to blast even with body shielding (Garman et al., 2011). Other animal models including the inertial rotational acceleration (Meaney

et al., 1993; Ross et al., 1994) and nerve stretch injury model (Gennarelli et al., 1989; Dieterich et al., 2002; Singh et al., 2006).

Despite differing opinions in selecting species for modeling human TBI, many investigators have accepted rodent as the most suitable choice for neurotrauma research (Cenci et al. 2002). The advantage of using rodent includes the relatively small size and cost of rodents, existing techniques for measurements of morphological, biochemical and behavioral parameters of rodents. However, others have suggested that the lissencephalic rodent cortex is not appropriate for modeling the changes in the anatomy of human cortex which is more complex, and the difference of physiological and behavioral responses to neurotrauma between rodent and human should also be taken into consideration (Povlishock et al., 1994). Nevertheless, rodents remain the most commonly used animal model for TBI studies (Cernak, 2005).

2.3.2 Marmarou Impact Acceleration Model

A challenge to the investigation of closed head diffuse traumatic brain injury is the difficulty of inducing an isolated but significant degree of axonal injury without concomitant focal contusion and skull fracture. Marmarou and his colleagues (1994) developed an impact acceleration device (Fig. 2-5) that can reliably produce axonal changes in a closed head injury in rodents. Briefly, the head of the anesthetized animals is placed unrestrained in a prone position on a foam bed, adjusted to the end of the device, and a head impact is delivered via a free falling weight. A 10 mm diameter metallic disc is glued on the rat skull to distribute the loading to prevent skull fracture and associated focal brain injury. The drop weight and height are controllable so as to produce a graded

axonal injury in various white matter tracts (Marmarou et al., 1994, Foda and Marmarou, 1994, Beaumont et al., 1999, Kallakuri et al., 2003). The Marmarou impact acceleration (IA) model reliably mimics a closed head injury induced by a combined linear and angular head impact and is capable of producing significant TAI in discrete WM tracts including corpus callosum (CC) and brainstem without concomitant focal contusion and skull fractures in rats (Marmarou et al., 1994).

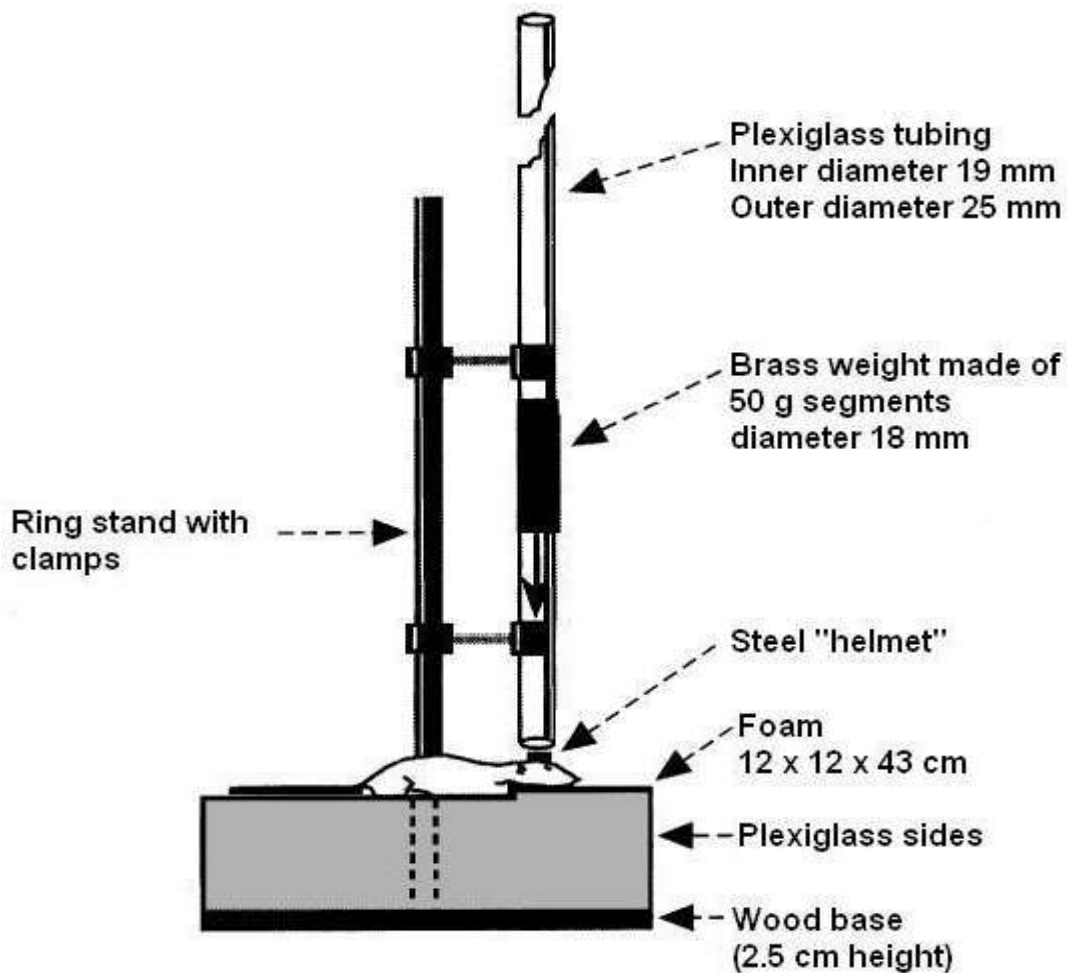


Figure 2-5: Original Marmarou impact acceleration injury model (Marmarou et al., 1994).

Since the model was developed in 1994, a total of over 150 publications were found upon a survey of the literature between 1994 and 2010 that used this rodent TBI model in a variety of studies. Some of the studies using this model were aimed at

understanding cellular and molecular responses to injury (Adelson et al., 2001; Thornton et al., 2006; Rafols et al., 2007; Kallakuri et al., 2007) as well as apoptosis and regeneration of neuronal cells following TBI (Park et al., 2001; Cernak et al., 2002; Tashlykov et al., 2007). Other studies were aimed at understanding the attenuation of IAT and neurofilament compaction (NFC) following TBI (Stone et al., 2004; Marmarou et al., 2006) and others studied the viscoelastic properties at pontomedullary junction and pyramidal decussation by combining finite element (FE) analysis with TBI induced by this model (Shafieian et al., 2009). Motor and cognitive deficits induced by this model (Adelson et al., 1997, 2000; Schmidt et al., 2000) have been studied as well as oxidative stress and mitochondrial related injury (Tavazzi et al., 2005; Vagnozzi et al., 2007). Diagnoses and treatment after TBI using this model have also been extensively studied due to the graded TAI induced (Health et al., 1999; Fei et al., 2006; Sengul et al., 2008).

Although studies illustrate the widespread utility of the Marmarou model in studying various aspects of TBI, there is very limited work on the mechanical responses of the model (Gilchrist, 2004; Wang and Ma, 2010b). No standard procedure has been developed to date to measure the mechanical response in the Marmarou IA model.

In an earlier kinematic study of the Marmarou IA device, Piper et al (1996) measured velocity by placing a photo-conductance cell near the bottom of the Plexiglas tube, and they found that the velocity of a 450 g weight dropped from a height of 2 m can vary by as much as 40% depending on the degree of initial friction. They indicated the use of supporting fishing line through the eye of metal wing nut resulted in less variation in weight drop velocity with fewer episodes of line breakage or depressed skull fracture. Others reported that friction between metal weight and vertical tube changed over time

(Ucar et al., 2006; Carre et al., 2004), which can also lead to variations in velocity. Other system errors include stiffness of foam bed (Piper et al., 1996) and lateral movement of the weight inside the Plexiglas tube (Cernak, 2005). The potential variations in the mechanical system described may also be major contributors to the varying mortality rates reported by different groups: 56.8% by Pascual et al. (2007), 78.5% by Ucar et al. (2006), 60% by Geeraerts et al. (2006), 35.7% by Rhodes (2002), 31% by Ueda et al. (2001), 20% by Fei et al. (2007), 15% by Suehiro et al. (2001) and 10% by Marmarou et al. (2006). In addition, information on the relationship between measured rat head kinematics and the quantified axonal changes and other neuronal changes has not been published. Therefore, a modified Marmarou impact acceleration model which accurately record various mechanical responses induced by this model could help to investigate the correlation between biomechanics and TAI produced by this model.

CHAPTER 3

BIOMARKERS FOR TRAUMATIC AXONAL INJURY

3.1 BACKGROUND OF BIOMARKERS FOR TBI

Acute brain injuries resulting from TBI, cardiac arrest, or stroke result in lasting neurologic and cognitive problems to highly variable degrees (Siman et al. 2009). Currently, mild acute brain injuries, especially mild axonal injury, are difficult to diagnose and evaluate. The brains of patients with mild brain injury usually look normal in CT scans, the most frequently used test after brain damage. The lack of efficient prognostic methods leaves patients at great risk for developing severe and sustained abnormalities, and makes it difficult to evaluate the rehabilitation results. To help circumvent these problems, considerable effort is being devoted to the establishment and validation of biochemical surrogate markers for acute brain damage.

A biomarker is an indicator of a specific disease or biological state that can be measured using samples obtained from serum, CSF or directly from affected tissue (Dash et al. 2010). The change of biomarker levels results from various cellular events, such as altered enzymatic activity, changes in gene/protein expression, post-translational modification, or a combination of these changes. As a result, various strategies have been used to identify biomarkers including genomic profiling, proteomic profiling and metabolic approaches (Merrick and Bruno 2004, He 2006). The attributes of ideal TBI biomarkers have been summarized by Wang et al. (2005) in Table 3-1. Basically potential biomarkers should be brain-originated, include information on mechanism of neuronal injury, and have good correlation to magnitude of injury severity and with other

TBI benchmarks (GCS, MRI, CT and neuropsychologic scores). Besides, good sensitivity and specificity are also very important.

Table 3-1: Attributes of ideal TBI biomarkers (Wang et al., 2005).

-
- Information on mechanism of neuronal injury.
 - Marker level elevated within 24 h after TBI.
 - Brain originated.
 - Correlation to magnitude of injury severity or lesion size.
 - Correlation with other TBI benchmarks (Glasgow Coma Score, magnetic resonance imaging, computed tomography, neuropsychologic scores).
 - Sensitivity to subclinical or mild traumatic brain injury.
 - Selectivity to TBI over other nonbrain injury neurologic disorders.
 - Prediction of outcome (Glasgow Outcome Scale-Extended).
 - Direct translation from preclinical animal models to clinical environment.
 - Prediction of therapy efficacy.
-

TBI: Traumatic brain injury

There are numerous reports indicate that many proteins expressed in the nervous system changes concentration and are detectable in human biological fluid following acute brain injuries, including proteins that indicate axonal injury, astroglial damage, BBB integrity and neuroinflammation. The most widely studied serum and CSF markers for TBI has been illustrated in Fig. 3-1 by Zetterberg et al. (2013), and has been reviewed previously (Pineda et al., 2004; Wang et al., 2005; Berger 2006; Kovesdi et al., 2010;

Dash et al., 2010; Zetterberg et al., 2013; Papa et al., 2013).

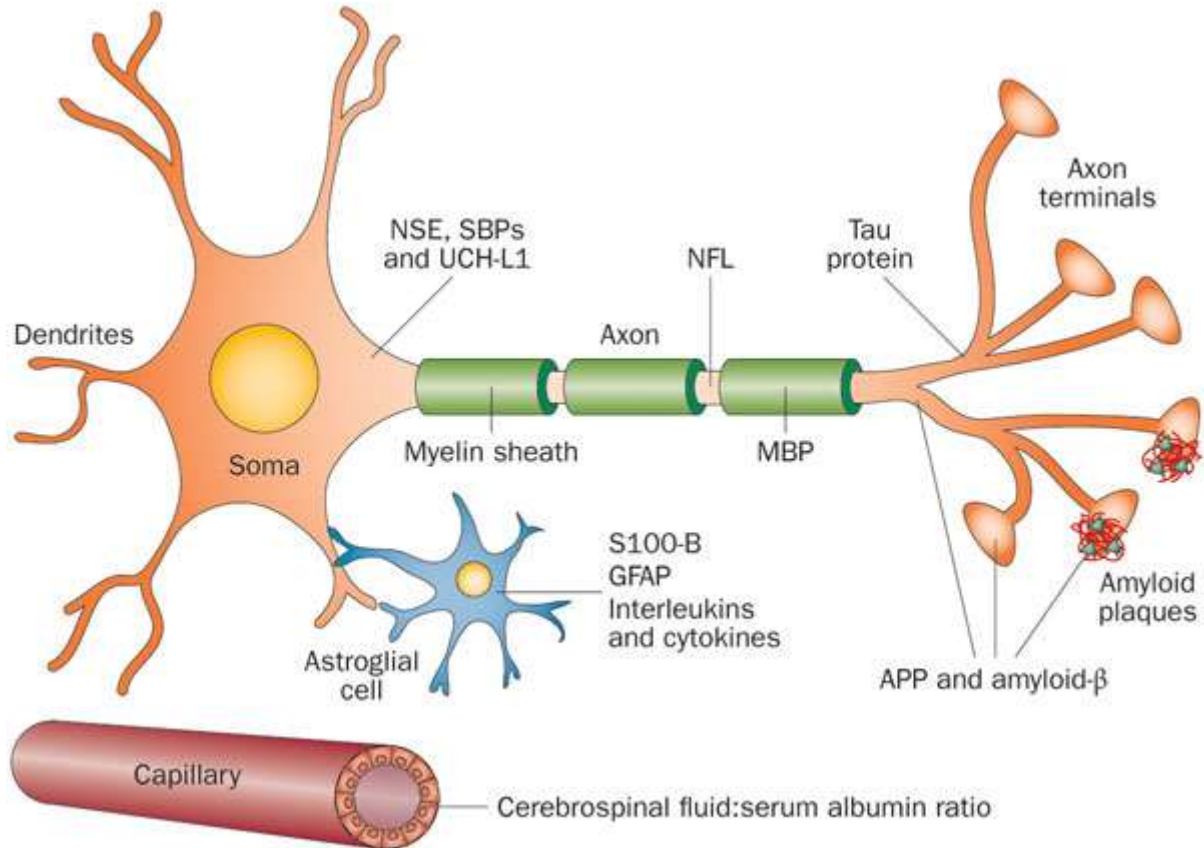


Figure 3-1: Biomarkers of TBI in CSF and Serum (Zetterberg et al., 2013).

Injury to neuron may lead to release neuron-specific enolase (NSE), ubiquitin carboxy-terminal hydrolase-1 (UCH-L1), spectrin breakdown products (SBDP). UCH-L1 is a marker of neuronal damage linked to TBI (Berger et al., 2012). UCH-L1 levels in blood are increased by compromised BBB integrity. In their pilot study of 96 patients with mild to moderate TBI, Papa et al. (2010) showed that UCH-L1 is detectable in serum within 1 h after TBI and its concentration is positive correlated with the Glasgow Coma Scale score, and damage seen on brain imaging. α II-spectrin is one of the major structural components of the cortical membrane cytoskeleton. It is specifically abundant in axons and presynaptic terminals and is a major substrate for calpain and caspase-3

cysteine proteases. The calpain-mediated cleavage of α II-spectrin results in the formation of calpain-signature spectrin breakdown products (SBDPs). The N-terminal fragment (SNTF) was recently reported as a biomarker for mTBI patients (Siman R. 2013).

Among axonal biomarkers, tau protein is most abundant in thin, nonmyelinated axons of cortical interneurons, whereas neurofilament polypeptides (NF) is highly expressed in the large-calibre myelinated axons that in deeper brain layers and the spinal cord. Distinct regional distributions of these two proteins in the brain might be helpful in determining the locations of brain damage that have been produced by TBI. Elevated levels of total tau and neurofilament light chain (NFL) in CSF obtained by lumbar puncture have been reported in patients with mTBI, such as boxers (Zetterberg et al., 2006, Neselius et al., 2012). The Tau protein level has also been found increase in the serum of mTBI patients (Guzel et al., 2010). Amyloid precursor protein (APP) and amyloid- β are transported along axon terminals and thought to be involved in synaptic activity and plasticity.

Injured astroglial cells may release S100-B and GFAP into the extracellular matrix, while astrogliosis and post-injury neuroinflammation can lead to increased production of interleukins and cytokines. GFAP has received considerable attention as serum biomarkers of astroglial injury, since it shows high specificity to brain tissue, and its serum levels does not affected by multi-trauma (Pelinka et al., 2005). Recent work by Papa et al. (2012) has indicated that the concentration of GFAP break down product increased in the serum of mild and moderate TBI patients within a few hours of injury, and were correlated with GCS ratings, CT lesions, and neurosurgical interventions.

These proteins are currently being evaluated as serum or CSF biomarkers for detection of brain injury in neurologic patients (Pelsers, M.A.L. et al. 2004), and patients with cerebrovascular accidents (Aurrel et al. 1991), traumatic brain injury (Kobeissy et al. 2006), stroke (Romner et al. 2000), and vascular dementia (Paraskevas et al. 2009) with the aim to eventually illustrate the mechanism of injury. Among these biomarkers, a hypophosphorylated form of neurofilament H (NF-H) and a proteolytic fragment of tau are expressed in neurons predominantly within axons, and CSF alterations in these proteins have been proposed as indicative of axonal damage (Zemlan et al., 1999; Petzold et al., 2006).

However, several of these markers, such as S100B, suffer from a lack of specificity, often being induced or released into the serum in response to other diseases or bodily injuries. This lack of specificity has hampered the effort to identify markers of mild TBI, especially in the context of polytrauma (Dash et al., 2010). Given the extracranial sources of biomarkers and the failure to find a single biomarker that satisfies the criteria for reliable use as an accurate screening tool, some investigators have examined combinations of biomarkers to improve outcome prediction (Berger et al., 2005, 2008, Lo et al., 2009, Siman et al., 2009). For example, Lo et al. (2009) examined the predictive capacity of multiple biomarkers from different mediator families to determine whether combinations of two serum biomarkers could achieve better outcome prediction than individual biomarker levels in 28 children with TBI. Eight different neurospecific and inflammatory biomarkers (S100B, NSE, interleukin (IL)-6, IL-8, IL-10, SICAM, I-selectin, and endothelin) were quantified using ELISA on day 1 and compared with outcome assessed at 6 months after injury. None of the eight biomarkers evaluated

individually achieved an area under the ROC curve (AUC) of 0.95 for predicting TBI, but five of the 20 biomarker pairs assessed achieved this high degree (more than 0.95) of outcome predictability. Two combinations of biomarkers, S100B and L-selectin, as well as S100B and IL-6, achieved an AUC of 0.98, and their specificity and sensitivity for TBI prediction were 96% and 100%, respectively. They concluded that prognostic pairs combining serum levels of two biomarkers (inflammatory mediators and brain specific proteins) improved prediction for unfavorable outcome after childhood brain trauma compared to single markers. Siman et al. (2009) hypothesized that a large panel of brain-enriched proteins may greatly improve the diagnosis and clinical evaluation of acute brain injuries. They developed a panel of biomarkers originally released from degenerating cultured neurons, and subsequently verified in rodent models of TBI and ischemia.

These pilot studies lead us to believe that combinations of markers may be better suited to guide management, warn of secondary injury, and help prognosticate in TBI, considering the limitations of individual markers and the heterogeneity of various factors that influence outcome in TBI.

3.2 CHALLENGES OF BIOMARKER STUDIES

Unfortunately, owing to limitations in sensitivity, specificity, and standardized quantification across multiple laboratories and studies, none of the existing proteins has emerged as a widely accepted diagnostic or prognostic clinical tool or a validated biomarker for brain damage (Svetlov et al. 2009). The common practice of dichotomizing outcome to “good or bad” or “dead or alive” severely limits the ability to

accurately assess the clinical usefulness of the biomarkers (Berger et al. 2006). Another limitation relates to the calculation of cut-off values to predict poor outcome/mortality. In many of the studies in the literature, cut-off values were determined retrospectively in order to maximize specificity and sensitivity. It is essential that investigators begin to evaluate potential clinically relevant cut-off values in a prospective manner (Berger et al. 2006).

A disadvantage of current clinical examination is that the population being studied has not experienced similar level of TBI. Other characteristics, including age, sex, and race, are also not homogenous. In addition, acute non-trauma brain insults such as posttraumatic seizures or hypoxemia, chronic non-trauma brain insults such as strokes, and acute noncranial injuries such as bone fractures can all change CSF and serum biomarker level therefore affect predictive outcome of biomarkers (Berger et al. 2006). For example, although serum levels of S100B correlates with mortality and morbidity, as well as long-term neurologic outcome, the protein also markedly increases in serum during surgical procedures or in disorders unrelated to acute brain injuries (Anderson et al., 2001; Siman et al., 2008). Consideration of extracranial injuries and their effect on functional outcome is also an important issue that should be addressed in future studies.

As discussed above, there is still significant work that needs to be done before biomarkers can be used to guide clinical decision making. A lack of unified models with defined injury criteria has contributed significantly to existing controversies. The use of large, homogenous study populations with appropriate control populations, consistent and refined outcome measures, and prospectively defined cut-off values for the biomarkers

are all important considerations for future studies. Therefore, a well-controlled animal model could facilitate the development of potential TBI biomarkers before clinical trials.

CHAPTER 4

SIGNIFICANCE OF THIS STUDY

4.1 MODIFIED MARMAROU IMPACT ACCELERATION MODEL

In spite of the widespread utility of the Marmarou model in studying various aspects of TBI there is very limited work on the mechanical responses of the model (Gilchrist, 2004; Shafieian et al., 2009; Wang and Ma, 2010b). As part of the current study, the model has been modified and expanded to monitor velocity, displacement into the foam, head linear kinematics and head angular kinematics during impact injury of various severities (Chapter 5). Results from this study offer for the first time the relationship between measured rat head kinematics and the quantified axonal changes (Chapter 6), and between kinematics and biomarker change in both CSF and serum (Chapter 7).

The lack of control over precise conditions of impact can result in a high degree of variability in the original Marmarou model, making injury response hard to reproduce between different investigators and laboratories. In order to standardize the use of this model, especially when TAI severity needs to be quantified, we recommend monitoring the following parameters: 1) weight drop velocity, it can be obtained either by velocity trap device (Piper et al. (1996) or high-speed video analysis (in our study); 2) foam stiffness, the elastic properties of foam bed need to be pre-determined and tracked periodically (Piper et al. 1996), and foam bed is suggested to be changed after 10 impacts based on our previous study (Zhang et al. 2005); 3) impactor-helmet interface, since lateral movement of impactor and helmet surface angles may potentially cause uneven

distribution of the impact energy, and increase variability of outcomes, a laser beam could be used in our study to guide the positioning of rat head under the Plexiglas tube and high-speed video could be checked to confirm the two surfaces of impactor and helmet are parallel at initial impact; 4) post-injury behavior, such as loss of consciousness, may indicate injury severity and help to exclude outliers. We also strongly suggest to monitor dynamic response of the rat head if applicable, which correlates with injury severity and can enable comparison of TAI levels between different research groups.

On the other hand, assessing which characteristics of an impact (force, energy, acceleration etc.) best predict the risk of TAI is of particular importance in developing injury criteria used by regulatory agencies that provide standards in the design and manufacture of safety equipment and motor vehicles. The Wayne State Tolerance Curve (WSTC) demonstrated that the severity of head injury was dependent both on the magnitude and duration of average or effective impact acceleration. The average head acceleration is also the basis of the existing Head Injury Criterion (HIC) used by most regulatory agencies in assessing the safety of motor vehicles (Prasad and Mertz, 1985). Accordingly, we attempted to directly correlate rat kinematics with TAI level, and sought to identify the best injury predictor for TAI and investigate injury threshold based on additional measured biomechanical parameters.

4.2 QUANTIFIED IMMUNOHISTOCHEMICAL TECHNIQUE

A more detailed quantification of TAI in CC was undertaken in this study than in previous studies using the Marmarou AI device. One silver impregnation study reported profiles of TAI as swellings, retraction balls and axons with vacuoles in four sections

through CC for each rat, using three rats at each drop height (Kallakuri et al., 2003). Another study (DiLeonardi et al., 2009) identified TAI in 2D panoramic images of CC from three anatomic locations, and described temporal and spatial progression of TAI at these locations, but TAI counts were not reported. Furthermore, by utilizing 12-14 sections across the entire CC, the spatial profiles of TAI maps revealed non-uniform distribution longitudinally along the CC, with the area directly under the helmet (bregma 0.60/0.84 mm) showing higher density of TAI in some rats.

Smith and Meaney (2000) showed that the pattern of axonal damage in the white matter is more accurately described as ‘multifocal’ rather than diffuse. Therefore TAI from a limited number of selected locations may not be an accurate representation of injury profiles in the entire CC. Utilizing the quantified data from many sections in our study, 3D injury maps were constructed and graded for the entire CC, permitting an element-by-element correlation with the mechanical response (such as the brain strain along with the rate at which the strain is applied) predicted at that location by the FE rat head model.

FE models provide a promising technique to study the mechanical response of the human brain to blunt trauma and the stresses and strains in brain tissue that lead to brain injury. Cadaver tests have been used to validate the mechanical response of FE models (King et al., 1995; Zhang et al., 2001, 2004). However, cadavers lack viable neural tissue, and although precise mechanical input can be measured, TAI cannot be assessed. The TAI injury maps developed in the current rat study are being correlated to tissue level stresses and strains in a rat head FE model. Hence, this will allow determination of tissue thresholds for TAI. Such tissue thresholds can later be translated to human head models

and therefore will enhance the capability of the human head model in predicting brain injury.

4.3 A PANEL OF BIOMARKERS

In this study, quantitative and qualitative TAI findings in specific white matter tracts were correlated with biomarker assays using a well-established rat impact-acceleration head injury model.

The modified impact acceleration model has some noticeable advantages over human clinical study: 1) our model is able to closely monitor the mechanical parameters that produce the injury; 2) the TAI quantification in CC region by β -APP enables accurate evaluation of the outcome of axonal injury; 3) our animal model restricts evaluations to CSF biomarker levels measured at exactly 24 h and only in isolated accidental brain trauma. These advantages help to eliminate the uncertain factors in human study, and standardize quantification across multiple laboratories and studies. Our study also allows us to screen reliable biomarker in short time period before translating it into clinical trials.

Many potential TBI biomarkers have been reported, but few previous studies have described outcome prediction using combinations of biomarker levels. Previous studies using individual biomarkers rarely yielded sensitivity and specificity of more than 85% (as reported here) for unfavorable outcome prediction. A recent report (Jain 2008) pointed out the need for multiple biomarkers and their correlation. We aim to evaluate multiple biomarkers from different cell type and to determine whether combinations of

two CSF biomarkers may achieve higher predictive values than individual biomarker levels.

4.4 HYPOTHESES AND SPECIFIC AIMS

Hypotheses: 1) TAI is produced by linear and/or angular acceleration. TAI severity can be quantified by histologic technique and is correlated to mechanical responses. 2) TAI is a subsequence of a cascade of cellular changes after impact. TAI severity is correlated to the concentration of biomarkers which are released to the CSF and serum by the cellular changes in the brain after injury.

Specific Aim I: Develop an improved head impact acceleration device for quantifying head biomechanical responses in a rodent model of traumatic axonal injury. This was accomplished by:

1. Investigate the biomechanical performance of the original Marmarou impact acceleration model.
2. Develop an improved head impact acceleration device for quantifying head biomechanical responses.
3. Compare the new impact model with the original Marmarou model.

Specific Aim II: Investigate correlation between impact mechanics and traumatic axonal injury in a rodent model of traumatic axonal injury. This was accomplished by:

1. Characterize the kinematics of the rat head during dynamic impact of various severities.

2. Quantify the intensity and distribution of the axonal changes throughout the corpus callosum and brainstem using histopathologic techniques.
3. Determine correlation between head impact response and traumatic axonal injury, and identify potential injury predictors for traumatic axonal injury.

Specific Aim III: Establish a panel of biomarkers to assess the level of traumatic axonal injury in a rodent impact acceleration model. This was accomplished by:

1. Determine correlation between individual biomarker levels after impact and TAI counts and identify potential reliable biomarker for TAI.
2. Investigate if the combination of multiple biomarkers can provide better predictive value for TAI.
3. Study correlation between biomarker levels after impact and head impact responses.
4. Identify potential biomarkers for mild traumatic brain injury.

To our knowledge, results from this study offer for the first time the comparison of various mechanical parameters with TAI, the signature injury induced by this model. The quantitative and qualitative techniques to characterize TAI will help to identify potential biomarkers for TAI.

CHAPTER 5

**AN IMPROVED HEAD IMPACT ACCELERATION DEVICE FOR
QUANTIFYING HEAD BIOMECHANICAL RESPONSES IN A RODENT
MODEL OF TRAUMATIC AXONAL INJURY**

5.1 INTRODUCTION

A number of laboratory experimental models have been developed to reproduce specific features of human traumatic brain injury (TBI) in an effort to identify cellular processes contributing to the neuropathophysiological outcomes. A challenge to the investigation of closed head diffuse traumatic brain injury is the difficulty of inducing an isolated but significant degree of axonal injury without concomitant focal contusion and skull fracture. Marmarou and his colleagues (1994) developed an impact acceleration device that can reliably produce axonal changes in a closed head injury in rodents. Briefly, the head of the anesthetized animals is placed unrestrained in a prone position on a foam bed, adjusted to the end of the device, and a head impact is delivered via a free falling weight. A 10 mm diameter metallic disc is glued on the rat skull to distribute the loading to prevent skull fracture and associated focal brain injury. The drop weight and height are controllable so as to produce a graded axonal injury in various white matter tracts (Marmarou et al., 1994, Foda and Marmarou, 1994, Beaumont et al., 1999, Kallakuri et al., 2003). Since the model was developed in 1994, a total of over 150 publications were found upon a survey of the literature between 1994 and 2010 that used this rodent TBI model in a variety of studies. These included but were not limited to the understanding of impaired axonal transport and neurofilament compaction (Stone et al.,

2004; Marmarou et al., 2006), motor and cognitive deficits (Adelson et al., 1997, 2000; Schmidt et al., 2000) oxidative stress and mitochondrial changes (Tavazzi et al., 2005; Vagnozzi et al., 2007) as well as the diagnoses and treatment after TBI (Fei et al., 2006; Sengul et al., 2008).

The impact energy calculated from the known mass and impact velocity of the weight for a given height is commonly used as a measure to imply injury severities. The actual velocity of the weight prior to impacting on the rat skull/helmet, however, can be affected by the drag force and frictional force between the weight and the plexiglass tube where the weight is falling through (Carre et al., 2004, Ucar et al., 2006). Additionally, the stability of the drop stand and the alignment of the tube with respect to the ground surface can induce variability in drop velocity from test to test. In the literature, velocity of a 450-g weight dropped from a height of 2m can vary as much as 40% (Piper et al., 1996) and some studies suggested minimizing the friction between the cylindrical weight and the plexiglass tube (Carre et al., 2004; Ucar et al., 2006). Despite the potential loss of velocity during drop, previous studies used drop height to define impact velocity. The actual impactor velocity has not been directly monitored and the degree of the velocity loss has not been quantified. Since the kinetic energy is proportional to the square of velocity, velocity change could lead to amplified changes in impact energy.

Biomechanically, the head kinematics in response to the impact force affects the internal brain responses, therefore affecting the severity and pathology of brain injury. In this rat impact model, the falling weight impacts the helmeted head, driving the head and compressing the underlying foam a considerable degree. Both the alignment of helmet center with the cylindrical weight prior to the impact and the head orientation can

introduce variability to the head motion during impact. Up to now, the precise kinematic response to the rat head, including the impactor force and the linear and rotational motion during the head impact has not been reported. Knowing the head kinematics will help in the understanding of the underlying biomechanical causes of brain injury in this model and provide the correlates for severity and extent of axonal pathology. No standard procedure has been developed to date to measure and quantify the mechanical response of the rat head in the Marmarou impact acceleration model. Without precise biomechanical measurements the relationship between the head kinematics and neuropathological changes following impact cannot be defined in this rodent TAI model.

The current study reports an improved rodent head impact device that was designed to monitor velocity, displacement into the foam, head linear acceleration, and head angular velocity through attached miniature sensor and high speed video analysis during impact injury of various severities. The new measuring systems which can directly monitor the impact energy and kinematics of the head during the entire dynamic impact were developed to in order to characterize the biomechanical response involved in brain injury production in this rodent model.

5.2 MATERIALS AND METHODS

5.2.1 Design of the head impact device

The original design of the impact acceleration rodent TAI device described by Marmarou et al. (1994) was modified and improved for the current study. In the original design, the impactor (drop weight) is made of a series of brass cylindrical segments at a diameter of 18 mm with each weighing 50 grams. The impactor is held at a desired

height by a string and then released through a 20 mm-diameter plexiglass tube (Fig. 5-1A). In the new design, a 2.5 m long and 57 mm in diameter plexiglass tube is used and attached to a rigid drop tower frame made of 80/20 3"x2" extruded aluminum bolted

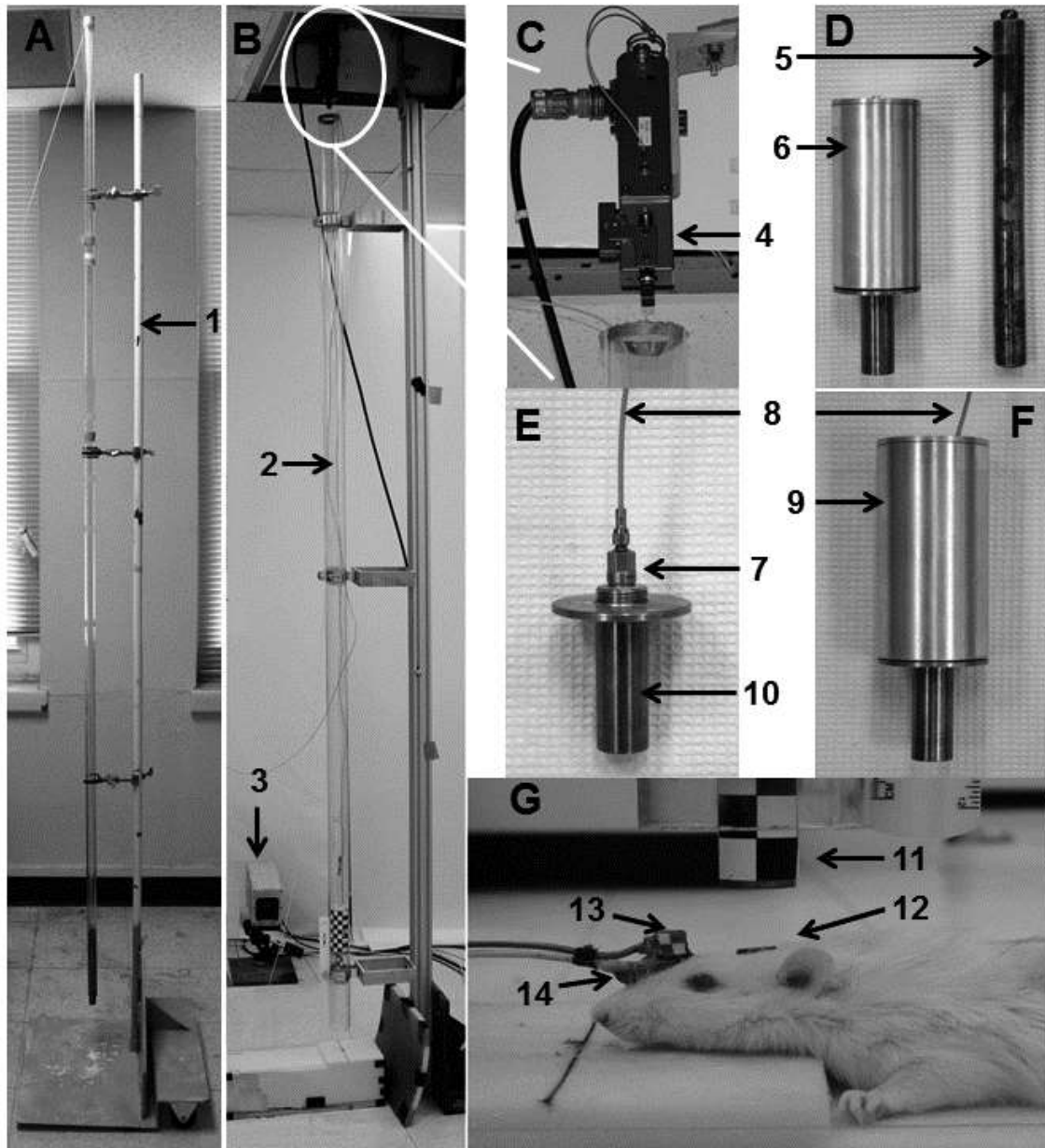


Figure 5-1: Comparison of the original Marmarou device (A) and the modified impact acceleration injury model with instrumentation (B-E). 1: original Marmarou device; 2: modified impact device; 3: high-speed camera; 4: solenoid automatic releases device; 5: old 450 g impactor; 6: new 450 g impactor; 7: accelerometer; 8: accelerometer cable; 9: aluminum cylinder; 10: brass impact end; 11: impactor; 12: helmet; 13: angular rate sensor; 14: accelerometer.

to a heavy steel base anchored to the floor (Fig. 5-1B). The impactor consists of a solid brass cylinder and an aluminum tube (Figs. 5-1E, F).

The lower end of the brass cylinder directly impacts the helmet/rat head and has a diameter of 19 mm to create an impact interface similar to the original design. The top surface of the brass impactor has a large diameter to provide a mounting surface for a small piezoelectric accelerometer 8084 (Kistler Instrument Corp., NY). The aluminum cylindrical tube (51 mm diameter) is threaded on the upper end of the brass cylinder to accommodate this mounted accelerometer. The accelerometer cable is connected to the data acquisition system through the opening of the top surface of the aluminum tube. The accelerometer allows recording of the impactor acceleration and to derive the velocity change of the impactor. The entire impactor weighs 450 grams. A custom-made solenoid automatic release device is installed on the top of the drop tower to release the impactor from any given height (Fig. 5-1C).

5.2.2 Comparison of impact velocities between the existing and new devices

The actual velocity of the impactor (weight) just prior to impacting the rat head was measured using a custom made velocity timer laser system (KME Company, MI). The laser beam was aligned at 20 mm below the bottom of the Plexiglass tube when the impactor contacts the helmet on the skull of the rat head. A series of tests (N=5 for each group) were conducted by dropping the impactor from 2 m height into the helmeted head of a freshly expired rat to measure impact velocity. The consistency/repeatability of the pre-impact velocity produced by the current new device and original device were assessed and reported.

The interaction of the impactor with the helmet and the motion of the rat head during impact were recorded by a high-speed digital video camera (MotionXtra HG-100K, Redlake MASD, CA). The camera was placed at 0.5 m from the side of the animal head and aligned to the surface level of the helmet/head. The digital video data captured at frame rate of 10,000 frames/second (fps) were then analyzed using ImageExpress software (MotionPlus, SAI, NY) to track the displacement of the marker placed on the impactor. The pre-impact velocity was then calculated from video displacement data. The accuracy of the pre-impact velocity analyzed from video footage was assessed in comparison to the velocity measured directly from the velocity timer.

The velocities recorded for a 450g-weight dropped from 2 m height were compared between two group tests conducted using Marmarou's original device and newly designed impact acceleration device with various impactor release mechanisms (N=5 for each subgroup). For group A, all tests were conducted using the original device but with two different weight hold-release mechanisms. In subgroup A₁, the weight was held and released through an attached cotton line through a pulley installed at the top of the Plexiglass tube. In subgroup A₂, the weight was held at the same height and released using a nylon fishing line. For group B, all tests were conducted using the new impact acceleration device. In the subgroups B₁ and B₂, the impactor release mechanisms were the same as those used in the subgroups A₁ and A₂, respectively. In subgroup B₃, the top of the impactor was held in place by an automatic release system via a pair of clamps and was then released through an in-house electronic control unit. No string was used for subgroup B₃. For B₁-B₃ subgroups, the cable which connects the accelerometer (seated inside of the impactor) to the data acquisition system was disconnected from the

accelerometer. In subgroup B₄, the entire test configuration was the same as that of subgroup B₃ except for the addition of the accelerometer cable (5 m long) which was attached to the top of the sensor mounted inside of the impactor. Each test condition was repeated five times. Upon release of the impactor, the cable fell through the tube as the impactor traveling downward within the tube. Test subgroup B₄ was compared B₃ to determine the existence of the cable drag on the falling velocity of the impactor.

5.2.3 Impact velocity as a function of drop height using new device

In published TBI studies using Marmarou device, 1.0, 1.5, and 2 m drop heights were chosen to deliver controlled mechanical insult to produce varying severities of traumatic axonal injury. The current study determined the differences between measured pre-impact velocity in all groups tested above and the theoretical values for each height. The corresponding heights required to achieve desired velocities or kinetic energies were also investigated. To do so, a series of drop tests were conducted at 1, 1.25, 1.5, 1.75, 2 and 2.25 m to obtain corresponding pre-impact velocities from each of the impact heights. The test setup was the same as that used in the subgroup B₄ in which the accelerometer within the impactor was connected to the cable and cable fell through the tube with the impactor. Five repeated tests were performed at each height. Velocity vs drop height was fitted to a linear regression function so that the desired rat head impact velocity could be determined from a known height by using this new device.

5.2.4 Rat head kinematics measurements

To measure the acceleration and angular rate of the head during the impact, a miniature-sensor system was designed to fit on the rat skull. This miniature sensor system included a modified accelerometer 7269 (Endevco Corporation, San Juan Capistrano, CA) and an angular rate sensor ARS-12k model (DTS, Seal Beach, CA) (Fig. 5-1G). The part of the mounting case of the 7269 accelerometer was removed to reduce the size and weight. The modification to the ARS sensor included the removal of the sensor enclosure followed by the proper sealing of the sensor to reduce the weight and size. The ARS sensor was rigidly secured to the top surface of the accelerometer using cyanoacrylate.

Recently expired rats (394 ± 11 grams) were used and the stainless disc with size of 10 mm in diameter was attached to the rat skull between the bregma and lambda using cyanoacrylate. Then the base of the accelerometer was attached to the midline of the dorsal surface of the skull at 5 mm anterior to the bregma by cyanoacrylate (Fig. 1G). The instrumented expired animals (N=17) were placed prone on an open-cell flexible polyurethane (PU) foam bed (12x12x43 cm, Foam to Size Inc., Ashland, VA) fitted in a Plexiglas box. The foam bed was then placed under Plexiglass tube. A laser pointer was used to guide the positioning of helmeted head to ensure that the impactor hit the center of the stainless steel disc (helmet). The high-speed video camera was used to record the impact event at 10,000 fps. Rats were impacted from 1.25 m at impact velocity of 5.51 m/s (N=6) and 2.25 m at impact velocity of 6.15 m/s (N=11).

The accelerometers and angular rate sensor signals were collected at a sampling rate of 50 kHz by a TDAS data acquisition system (DTS, Seal Beach, CA). The solenoid

release device, the sensors, the camera and the data acquisition systems were synchronized through an in house trigger switch during each experiment.

The displacement of the impactor and the helmeted head was obtained digitally by tracking the attached target using an image tracking software (ImageExpress) assuming 2D sagittal motion. Velocity change (dV) was determined from the derivative of the displacement-time histories of digitized video data. The velocity change in the rat head was also derived by integrating the head linear acceleration-time history measured from the transducer. A reliable measurement of the rat head motion was ascertained when head dV from the integrated acceleration signals reasonably matched to the head dV from video tracking, indicating that the sensors were rigidly attached to the skull during impact.

5.2.5 Statistical analysis

Given values were mean \pm standard deviation (SD). Linear regression were used to evaluate the correlation between drop height and impact velocity.

5.3 RESULTS

5.3.1 Pre-impact velocity

The theoretical terminal velocity of the impactor falling from 2 m height is 6.26 m/s. The actual terminal velocities from 2 m height measured from various test conditions were found to be consistently lower than the theoretical values in all test groups. In all group A tests, the mean (\pm standard deviation, SD) velocity was 5.84 ± 0.05 m/s for subgroup A₁ and 5.92 ± 0.02 m/s for subgroup A₂. The corresponding velocity reduction was 6.74% for subgroup A₁ and 5.37% for subgroup A₂. For group B tests

using the new device, the mean velocity was found to be 5.9 ± 0.02 , 6.01 ± 0.04 and 6.07 ± 0.02 m/s, respectively using cotton line (subgroup B₁), fish line (subgroup B₂) and automatic release mechanisms (subgroup B₃). The corresponding velocity reductions were 5.81%, 4.03% and 3.10%, respectively. For subgroup B₄, the mean velocity and percentage velocity reduction was 5.79 ± 0.03 m/s and $7.44\%\pm 0.0047$ m/s, respectively. Comparing the velocity produced by subgroup B₄ to subgroup B₃, the use of the accelerometer cable significantly slowed down the impact velocity. This was largely due to the cable dragging against the side of the tube during the fall of the impactor/cable.

Table 5.1 Comparison of pre-impact velocity from 2 m drop height between various devices and release mechanisms

<i>2m Drop</i>	<i>Original Device</i>		<i>New Device</i>			
	A ₁	A ₂	B ₁	B ₂	B ₃	B ₄
Sample Size (N)						
Mechanism of Weight Release	Cotton Line	Fishing Line	Same as A ₁	Same as A ₂	Automatic Release	B3 + Cable
Mean (\pm SD)(m/s)	5.84 (0.05)	5.92 (0.02)	5.90 (0.02)	6.01 (0.04)	6.07 (0.02)	5.79 (0.03)
Theoretical Velocity (m/s)	6.26	6.26	6.26	6.26	6.26	6.26
Velocity Lose (%)	-6.74%	-5.37%	-5.81%	-4.03%	-3.10%	-7.44%
Coefficient of Variance	0.0083	0.0031	0.0028	0.0059	0.0030	0.0047

5.3.2 Drop height and impact velocity relationship

The measured impact velocities from 6 different drop heights using the new device with automatic release mechanism (subgroup B₄) are plotted in Fig. 5-2. When compared to the theoretical velocity of the impactor calculated for the respective height, the velocity reduction increased as drop height increased. A linear regression fitted to data showed a significant correlation between the height and measured velocity ($R^2=0.99$). The linear function between the impact velocity and drop height therefore is

expressed by: $velocity (m/s) = 1.541 \text{ height } (m) + 2.710$. By using the equation, the desired velocity can be achieved based on the adjusted height. For an example, to achieve the velocity of 6.26 m/s (2m), the adjusted height would be 2.29 m using the current new device. The measured actual velocities from a series of repeated drop tests at 1.25 m and 2.25 m were 4.61 ± 0.05 m/s and 6.15 ± 0.04 m/s, respectively which were in good agreement with those calculated from the equation above ($<0.5\%$ error).

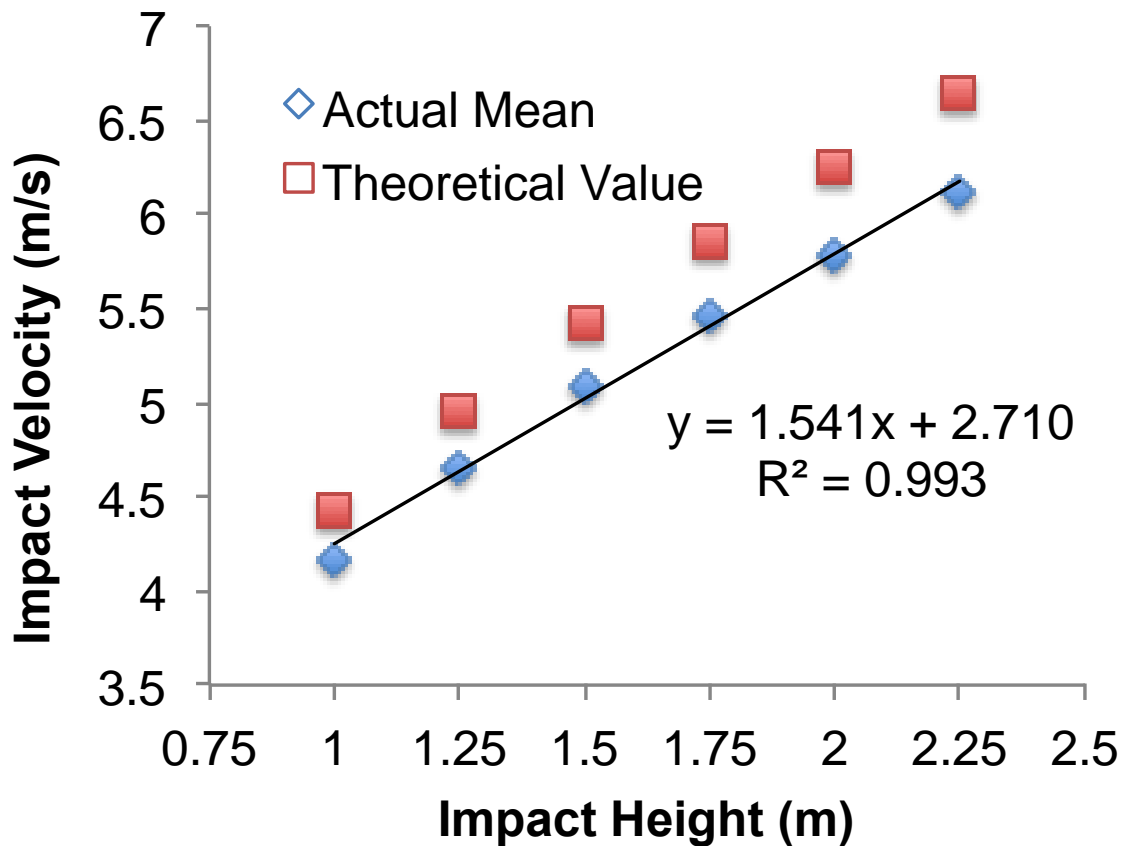


Figure 5-2: Impact velocity as a function of drop height determined for the new impact acceleration device

5.3.3 Measurements of rat head kinematics

The incidence of skull fracture was 20.4% from all 2.25 m impacted rats and was absent in 1.25 m impacted rats. Fig. 5-3A showed a series of snapshots of the impact

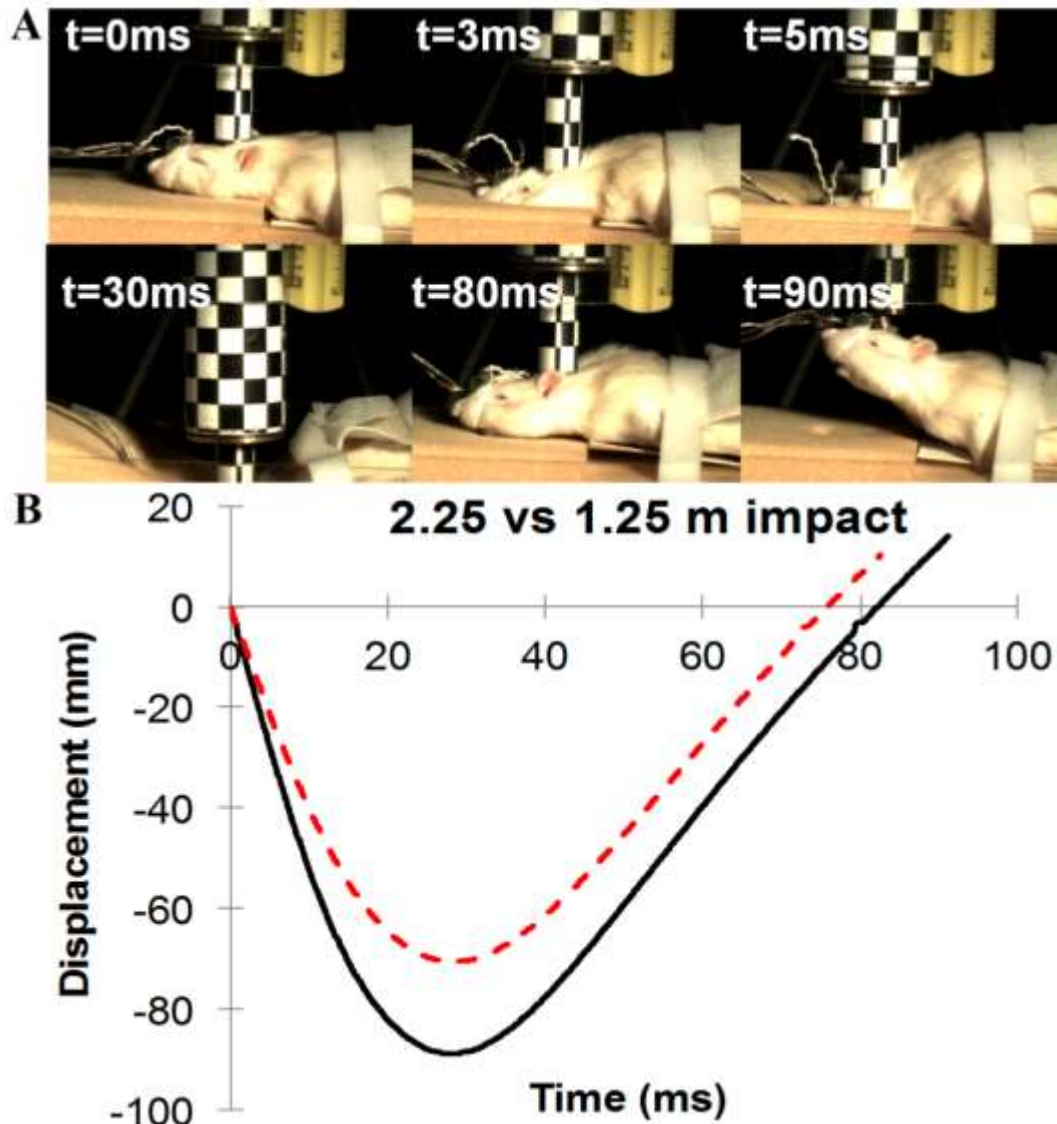


Figure 5-3: Rat head impact event. (A) Snapshots of impacted rat head at various time points during the 80-90 ms event produced by a modified rat head impact acceleration injury device. The head reached the maximum excursion into the foam at about 30 ms before rebounding to the foam surface at about 80 ms. (B) The head displacements tracked from the video footage captured at 10,000 frames/second for 2.25 and 1.25 m impacts.

event from a high-speed video camera that recorded the impacted rat head at various stages over 80 ms before the head rebounded upward above the initial position. The amount the rat head displaced into the foam upon impact and rebound from the foam surface after impact were analyzed and quantified from the video data. Fig. 5-3B showed

the time histories of quantified head displacements in the vertical direction (z axis) resulting from 2.25 m and 1.25 m tests. The average peak displacement and time when the rat head compressed into the foam was 89.7 ± 1.7 mm and 28.9 ± 0.49 ms for 2.25 m, and 71.3 ± 1.4 mm and 28.2 ± 0.47 ms for 1.25 m drops, respectively. The average time before the rat head rebounded to the pre-impact position was about 83 ms for 2.25 m and 76 ms for 1.25 m.

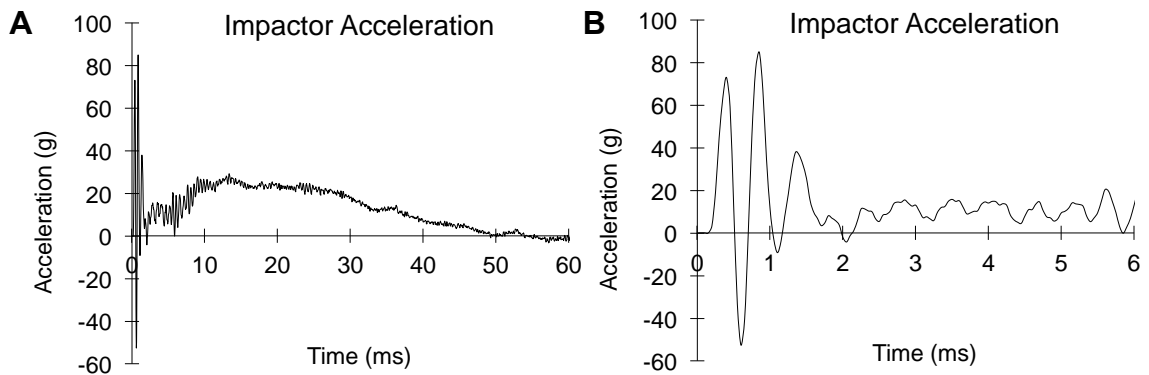


Figure 5-4: (A) Rat head impact acceleration measured on impactor over 60 ms duration and (B) during first 6 ms where peak acceleration magnitude occurs.

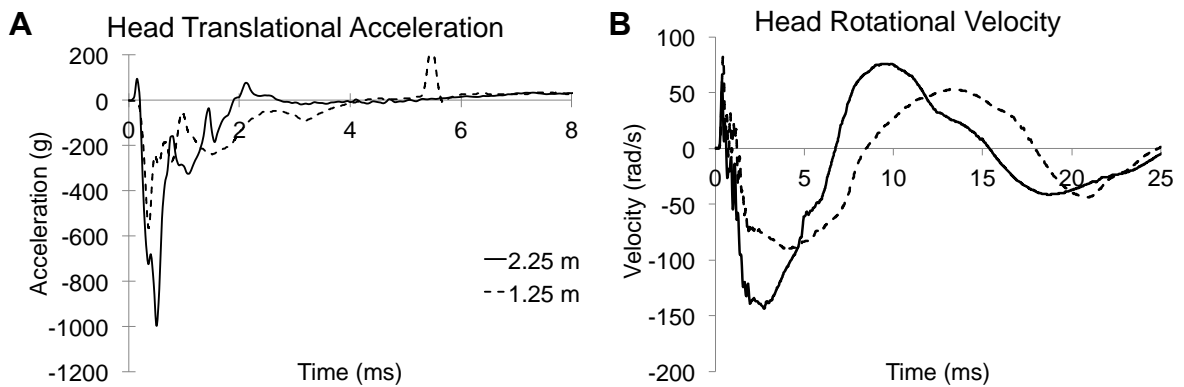


Figure 5-5: Typical time-history traces of (A) translational acceleration and (B) rotational velocity measured on the rat head in 1.25 and 2.25 m head impacts, respectively.

The maximum deceleration of the impactor in all 2.25 m impact tests ranged 48 to 96 g, with an average of 69.9 g. Fig. 5-4 showed the acceleration-time histories measured by the sensor within the impactor from 2.25 m impact. The initial high g deceleration pulse of the impactor resulted from the initial metal on metal impact. This initial acceleration pulse peaked at about 0.9 ms and lasted approximately 2 ms. The second deceleration pulse was mainly caused by the resistance of foam. It started 2 ms after initial impact with the rat helmet, reached a peak value of 25 g at about 12-13 ms, and lasted about 50 ms. During the deceleration process, the velocity of impactor gradually reduced to zero, and then the impactor started to rebound back from the foam bed.

Fig. 5-4 and 5-5 shows the typical head translational acceleration and rotational velocity time histories measured from the sensors on the rat head subjected to two impact severities. The rat head sustained linear acceleration of 918 ± 281 g and 609 ± 142 g, respectively from 2.25 m and 1.25 m impacts. The corresponding peak rotational velocity on the rat head was 116 ± 45 rad/sec, 98 ± 31 rad/sec, respectively at the two drop heights. The average acceleration peak time was 0.49 (± 0.2) ms. The rotational velocity peaked at about 2.5-3 ms after initial impact with the major response pulse lasting about 25 ms.

5.4 DISCUSSION

The Marmarou impact acceleration model has been one of the most widely used TBI animal models and the most relevant closed head injury model that mimics human pathology after TBI. An improved impact acceleration rodent TBI model which retains

the major characteristics of the original design has been developed and tested. The new system incorporated a number of design improvements, including enhanced structural rigidity for the drop stand, the use of a larger diameter tube for improved flexural rigidity and the addition of an automatic release mechanism. By monitoring the impact velocities between two designs, it was discovered that the actual terminal velocity of a 450 g impactor falling within the tube was consistently lower than the theoretical value calculated from a given height. One of the factors responsible for the velocity loss was likely the frictional effect between the wall of the plexiglass tube (~0.7 coefficient of friction) and the cylindrical impactor. The existence of the friction problems was also reported by Ucar et al. (2006). Carre et al. (2004) suggested replacing the plexiglass tube with a metal tube to reduce the friction. Another influential factor is that in the previous design, the impactor was released from a string through the pulley, which could add additional friction as well as induce additional lateral instability inside of the tube (Cernak et al., 2004) leading to further reduction in terminal impact velocity. The variability of impact velocity produced by the original form of the Marmarou device was reported as high as 40% from a 450-g weight dropped from 2 m height (Piper et al., 1996). Up to now, none of above studies measured the actual velocities from different falling mechanisms and quantified the velocity loss inherent in the systems. With the new design, the impact velocity and energy were more consistent and repeatable than the original design (Table 1). Furthermore, a linear relationship was established between any given impact height and actual impact velocities. This relationship is of importance for designing the test that allows the control of desired severities for trauma on the animal

head. The current new device improved consistency, reproducibility and reliability in terms of impact energy imparted to the rat head.

Using the original Marmarous device, different mortality rates were reported between different research groups including 56.8% by Pascual et al. (2007), 78.5% by Ucar et al. (2006), 60% by Geeraerts et al. (2006), 35.7% by Rhodes (2002), 31% by Ueda et al. (2001), and 10-20% reported by the Marmarou group (Marmarou et al., 1994; Foda and Marmarou, 1994). There were several factors that likely contribute to the variability of injury severities sustained by the animals from different groups using the same device. Firstly, the velocities quantified from the current study ascertained the inherent variability of impact velocity in the original device and therefore contribute to the differences in resulting injury severities. Secondly, the different body weight/ages of animals used by different groups (ranging from <300 to 400 g body mass) could also affect the mechanical responses of the head to the same impact. The skull thickness and head mass associated with body weight of the rodent increase with advancing age, resulting in differing mechanical responses and tolerances to a given insult. Thirdly, the foam bed in Marmarou model serves as an energy absorber and helps lengthen the impact duration. The degradation of mechanical properties of the foam during cyclic loading has been reported in our previous study (Zhang et al., 2011a). The study recommended that adequate foam recovery time would be essential to maintain the same energy absorbing capability if the foam would be repeatedly used in the subsequent impact test. In addition, marked difference in stress-strain relationship as high as 30% was observed between a used foam and a new foam. This implied that the changes of foam mechanical properties

could potentially affect the mechanical loads transmitted to the head and thus the degree of injury sustained by the rat (Piper et al., 1996; Li et al., 2011a,b; Zhang et al., 2011a).

In the original Marmarou model, the peak acceleration of rat head was estimated from a mathematical damper-spring system (Marmarou et al., 1994). The reported acceleration lasted approximately 0.2 ms from peak to zero, with peak magnitudes of 900 g for 2 m and 630 g for 1 m impact. The current study utilizing a miniature sensor system allows direct measurements of both the translational and rotational motion experienced by the rat head during each impact. The measured data revealed that the head underwent significant translational acceleration in the first 3ms followed by large rotational motion occurring around 5ms. Results from our current study showed similar average peak linear acceleration of 918 and 609 g for 2.25 and 1.25 m drop, respectively, albeit with a longer duration of approximately 2ms compared to the mathematical model results of Marmarou. The longer duration in acceleration from the current study may be related to differences in material properties of the rat head compared to those spring-damper properties assumed in the mathematical model. The average peak rotational velocity was 116 rad/s and 98 rad/s with for 2.25 and 1.25 m, respectively. The calculated mean peak angular acceleration was 180 krad/s^2 (2.25 m) and 161 krad/s^2 (1.25 m) by Marmarou et al (1994). The values at 2.25 m from the current study were lower than those reported by Fijalkowski et al. (2007) in their concussion rodent injury model subjected to prescribed average angular accelerations of 368 krad/s^2 . Another rat model combining linear and angular accelerations of $137 \pm 12 \text{ krad/s}^2$ resulted in brain injury but not with angular acceleration alone (Wang et al., 2010).

The measured head kinematics from the use of the new impact device revealed variation between repeated tests. In the new design, a laser beam was added to assist in alignment of the helmet center with the impactor center before each test. However, a slightly misalignment or offset of the impactor surface with respect to the helmet surface at the initial impact could still exist. A computer model simulation was therefore conducted to help identify the degree of the influences of helmet surface angles on the resulting head kinematics. The model simulation results showed that as the helmet tilted about 5 degrees from horizontal in the coronal plane, the condition resulted in 56%, 17%, and 10% increases in posterior-anterior, ventral-dorsal direction and resultant accelerations, respectively, with additional lateral acceleration of 400 g as compared to the helmet surface aligned at a perfectly horizontal level. Similarly, in head rotational acceleration, the angled impact resulted in a decrease of rotational acceleration in the sagittal plane and induced an additional rotation in coronal plane. The model simulation along with the measurements of test results (918 ± 281 g and 116 ± 45 rad/sec) imply that the initial impactor/helmet contact condition could affect the consistency of the head kinematics sustained by rats from the same impact velocity and this could be a major contributor to variability in injury outcome among tests at the same drop height. Such results were found in the tests conducted on anesthetized rats (Li et al., 2011a,b). Future tests will include a tri-axial angular rate sensor to capture the head kinematics in all axes.

CHAPTER 6

CORRELATION BETWEEN IMPACT BIOMECHANICS AND TRAUMATIC AXONAL INJURY

6.1 INTRODUCTION

In the United States, 1.4 million people sustain TBI each year, resulting in 235,000 hospitalizations and 50,000 fatalities annually. The leading causes of TBI are falls, motor vehicle accidents (MVAs), accidental impacts and assaults. The direct and indirect costs of TBI are estimated to be \$60 billion annually (Finkelstein et al., 2006). TAI is a predominant injury in 40-50% of TBI cases requiring hospitalization in the United States and is associated with one-third of deaths in severe TBI (Meythaler et al., 2001). There is a need to develop a better understanding of axonal injury tolerance in TBI so that car crash dummies and finite element models can more accurately be used to design safety devices that reduce the consequences of both linear and rotational brain motion in vehicles crash or in sports impact.

TAI is an important consequence of severe brain injury. TAI results from tension or shear on the axons in the white matter tracts of the brain and is produced by rapid head acceleration/deceleration during blunt head impact as described in Chapter 2. Several previous studies examined the relationship between axonal injury and mechanical loading in species other than rat. Gennarelli et al. (1982) published one of the earliest studies on the relationship between mechanical response of the tissue and axonal injury in primates subjected to acceleration injury. They found the amount of TAI strongly correlated with the direction of the head angular motion, with motions about the coronal plane producing

highest TAI magnitude and duration of coma. Further studies suggested that increased TAI severity was related to rotational kinematics, including angular velocity (Meaney et al., 1995), angular acceleration (Margulies and Thibault, 1992) and duration of acceleration (Gennarelli et al., 1982) using non-impact rotational acceleration models. Anderson et al. (2003), using a sheep blunt impact acceleration model, suggested that the most reliable predictors for the extent of axonal injury were peak linear velocity and peak angular velocity.

However, studies aimed at correlating biomechanical responses with injury level in rat IA models are limited. Most previous studies assess TAI level based on drop height (Sawauchi et al., 2004; Czeiter et al., 2008; Vagnozzi, 2005) but do not quantify the mechanical response of the head. Results from our study showed that in spite of minimal variation in impactor velocity, biomechanical responses in rat head can vary widely within the same drop height. This may be related to small variations between the angle of impactor surface and the helmet surface, variations in head shape and size, eccentric line of action of the contact force, and thickness of the skull. On the other hand, assessing which characteristics of an impact (force, energy, acceleration etc.) best predict the risk of TAI is of particular importance in developing injury criteria used by regulatory agencies that provide standards in the design and manufacture of safety equipment and motor vehicles.

Therefore, a biomechanical model of traumatic axonal injury was developed in our lab (Chapter 5) to record various mechanical responses induced by this model and their correlation to TAI produced by this model. As part of this investigation, both linear and angular acceleration of rat head were measured, and injury-specific tolerance criteria

for TAI at different brain regions was established. Overall, this study provides further insight into the mechanical input that produces TAI and may aid in developing preventative strategies for brain trauma.

6.2 METHODS

6.2.1 Animal Handling and Preparation

Thirty-one anesthetized male Sprague-Dawley rats (392 ± 13 grams) were used. All rats were administered Buprenex (0.3 mg/kg) subcutaneously 20 minutes prior to impact. Fifteen minutes prior to impact, rats were placed in a sealed acrylic chamber. Anesthesia was induced and maintained by a mixture of Isoflurane (3%) and oxygen (0.6 L/min). The skull was then exposed by a midline dorsal incision of the skin and a round stainless steel disk (helmet) of 10 mm in diameter and 3 mm in thickness was positioned midline between bregma and lambda and affixed to the skull vault using cyanoacrylate (Elmer's Products, Columbus, OH). All animal surgical procedures were approved by Wayne State University Animal Care and Use Committee.

6.2.2 Instrumentation and Experimental Preparation:

The modified weight drop device previously described in Chapter 5 was used in this study to record various biomechanical parameters. Briefly, TBI was induced by dropping a custom-made 450 gram impactor housing a miniature accelerometer (Kistler 8044) (Fig. 6-1B, C) from a height of 1.25 m ($n = 15$) and 2.25 m ($n = 16$) respectively to induce mild or severe TBI (Fig. 6.1). The heights of 1.25 m and 2.25 m, although higher than those used in the original Marmarou model, were chosen to compensate for the loss

of velocity caused by the accelerometer cable dragging against the tube and the friction between impactor and the Plexiglas tube (Zhang et al., 2010a). At these increased heights, the actual impact velocities of 4.54 ± 0.06 m/sec and 6.14 ± 0.07 m/sec are close to the theoretical velocities of 4.43 m/sec and 6.26 m/sec, respectively from drop heights of 1 m and 2 m reported originally by Marmarou et al (1994). Linear and angular responses of the rat head were measured with an accelerometer (Endevco 7269) along the z axis and an angular rate sensor (DTS AR12k) in the yz plane glued to the skull approximately 5 mm anterior to the helmet using cyanoacrylate (Fig. 6-1D). The entire impact event was captured at 10,000 fps by a high-speed video camera (MotionXtra HG-100K) placed 0.5m away from the animal (Fig. 6-1E), and the image resolution in the yz plane was 0.41 ± 0.02 mm/pixel. Signals from all of the transducers were acquired at a sampling rate of 50,000 Hz using the TDAS1R4 data acquisition system (Diversified Technical Systems, Inc, Seal Beach, CA).

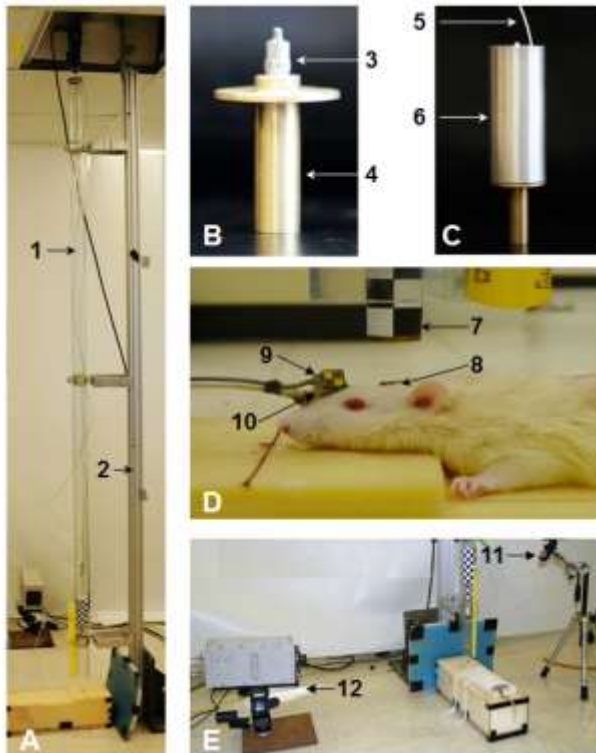


Figure 6-1: Diagrams of the modified impact-acceleration injury model and instrumentation setup. 1 = Plexiglas tube; 2 = aluminum pole; 3 = accelerometer (Kistler 8044); 4 = brass impact end; 5 = accelerometer cable; 6 = aluminum cylinder part of impact housing accelerometer; 7 = brass impactor end with tracking label; 8 = helmet; 9 = angular rate sensor (DTS AR12k); 10 = accelerometer (Endevco 7269); 11 = IR laser pointer; 12 = high speed camera (MotionXtra HG-100K HG-100k)

6.2.3 Induction of Traumatic Brain Injury

The instrumented animals were placed prone on an open-cell flexible polyurethane foam bed in pre-cured shape (12x12x43 cm, Foam to Size Inc., Ashland, VA) in a Plexiglas box under a 2.5 m long and 57 mm in diameter Plexiglas tube, with the helmet centered directly under the lower end of the tube. A laser beam was used to guide the positioning of the helmeted head to ensure that the impactor hits the center of the stainless steel disc (helmet) (Fig. 6-1E). Just prior to impact, the anesthesia was turned off and the rats were subjected to TBI by dropping the impactor from either 1.25 m or 2.25 m. Immediately after the impact, the Plexiglas box was manually removed to avoid a second impact to the rat head. After the removal of stainless steel helmet and the transducers, the skull was examined for fractures and then the skin was closed by staples.

6.2.4 Head impact data processing and analysis

The displacement of the impactor and the helmeted head in z direction were obtained digitally by tracking the attached target on the impactor using an image tracking software (ImageExpress MotionPlus, SAI, Utica, NY), since the impactor remained in close contact with the rat head during the impact. The velocity at the end of the initial acceleration pulse was calculated from both digitized video data and accelerometer curve. From the displacement-time histories of the helmeted head, the velocity (V) of the impactor and the helmeted head were calculated as the slope of displacement vs. curve. From the acceleration-time histories, the velocity (ΔV) of the head was calculated as the area under the curve of the initial acceleration pulse (Fig. 6-2A). A reliable measurement of the rat head motion was ascertained when the ΔV from accelerometer matched V from

the video tracking (within two standard deviation of the mean of V), indicating that the sensors were rigidly attached to the skull during impact.

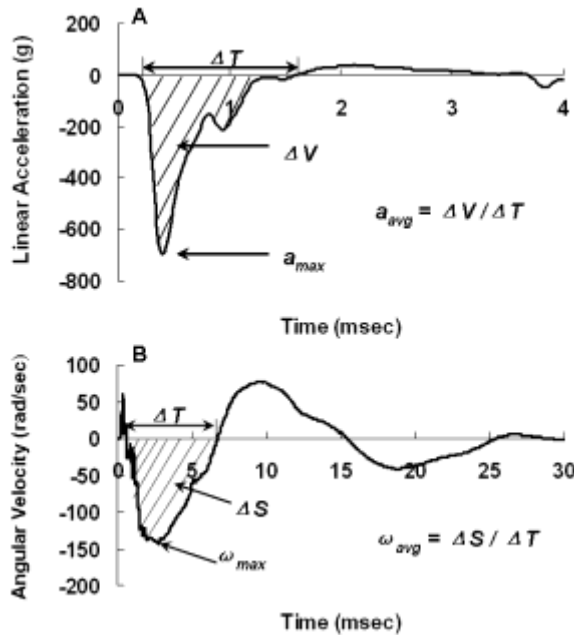


Figure 6-2: Diagrams illustrating data processing from accelerometer and velocity sensors. (A) Methodology for calculating peak and average linear acceleration from linear acceleration time history curve. (B) Methodology for calculating peak and average angular velocity from angular velocity time history curve.

Peak instantaneous linear acceleration a_{max} and average linear acceleration a_{avg} of the head were determined from the acceleration-time curve recorded from the head-mounted accelerometer. a_{max} was the maximum absolute value of the negative portion of the head acceleration curve, and a_{avg} was the area under the negative portion of the curve divided by the time interval of that portion (Fig. 6-2A). Peak angular velocity ω_{max} and average angular velocity ω_{avg} were determined from the angular velocity-time history curves. ω_{max} was the maximum absolute value of the negative portion of the curve (counter-clockwise rotation when rat nose tipping downward) and ω_{avg} was the area under the negative portion (ΔS , radians) divided by the time interval of that portion (Fig. 6-2B).

The angular velocity-time curve recorded from the angular rate sensor was filtered with SAE (Society for Automotive Engineers) Channel Frequency Class 1,000 Hz (SAE J211) and angular acceleration was obtained from the derivative of the angular velocity with respect to time. Peak α_{max} and average α_{avg} angular acceleration were then determined from the angular acceleration curve. α_{max} was the maximum absolute value of the negative portion of the curve and α_{avg} was the area under the negative portion of the curve (ΔV) divided by the time interval (ΔT) of that portion.

Head Injury Criterion (HIC) value was calculated using HIC software (UDS HIC, version: 1,2,4,5, NHTSA). HIC is widely accepted as a measure of head injury tolerance to translational mechanical impact and used by most regulatory agencies in assessing the safety of motor vehicles (Prasad and Mertz, 1985). The HIC is defined by the analytic expression:

$$HIC = \max_{t_1, t_2} \left\{ \frac{1}{(t_2 - t_1)^{3/2}} \left[\int_{t_1}^{t_2} a(t) dt \right]^{2.5} \right\} \quad (1)$$

where t_1 and t_2 are the initial and final time (in seconds) of the interval during which HIC attains a maximum value, and acceleration a is measured in g 's.

Power is an expression that is proportional to the rate of change of kinetic energy. In the equation below the mass term, which is considered constant, is removed and the equation reflects the rate of change of translational kinetic energy:

$$Power = \Delta V^2 / \Delta T \quad (2)$$

where ΔT is the time duration of effective acceleration, and ΔV is the change of velocity of the head in this period. Power provides the basis for a hypothesis that head injury

severity correlates to the magnitude of the rate of change of kinetic energy that the head undergoes during an impact (DiLorenzo, 1976; Newman et al., 2000).

Time to surface righting (SR) is the time spent by an animal to regain a normal ventral position after being placed on its back after impact. It is used as an indicator of duration of unconsciousness of rats (Adams 1986).

6.2.5 β -amyloid precursor protein (β -APP) immunostaining

After TBI, rats were allowed to recover and monitored for at least 6 hours. Rats with skull fracture or those exhibiting signs of severe distress were euthanized and were not used in this analysis. After a 24 h survival period, each rat was euthanized with an overdose of sodium pentobarbital (120 mg/kg, intra peritoneal) and exsanguinated. Rats were then transcardially perfused with heparinized (500 units/ml) normal saline followed by cold 4% paraformaldehyde in phosphate buffered saline (0.1 M PBS, pH 7.45). The brain was then carefully removed and post fixed (4% paraformaldehyde in 30% sucrose), after which the cerebral hemispheres were coronally cut into 40 μ m thick frozen sections from the genu of the CC (+2.3 mm anterior to the bregma (0.00 mm)) through the splenium of the CC (-5.2 mm posterior to the bregma) based on the rat brain stereotactic atlas (Paxinos and Watson, 2007, Figs. 6-3A, B). The rest of the cerebral hemispheres (-6.0 mm posterior to bregma) with the entire brainstem still being attached were processed for the analysis of TAI in the pyramidal tract. For this purpose, two bilateral longitudinal cuts were made in the brainstem ensured inclusion of regions encompassing midbrain, pons and pyramidal tract. Then serial sagittal sections of brainstem (40 μ m) were collected (Fig. 6-3A). All the coronal and sagittal sections

sections were individually placed in 1x PBS filled multi-well plates and stored at 4°C till further processing.

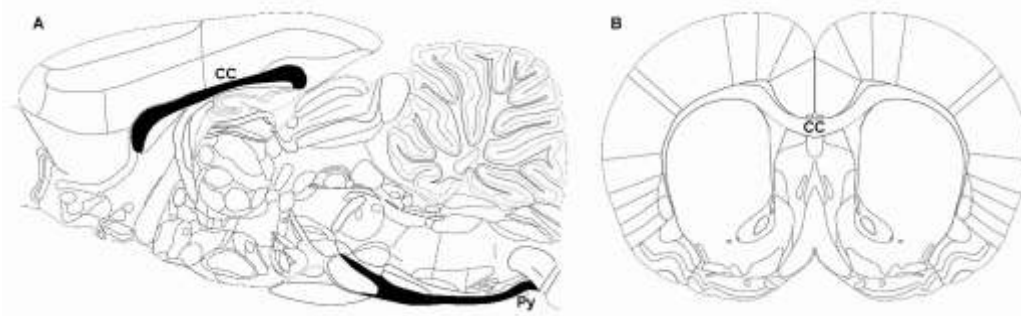


Figure 6-3: Illustration of corpus callosum (CC) and pyramidal tract (Py) in rat brain (highlighted in black). (A) Sagittal view demonstrating cut direction of Py; (B) Coronal view demonstrating cut direction of CC. Modified from Paxinos and Watson, 2007.

A set of successive coronal sections (13-15) spaced 0.48 mm apart were selected for investigating TAI in along the entire anterior to posterior aspects of corpus callosum. To assess TAI in pyramidal tract, a set of 7 sagittal sections, comprising midline (0 μm), $\pm 200 \mu\text{m}$, $\pm 600 \mu\text{m}$, $\pm 1000 \mu\text{m}$, were selected. These sections were processed for antigen retrieval by incubation in a citrate buffer (pH6.0) at 90°C for 1 h and then washed 3 times in 1x PBS and allowed to be cooled to room temperature. They were subsequently immersed in 0.3% H₂O₂ for 1 h to quench endogenous peroxidase activity. This was followed by an overnight incubation (at room temperature) in C-terminus specific APP (1 $\mu\text{g}/\text{ml}$; rabbit anti-C-terminus β -APP; cat #51-2700; Zymed, San Francisco, CA) antibody in 2% normal goat serum (Vector Laboratories, Burlingame, CA) and 1% bovine serum albumin. The following day, sections were washed 3 times for 5 minutes in 1x PBS and then incubated in goat anti-rabbit IgG secondary antibody (Vector Laboratories, Burlingame, CA) for 1 h. Sections were visualized via incubation in avidin biotin peroxidase complex (Vectastain ABC Standard Elite Kit, Vector Laboratories,

Burlingame, CA) and were developed by brief incubation in 3, 3'-diaminobenzidine (DAB) and hydrogen peroxide. Finally, the sections were washed, dehydrated and cover-slipped using Permount. Negative control incubations were performed in the absence of primary antibody.

6.2.6 Quantitative analysis of TAI

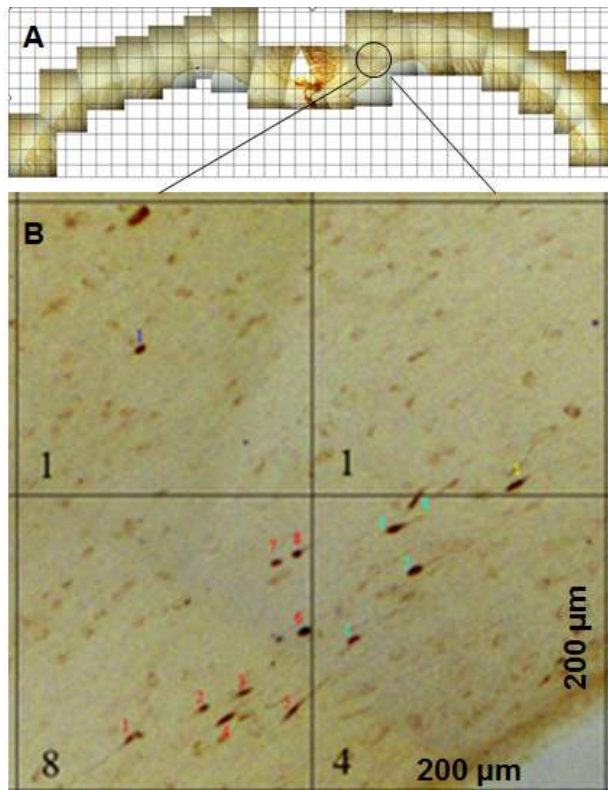


Figure 6-4: A representative panoramic view of corpus callosum used to quantify β -APP reactive (+) axonal (arrow) profiles. The number at left lower corner indicates TAI count in each box.

The total number of β -APP reactive axonal swellings and retraction balls (considered as total TAI counts) in CC or Py from all stained sections from each animal were quantified by a blinded observer. Each section was observed under a light microscope (Leica DMLB, Leica Microsystems Ltd, Heerburg, Switzerland) to visualize β -APP reactive axonal swellings and retraction balls. Then serial photomicrographs (x10 magnification) encompassing the whole CC or Py structure were taken with a digital

camera system (ProgRes C7, JENOPTIK Laser Optik Systeme, GmbH) for each section. These photomicrographs were taken at a single focal plane and were combined into a single panoramic image using Photoshop CS2 (Adobe Systems Incorporated, CA). Then grids measuring 200 x 200 μm were superimposed on each constructed panoramic image (Fig. 6-4). This enabled a direct correlation of the number of retraction balls and swellings to the level of mechanical strain in corresponding elements of the same resolution ($\sim 200 \times 200 \mu\text{m}$) in an anatomically detailed finite element (FE) model of the rat head (Zhang et al., 2010, 2011b). All β -APP reactive swellings and retraction balls in each grid were counted using ImageJ software (<http://rsb.info.nih.gov/ij/>), and added to obtain total TAI counts per section. The total TAI in CC or Py for each rat was the sum of TAI from panoramic images of all stained sections. In order to compare TAI level between rats with different section numbers, TAI counts were normalized based on equation 3. 14 was used as a normalizing constant in CC, since the majority of rats (18 out of 31) had 14 coronal sections. Similarly, 6 was used as the normalizing constant in Py, since 16 out of 28 rats had 6 quantified sagittal sections. The potential reason for variability in the number of sections stained may be related to minor variations in the selection of first section (starting after disappearance of forceps minor and beginning of genu of CC) and the last section (at end of splenium and appearance of forceps major), resulting in some variation in the total length of CC longitudinally. In addition, small variations in the volume and dimensions of rat head and brain may contribute to small variations in length of CC.

$$\text{Normalized TAI} = (\text{Total TAI} / \text{Number of section}) \times \text{Normalizing constant} \quad (3)$$

6.2.7 Statistical analysis

Given values are presented as mean \pm standard error of the mean (SEM). A p value < 0.05 was considered to be statistically significant.

Logistic regression is a form of regression which is used when the dependent variable is a dichotomy and the independent variables are continuous, categorical, or both. Logistic regression estimates the probability of occurrence for a given event. In this study, a logistic regression analysis was conducted to determine strong injury predictors and to establish injury tolerance or criterion for severe TAI. To form the regression model, the dichotomous dependent variable was the occurrence of severe TAI after impact. In the Marmarou model, the 2 m drop height is considered to lead to severe TAI because of the high mortality rate (Marmarou, et al. 1994). The axonal injury in this group can be categorized as having a grade 3 diffuse axonal injury (Adams, et al., 1989), where axonal abnormalities were more global and included the cerebellum as well as hemorrhages in the brain stem. Similarly in our tests, the 2.25 m drop height produced the highest levels of TAI and the longest time for surface righting. Therefore the critical value of severe TAI was determined as the lower limit (LL) of 95% confidence interval of normalized total TAI count in 2.25 m impact group, defined as:

$$\text{Lower limit} = \text{Mean} - t(\alpha, N - 1) * s / \sqrt{N} \quad (4)$$

where $t()$ is the test statistic, N is the sample size, α is the desired significance level, which is 95% in our case and s is the sample standard deviation. All rats with TAI number higher than the LL were grouped into category 1. All rats with TAI number lower than the LL were grouped into category 0.

The independent variables tested were: peak and average head linear and angular accelerations, peak and average head angular velocities, HIC, Power and time to surface righting. Various univariate and multivariate models were assessed to find a single predictor variable, or a combination of the variables, which best explained the data. To determine whether relationships between outcome and the predictor variables were statistically significant, -2Log Likelihood ratio, Wald Chi-Squared and H-L test were performed.

Receiver operating characteristic curve (ROC) analysis and area under ROC were also used to assess and compare the outcome prediction performance between single and paired combinations. The optimal threshold (specificity and sensitivity) for each individual and paired predictor was determined, which was defined as the point closest to the left upper corner of the ROC curve. The Logistic analysis and ROC analysis were performed using SPSS 13 (SPSS Inc. Chicago, Illinois).

6.3 RESULTS

6.3.1 Head Kinematics

The measured or calculated mechanical responses and post-injury behavior from 1.25 m and 2.25 m impacts are summarized in Table 6-1. The biomechanical and behavior responses were significantly different between the 1.25 m and 2.25 m groups ($p < 0.05$), except peak linear acceleration and peak angular acceleration ($p > 0.05$).

Table 6-1: Mechanical Responses of Rat Head in 1.25m & 2.25m Weight Drop

Test	Linear Biomechanical Responses, <i>mean</i> \pm <i>SEM</i>						Angular Biomechanical Responses, <i>mean</i> \pm <i>SEM</i>				Behavior
	Peak Linear Acc. (g)	ΔV (m/s)	ΔT (ms)	Average Linear Acc. (g)	Power (m ² /sec ³)	HIC	Peak Angular Vel. (rad/sec)	Average Angular Vel. (rad/sec)	Peak Angular Acc. (krad/sec ²)	Average Angular Acc. (krad/sec ²)	
2.25m (n=16)	855 \pm 118	5.29 \pm 0.23	2.27 \pm 0.27	296 \pm 41	14.59 \pm 1.72	4612 \pm 1031	132 \pm 11	67 \pm 5	187 \pm 14	80 \pm 7	24 \pm 2
1.25m (n=15)	660 \pm 44	3.96 \pm 0.19	3.10 \pm 0.34	153 \pm 12	5.69 \pm 0.36	1911 \pm 239	95 \pm 6	47 \pm 4	169 \pm 10	51 \pm 8	16 \pm 1

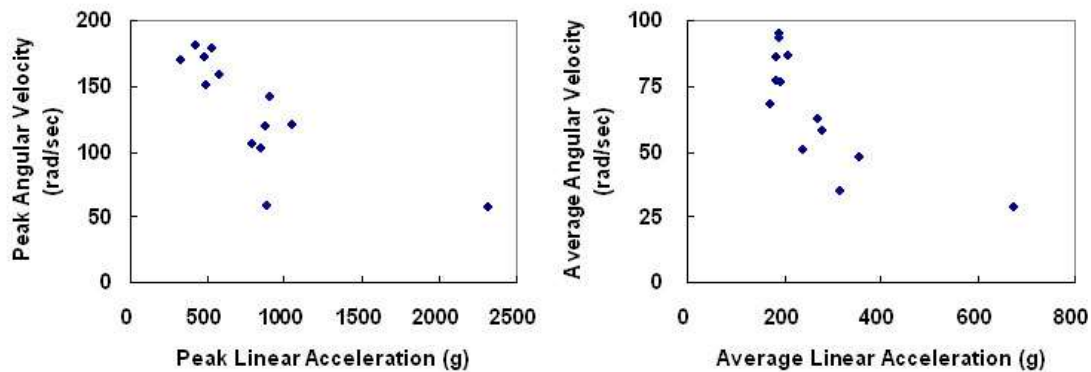


Figure 6-5: Correlation between linear component and angular component of head response in 2.25 m impact.

Both linear and angular responses had large variation. In 2.25 m drop, the peak linear acceleration and average linear acceleration ranged from 321 to 2313 g and 172 to 711 g, respectively. The peak angular velocity and average angular velocity ranged from 58 to 181 rad/sec and 29 to 95 rad/sec, respectively. But the linear responses showed a negative relationship pattern with angular responses (Fig. 6-5), although they had no statistical significant correlation ($p = 0.27$), suggesting the total energy transferred to rat head during impact was similar at the same drop height.

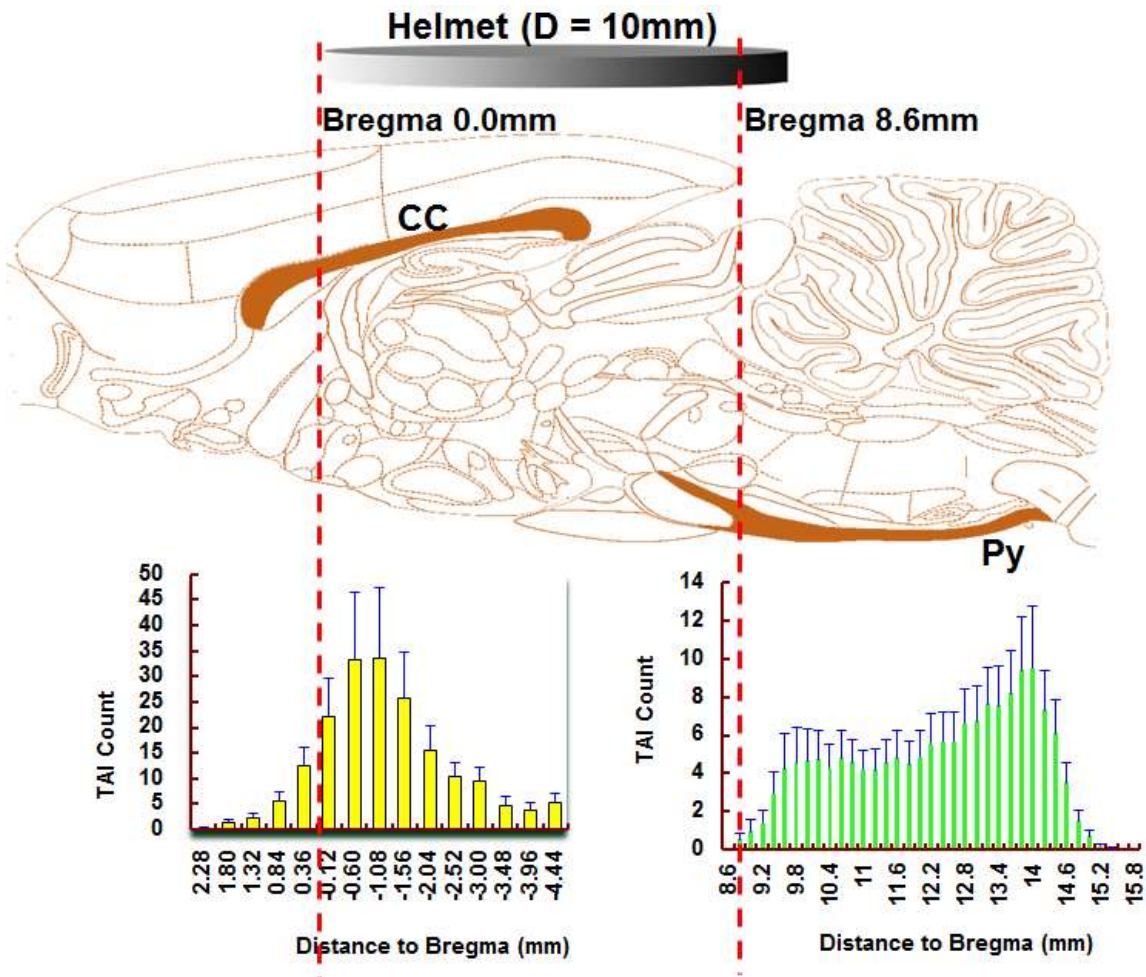


Figure 6-7: TAI distribution along the rostro-caudal direction in 2.25 m impacted rats. Relative position of the 10mm diameter helmet is also shown. The bar charts show average TAI number at given anatomical locations along the rostro-caudal direction in CC and Py.

The spatial profiles of TAI maps revealed a non-uniform distribution longitudinally along the CC, with the area directly under the helmet, in particular from 0.12 to 2.04 mm posterior to bregma, showing higher density of TAI (Fig. 6-7A). TAI maps also indicated a non-uniform distribution in Py, with the most caudal region of the pyramidal tract representing high levels for TAI (Fig. 6-7B).

6.3.3 Injury predictor for severe TAI

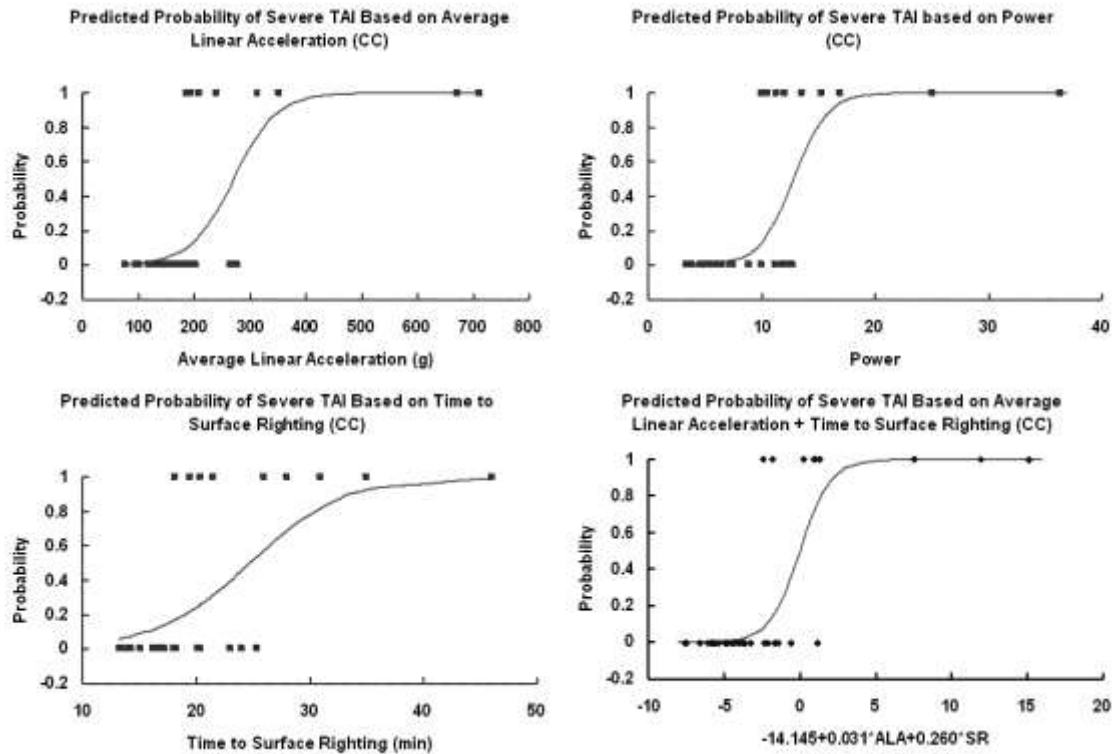


Figure 6-8: Logist plots of the predicted severe TAI probability in CC based on average linear acceleration (A), power (B), and time to perform surface righting (C).

The injury predictors for severe TAI evaluated in this study were biomechanical parameters, including existing head injury criteria, and post-injury behavior. Single and paired potential predictors were tested in CC and Py, respectively. In CC, 8 out of 16 rats in 2.25 m impact had severe TAI, whereas none of the 1.25 m impact rats had severe TAI. The best single predictor for severe TAI was the average linear acceleration, followed by the Power Index and time to surface righting (Appendix Table A1). The estimated average linear acceleration levels were 228, 270, and 325 g for 25%, 50%, and 80% probability of severe TAI (Fig. 6-8). The combination of average linear acceleration plus time to surface righting showed improved predictive ability than any

individual predictor. A multivariate model using these two combined predictors achieved an area under the ROC curve of 0.949, compared to 0.889 for average linear acceleration and 0.823 for time to surface righting. The optimal specificity and sensitivity of this model for severe TAI were 88.9% and 90.9%, respectively (Fig. 6-9).

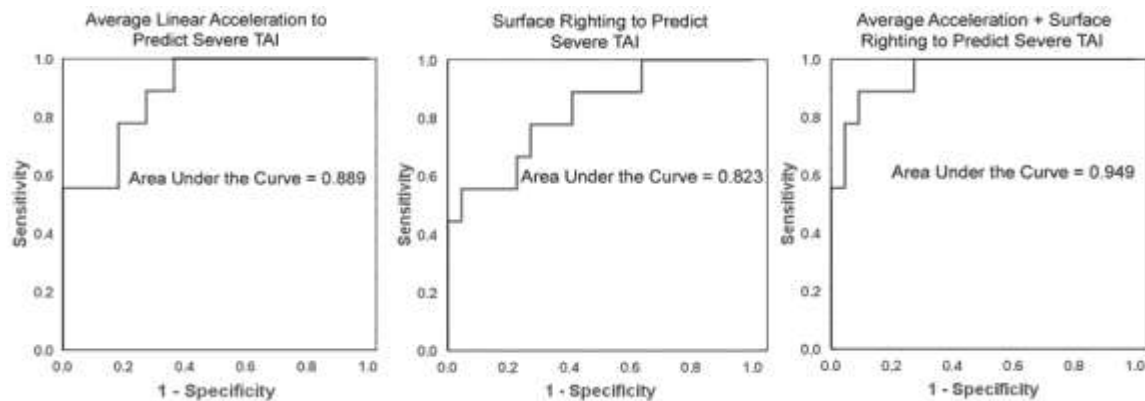


Figure 6-9: Specificity and sensitivity for predicting severe TAI in CC. The highest outcome predictive value for severe TAI was achieved when average linear acceleration was paired with time to surface righting.

In Py, 7 out of 16 rats in 2.25 m impact had severe TAI, whereas none of the 1.25 m impact rats had severe TAI. Angular components of head kinematics showed better predictive results than linear components. The occurrence of TAI was best predicted by time to surface righting, followed by peak angular velocity and average angular velocity (Appendix Table A2). The estimated peak angular velocity levels were 133, 154, and 180 rad/sec for 25%, 50%, and 80% probability of severe TAI (Fig. 6-10). The combination of peak angular velocity plus time to surface righting slightly improved the predictive results. The multivariate model achieved an area under the ROC curve of 0.898, compared to 0.881 for peak angular velocity and 0.818 for time to surface righting. The optimal specificity and sensitivity of these two combined predictors for severe TAI were 78.2% and 87.5%, respectively (Fig. 6-11).

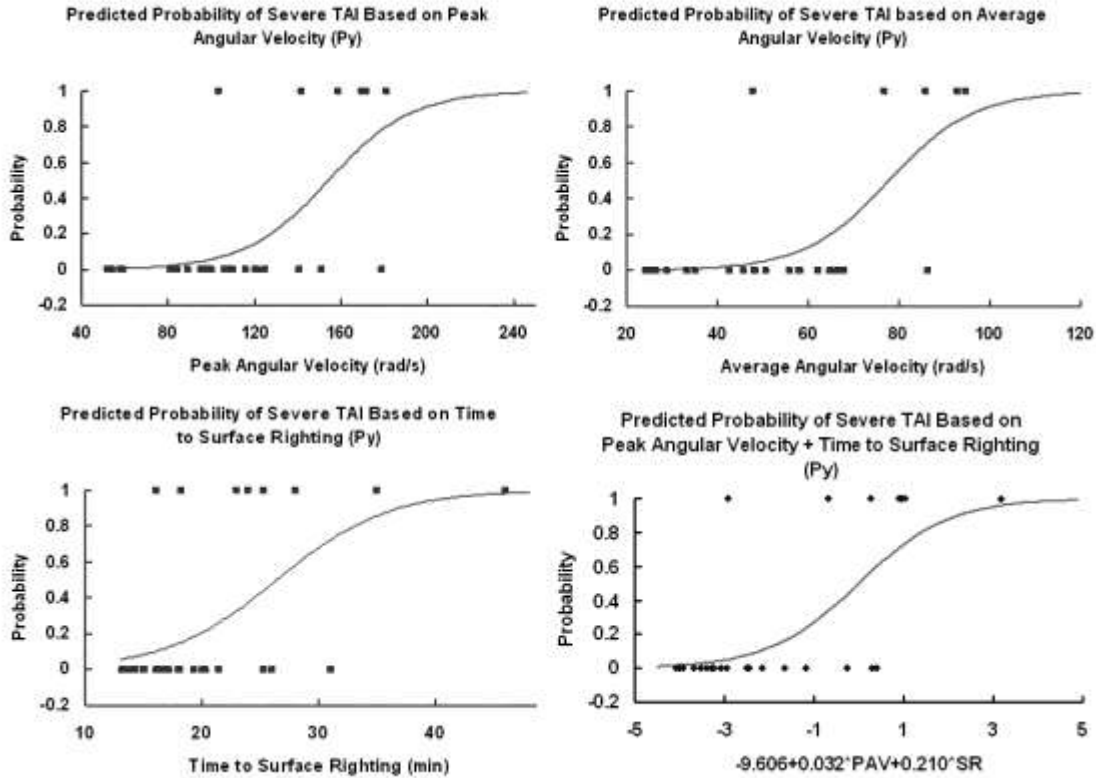


Figure 6-10: Logist plots of the predicted severe TAI probability in Py based on peak angular velocity (A), average angular velocity (B), and time to perform surface righting (C).

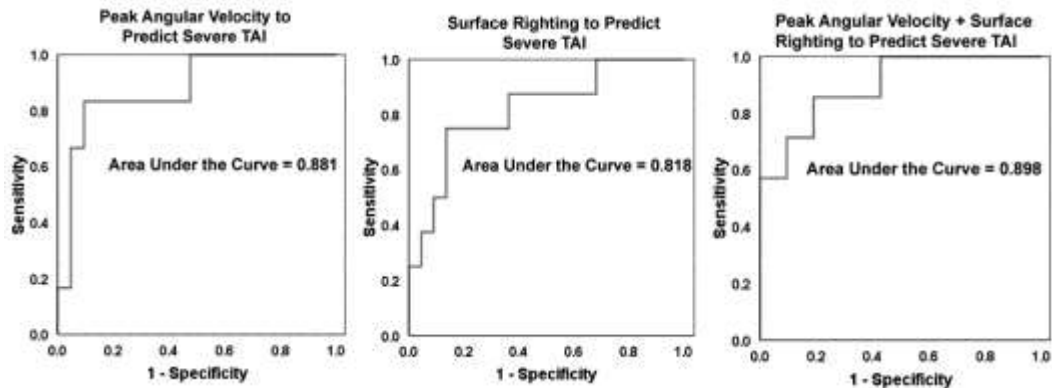


Figure 6-11: Specificity and sensitivity for predicting severe TAI in Py. The highest outcome predictive value for severe TAI was achieved when peak angular velocity was paired with time to surface righting predictor.

A predictor for severe TAI in both brain regions can be determined by defining the dependent variable as “1” in logistic model if severe injury occurred in either CC or

Py. By this definition, 11 out of 16 rats in 2.25 m impact had severe TAI, whereas none of the 1.25 m impact rats had severe TAI. In terms of univariate models, power showed best predictive result, followed by time to surface righting. There was also statistically significant relationship between TAI and average linear acceleration, average angular acceleration, peak angular velocity, average angular velocity (Appendix Table A3). The critical value of all potential predictors to predict 25%, 50%, and 80% probability of severe TAI are summarized in Table 2. However we observed that the risk curve for prediction using power is much steeper than that of other single predictors, which indicate it is a more sensitive predictor of severe TAI in CC and Py combined (Fig. 6-12). The paired predictors were tested using the multivariate model. The combination of power and time to surface righting, as well as average linear acceleration and average peak velocity showed better predictive results than other combinations (Appendix Table A3). The combined power and time to surface righting achieved an area under the ROC curve of 0.943, compared to 0.904 for power and 0.818 for time to surface righting. The optimal specificity and sensitivity of these two combined predictors for severe TAI were 89.5% and 91.7%, respectively (Fig. 6-13A). The combination of average linear acceleration and average angular velocity achieved an area under the ROC curve of 0.928, compared to 0.833 for average linear acceleration and 0.739 for average angular velocity. The optimal specificity and sensitivity of these two combined predictors for severe TAI were 83.3% and 90.0%, respectively (Fig. 6-13B).

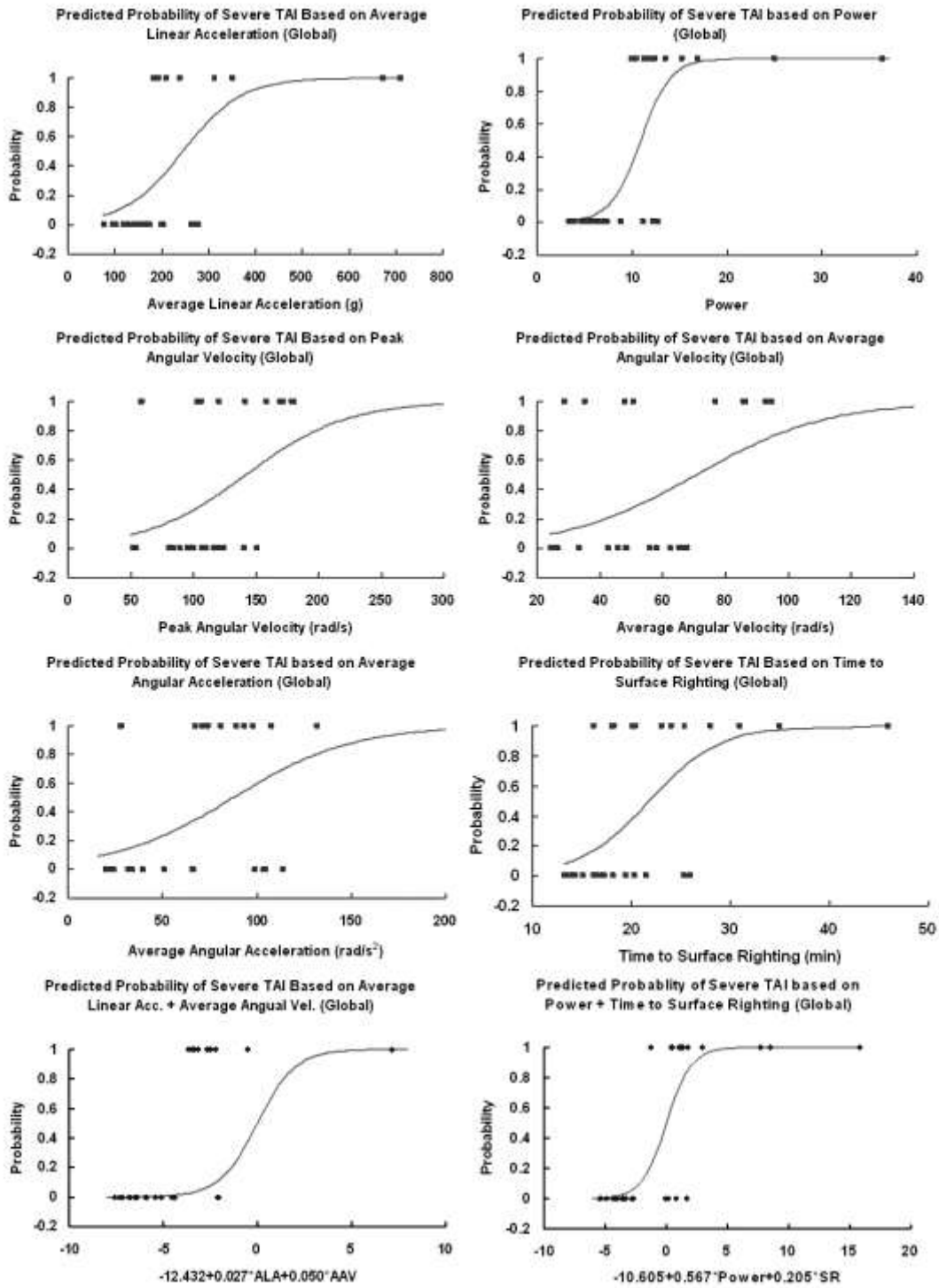


Figure 6-12: Logist plots of the predicted severe TAI probability in combined CC and Py brain regions based on average linear acceleration (A), power (B), peak angular velocity (C), average angular velocity (D), average angular acceleration and time to perform surface righting (E).

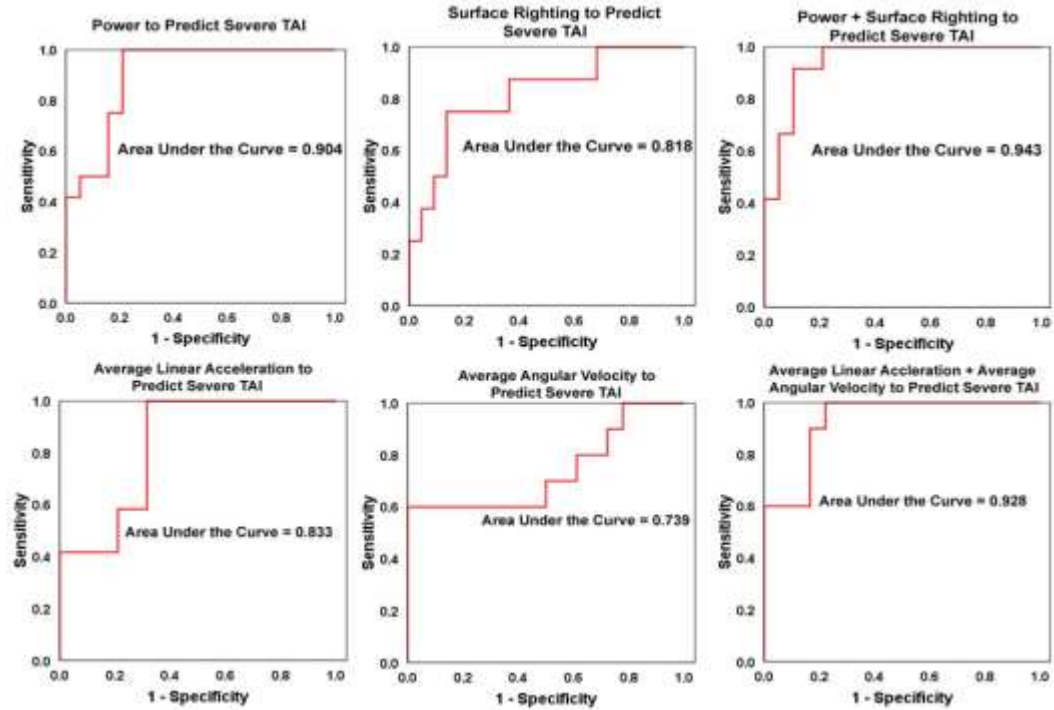


Figure 6-13: Specificity and sensitivity for predicting severe TAI in combined CC and Py brain regions. The highest outcome predictive value for severe TAI was achieved when power was paired with time to surface right, as well as average linear acceleration was paired with average angular velocity.

Table 6-2. Critical values of all potential predictors to predict 25%, 50%, and 80% probability of severe TAI in global brain.

Predictor	Injury Probability		
	25%	50%	80%
Power (m^2/sec^3)	9.2	10.9	13.1
Surface Righting (min)	16.9	21.8	26.7
Average linear Acc (g)	156	245	332
Peak Angular Vel (rad/s)	87	142	198
Average Angular Vel (rad/s)	42	71	100
Average Angular Acc (rad/s ²)	44	88	131

6.3.4 Injury tolerance for severe TAI

Logistic regression analysis described above shows that TAI severity correlates not only to the magnitude of acceleration but also to how long the acceleration is applied. Also both linear and angular acceleration contribute to TAI production during an impact. In order to develop the injury tolerance curve for severe TAI, two independent approaches were employed. Firstly, the combination of average linear acceleration and the duration of effective acceleration were plotted to define the asymptotes of the tolerance curve (Fig. 6-14A). The expression $a^2T = 100$, which is in a similar form of an approximation of WSTC, reasonably separated the injury and non-injury data. The tolerance curve has a straight line with a negative slope of 2, which is the exponent in the expression, if it is plotted on a log-log scale (Fig. 6-14B). It suggests short pulses of high acceleration can produce TAI and lower accelerations require longer pulses to produce TAI in rat, similar to the relationship for head injury tolerance in humans based on WSTC and HIC. Loads above this tolerance curve would be capable of producing severe TAI.

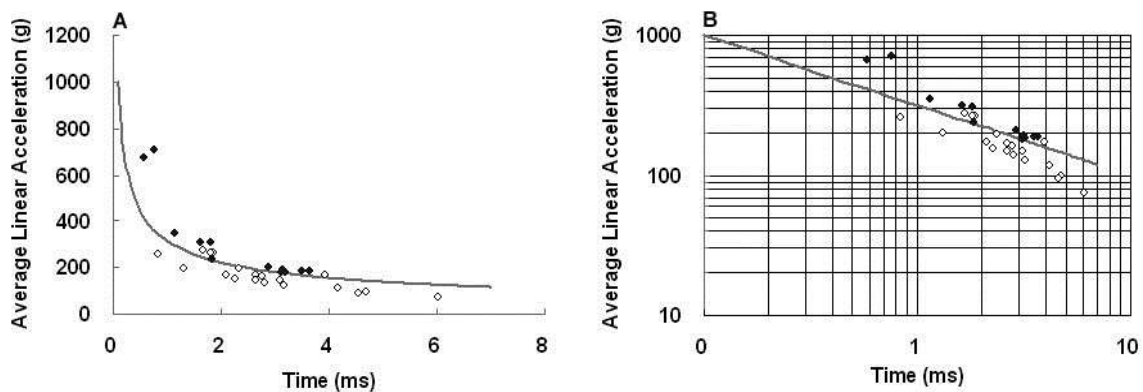


Figure 6-14: Severe TAI tolerance for rat head impact based on average linear acceleration and time duration. Solid points represented rats with severe TAI (category 1 in logistic regression), hollow points indicated mild or no injury (category 0 in logistic regression).

A second consideration was an injury tolerance curve based on average linear acceleration and average angular velocity (Fig. 6-15A). This curve showed that the brain can tolerate higher linear accelerations if the angular velocity was lower, and vice versa. The tolerance curve is expressed by expression $a^2\omega=15000$, which represents a threshold of severe TAI in a closed rat head impact model. Similarly, the exponent 2 in the expression was determined in the log-log plot (Fig. 6-15B).

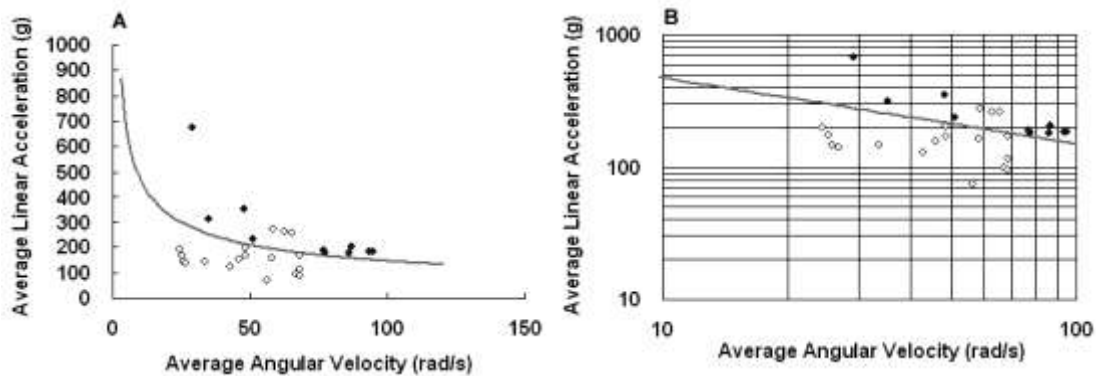


Figure 6-15: Severe TAI tolerance for rat based on average linear acceleration and average angular velocity. Solid points represented rats with severe TAI (category 1 in logistic regression), hollow points indicated mild or no injury (category 0 in logistic regression).

6.4 DISCUSSION

6.4.1 Model development

Development of injury criteria for TAI is difficult because the cause of injury is often unknown, and the pathology is difficult to quantify using current imaging techniques. In cadaver studies, true neurological injury is not produced. Therefore, animal models are useful to validate TAI criteria. The Marmarou IA model is one of the most widely used preclinical models to study diffuse brain injury using rats. The lack of control over precise conditions of impact can result in a high degree of variability in this model, making injury response challenge to replicate between different investigators and

laboratories (Piper et al., 1996; Cernak, 2005; Wang et al., 2010; Li et al., 2011). As part of the current study, the model was modified and expanded to monitor velocity, displacement into the foam, head kinematics and post-injury behavior of two different impact severities.

A more detailed quantification of TAI in CC and Py was undertaken in this study than in previous studies using the Marmarou AI device. Smith and Meaney (2000) showed that the pattern of axonal damage in the white matter is more accurately described as ‘multifocal’. Therefore TAI from a limited number of selected locations may not be an accurate representation of injury profiles in the entire CC. Utilizing the quantified data from multiple sections across white matter tracts as in our study, 3D injury maps were constructed for the entire CC and Py. Furthermore, the spatial profiles of TAI maps revealed non-uniform distribution longitudinally along the CC and Py, enabling further investigation of injury biomechanics during impact at different brain region.

The modified injury model quantitatively monitors the inherent mechanical response variability during an impact acceleration event. The comprehensive map of axonal damage throughout the CC and Py makes it possible to establish more accurate TAI criteria. These detailed injury data and biomechanical response can be used as references for future studies both in animals as well as in finite element simulations to develop tissue level injury criteria.

Because of the small size of the rat head, one limitation of this study was that only one accelerometer was used to record the linear head acceleration. Since the linear acceleration was measured in the local frame, it is not exactly the acceleration in the

laboratory vertical axis, which is the cosine of actual measurement due to rotation. However, in current study, this error is relatively small, and can be neglected. During initial linear acceleration pulse, the rat head rotated 7.2 (± 6.0) and 5.3 (± 3.1) degree, respectively, for 2.25m and 1.25m impacts. Thus the error levels of linear acceleration are approximately 0.8% ($\pm 0.5\%$) and 0.4% ($\pm 0.1\%$). Another potential limitation is the accelerometer was not located at the center of gravity (C.G.) of the head and thus is not the acceleration at the C.G. Ideally, two accelerometers placed on the rat head at equal distance anterior and posterior to the C.G. could be used to calculate the linear acceleration at C.G. But there is not enough bony area posterior to ensure a rigid attachment of accelerometer in practice. Future tests will include a tri-axial angular rate sensor to capture the head kinematics in all axes, and therefore the resultant acceleration at surface can be transformed to the C.G..

This study focused on impaired axoplasmic transport (IAT) by analyzing β -APP immunoreactivity of axons. IAT does not represent all the injured axons. Mechanistic insults to the brain may initiate other cellular changes in neurons (Geddes-Klein, et al. 2006). These changes include impaired restoration of ion homeostasis (Stiefel, et al. 2005), increased intracellular free calcium levels, increased extracellular potassium levels (Reinert, et al. 2000), or the promotion of cytokine production (Hadjigeorgiou, et al. 2005; Woiciechowsky, et al. 2005), which in turn lead to necrosis, apoptosis or both. Therefore, additional staining methods targeting other cellular events in the future will help us fully understand the relationship between mechanical input and the subsequent cell death after TBI.

6.4.2 Injury mechanics in different brain regions

TAI can result from angular as well as linear acceleration of the head (Gennarelli et al., 2003; McLean, 1995; King, 2000; Zhang et al., 2001b). However, there is debate on what role the linear or angular accelerations play during impact. Several studies have proposed angular acceleration as the main condition responsible for TAI (Gutierrez et al., 2001; Smith et al., 2003; Zhang et al., 2006), and TAI tolerance based on angular acceleration was proposed (Margulies et al., 1992). Others suggested that high non-impact rotational acceleration alone may not be sufficient to produce TAI (Prange et al., 2003), and showed by FE stimulation that linear acceleration can also induce TAI (Nishimoto et al., 1998). In this model, the center of the impact was not perfectly in the center of gravity of the brain; hence the brain was exposed to a combination of linear and angular accelerations. Our study suggested that TAI in different brain regions may result from different mechanical input and loading modes. One factor that causes the TAI in CC could be the strain in the cortical tissue under the impact site, which is caused by the depression in its superficial layers. Marmarou et al. (1994) reported that the skull undergoes a maximum of 0.3mm deflection during a 2 m impact. Pai et al. (2006) found axonal injury in well-defined areas of cortical layers IV and V under the impact site using their weigh drop model. Since the axons in CC run perpendicular to the impact force vector, a sudden stretch in the cortical tissue under impact site may contribute to the development of the axonal damage. Another significant factor to consider is intracranial pressure. Sudden increase in intracranial pressure at the impact site of the brain has been reported previously (Denny-Brown and Russell, 1941) in experimental cerebral concussion. Manley et al. (2006) showed intracranial pressure immediately increased

following controlled cortical impact and the value increased with increasing depth of depression. Zhang et al. (2004) indicated intracranial pressure had the highest correlation with translational acceleration, while strain had the highest correlation with rotational acceleration in their FE analysis. In a dynamic cortical deformation model, sudden changes in intracranial pressure were reported to cause morphological damage to the rat brain and causing the axonal damage. These axonal injuries were observed in the subcortical white matter and in the ipsilateral internal capsule, but not in the contralateral hemisphere or in any remote regions (Shreiber et al., 1999). These studies suggest that in the current study increased pressure under the impact site may be related to the higher density of TAI in the CC region directly under the helmet (Fig. 6-7).

Interestingly, previous studies (Witelson, 1989; Hofer and Frahm, 2006) in the human brain showed that the axonal fibers with a relatively small diameter are most pronounced in the anterior and posterior third of the CC and fibers with a larger diameter are more frequent in the midbody of the CC and gradually reduce laterally. The distribution of larger diameter axon is somehow in agreement with the distribution of β -APP stained axon after injury (Fig. 7). This finding might suggest that the thick axonal fibers are more sensitive to rapid head acceleration compared to thin fibers.

Secondly, the bundles of neural fibers in CC connect the left and right cerebral hemispheres, and pass through the mid-sagittal plane vertically (Xu et al., 2002; Hofer and Frahm, 2006), parallel to the axis of sagittal rotation. Thus the induced tensile forces by rotation aligning with the axonal fiber orientation were expected to be small. Similar observation was found by Gutierrez et al. (2001) in their rabbit's rotational acceleration model to study diffuse brain injury. They indicated that the astrocytosis was absent in the

corpus callosum after injury, since the rotation was in the sagittal plane. Therefore, linear acceleration showed higher predictive value for TAI in CC.

On the other hand, the Py is located on the ventral aspect in the brainstem, between the cerebral cortex and the spinal cord. In sagittal plane rotation, the caudally projecting axons in brainstem are perpendicular to the axis of rotation in the Marmarou impact model, producing greater tensile strains and shear forces compared to the CC. The correlation of TAI in Py to angular velocity/acceleration is consistent with this mechanism of loading to the brainstem. Smith et al. (1997) reported that axonal injury was primarily found in the brainstem, the only region in which severe axonal damage was demonstrated following head rotation in pigs. Sheng et al. (2000) also suggested that the axonal injuries were most severe in the brainstem in their rat's lateral head rotation model. These results indicate that the combined linear and angular accelerations may produce higher TAI than linear or angular acceleration alone. The preliminary simulation of rat head impact using a new rat head FE model showed relatively moderate principal strain in the CC compared to that on the brainstem region (Zhang et al., 2010, Zhang et al., 2011b). The role of tissue level biomechanical correlates to TAI occurrence and severity in various regions needs further FE analysis in this TBI model. Taken together, our study provides further understanding of the contributions of linear and angular response to traumatic brain injury. These findings indicate that different impact sites, the direction of linear acceleration and the axis of head rotational acceleration may result in different TAI distributions and injury types. Thus, TAI is not necessarily a diffuse injury (Smith and Meaney, 2000), but rather a reflection of the mechanism of loading to the brain.

6.4.3 Head kinematics-based predictors for severe TAI

Previously, several tissue-level injury tolerance criteria were proposed to predict TAI. These measures of injury include pressure (Ward et al., 1980; Gennarelli et al., 1982; Deck et al., 2008), von Mises stress (Zhang et al., 2004; Deck et al., 2008), maximum principal strain (Strich 1961; Margulies et al. 1992; King et al., 2003; Zhang et al., 2003; Bandak and Eppinger, 2005; Viano et al., 2005; Kleiven et al. 2007), and angular motion (Margulies et al., 1992; Maxwell et al., 1993). However the details of the motion in most of the previous studies have been derived from accident reconstructions or national football league (NFL) data where there is always a degree of uncertainty whether the data accurately represent the mechanical response of the head in the accident. Newman et al. (2005) reported a potential error in the relative velocities of the NFL data of 11% as well as maximum errors of 17% for the linear accelerations and 25% for the angular accelerations. Secondly, some previous studies used concussion as an indicator of mild TAI as it was difficult to detect the structural signature of TAI in humans. However, our model is not constrained by such limitations and provides an accurate comparison between mechanical parameters and the observed brain pathology.

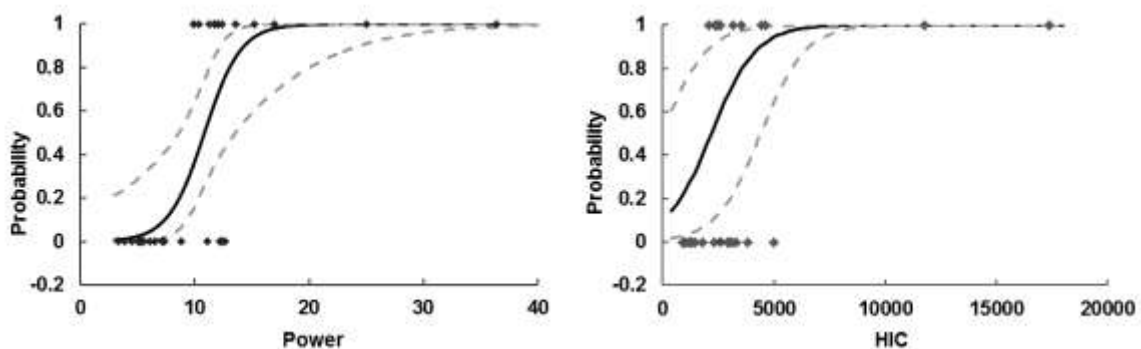


Figure 6-16: Logist plots of the predicted severe TAI probability in combined CC and Py brain regions based on Power and HIC. The dot line shows the 95% confidence intervals.

In our study, the loading condition was well characterized, and the biomechanical responses were measured directly from head motion. Furthermore, our quantification technique enabled us to correlate potential predictors to the actual magnitude of TAI pathology. Based on logistic regression analysis, power, as a function of average linear acceleration and duration, was the best single predictor for severe TAI. It has better predict value (Table A3) and narrower confidence intervals (Fig. 6-16) compared to HIC, which is used by most regulatory agencies as a criteria in assessing TBI. This finding suggested an alternative injury predictor specific for TAI is needed in designing safety measures either in vehicles or in sports helmets. However, considering the difference of brain structure between rat and human, and the limitation in HIC calculation described previously, more work is required to justify this conclusion.

Our results also provided the possibility to establish a TAI tolerance curve based on both linear and angular velocity/acceleration (Fig. 6-15). In addition, we proposed that combined biomechanical and behavior responses could achieve better predictive value for severe TAI for the first time. Glasgow Coma Scale (GCS), which is also an indication of the physiological state of the patient after injury, has been frequently used to predict the severity of TBI (Teasdale and Jennett, 1974; McNett, 2007). However, a low GCS score does not always accurately predict the outcome of severe TBI (Lieh-Lai, et al. 1992). Gill et al. (2004) showed only modest agreement between ED staffs assessing GCS. The GCS has also been criticized from a purely mathematical point of view by Bhatti and Kapur (1993). By combining with the mechanical inputs when possible, the GCS, as well as other scoring systems assessing behavior after TBI, may achieve better

predictive results regarding recovery and may provide further information on injury mechanisms and guide treatment selection.

One of the limitations of logistic regression and ROC analysis is that the data must be divided into two states. Since the TAI counts in our study are on a continuous scale, the selection of the cutoff value separating severe and non-severe TAI is crucial. The ROC area may vary as the cutoff varies. Another possible limitation of our study is the sample size. Logistic regression usually requires large samples (Bland, 2000), at least 10 in each category (Peduzzi et al., 1996). The sample size of ROC analysis must also be large enough for the effects to be real and significant (Beck, 1986). In our study, the injury cases in either CC or Py are less than 10, although injury cases exceeded 10 when combining both regions to identify predictors of combined injury. In addition, more data points are required to establish a more reliable injury tolerance curve (Fig. 6.14A, 6.15A). It should be emphasized that the head rotation occurring in the current rat head impact model was predominately in the sagittal plane. The complex multi-planar motions often seen in real-world cases can induce different distributions of injury location from a non-uniform head impact. A thorough investigation of TAI responses from a combination of translational and rotational acceleration in three-dimensional fashion is needed before a generalized mechanical threshold can be determined with high confidence.

CHAPTER 7

CORRELATION BETWEEN BIOMARKERS AND TRAUMATIC AXONAL INJURY

7.1 INTRODUCTION

Traumatic axonal injury (TAI) accounts for 40-50% of the 500,000 new cases of traumatic brain injury (TBI) each year and is responsible for one third of mortalities resulting from TBI (Meythaler et al., 2001). Current research has identified TAI to be an ongoing process, in which the mechanical forces that cause axonal deformation also induce continued biological responses (Gennarelli et al., 1998; Povlishock, 1995). The gradual degeneration of the axon suggests that TAI could be treated therapeutically (Büki and Povlishock, 2006; Sandler et al., 2010). To accurately determine various treatment options and to assess the risk for continued axonal degeneration, a clear diagnosis and prognosis of TAI is essential. However, considering the microscopic nature of this type of injury, current imaging modalities are limited in their capabilities to sufficiently diagnose TAI (Gennarelli et al., 1998; Sandler et al., 2010) and leaving a need for improved sensitive diagnostic methods.

A growing number of biomarkers in serum and CSF have been studied and proposed for assessing brain injury (Wang et al., 2005; Berger et al., 2007; Sandler et al., 2010; Dash et al., 2010). Although many biomarkers have been investigated and proven to reflect some quantitative association with TBI severity, secondary pathologies and patient outcomes, and issues of specificity and sensitivity of individual biomarker persist (Pineda et al., 2004; Siman et al., 2004; Dash et al., 2010). This has lead researchers to

investigate panels of biomarkers that may be appropriate for assessing TBI (Berger et al. 2005, 2008, Lo et al. 2009, Siman et al. 2009). These biomarkers range in size, function and molecular structure. Some proposed biomarkers are specific to brain tissue and others are not. Given the large range of biomarkers associated with TBI, comparisons between different studies are essential to determine the most useful biomarkers and combinations for clinical diagnosis and prognosis.

Currently, there are two general approaches to assessing biomarkers. One relies on clinical evaluations and the other involves the use of animal models (Wang et al., 2005). The clinical models use samples of CSF, serum, urine and/or the brain parenchyma to evaluate biomarker expression (Winter et al., 2004; Zemlan et al., 1999). Correlations between patient outcome and biomarker expression are then determined. The main limitation of clinical models is the inability to fully understand the circumstances of the injury, which results in an inability to quantitatively correlate the severity of the injury to biomarker expression. Furthermore, in clinical settings, correlations are usually drawn based on less specific measures such as the Glasgow Coma Scale, CT scans and the number of days the patient was hospitalized. In contrast to clinical models, animal models provide advantage with regard to their reproducibility. TBI in animal models which utilized measured mechanical input can be induced in a well-controlled laboratory environment, and it is possible to detect injuries from defined brain regions (Wang et al., 2005; Saatman et al., 2008) by histological analyses.

The Marmarou impact acceleration (IA) model reliably mimics a closed head injury induced by a combined linear and angular head impact and is capable of producing significant TAI in discrete WM tracts including corpus callosum (CC) and brainstem

without concomitant focal contusion and skull fractures in rats (Marmarou et al., 1994). The linear and angular acceleration of the head are the clinical cause of TAI (Adams et al., 1982; Gennarelli et al., 1998; Povlishock, 1995). Previous studies have quantitatively linked linear and angular responses to the severity of TAI (Adams et al., 1982; Li et al., 2011). Although there is strong evidence that TAI severity could be graded by several biomarkers, published research to date has not correlated the severity of mechanical inputs to the head with biomarker expression. An animal model which can precisely measure mechanical response in mild to severe TBI can facilitate the development of reliable biomarkers before clinical trials.

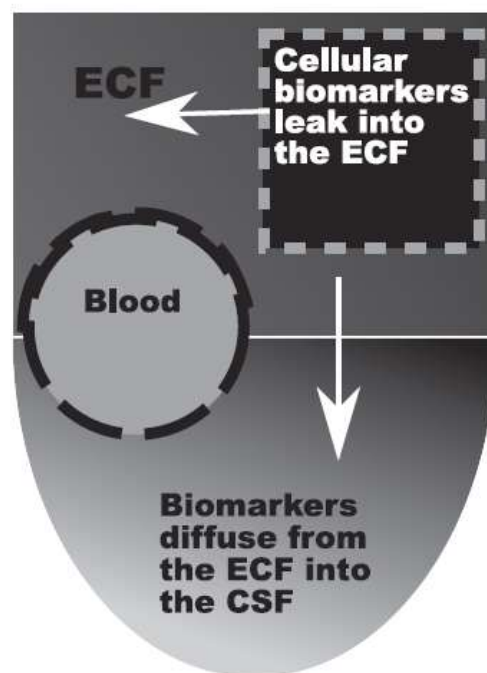


Figure 7-1: Origins of CSF and serum biomarkers

Biomarkers of TBI are usually evaluated in CSF and serum using ELISA. In TBI events, biomarkers in the cytoplasm leak through the damaged cellular membrane into the adjacent extracellular fluid (ECF). These biomarkers then diffuse into the CSF

(Petzold et al., 2007). In the case of BBB damage or breakdown during TBI, biomarkers can directly enter into blood from ECF (Fig. 7-1).

Biomarkers may be released specifically in response to brain injury or may be associated with inflammation or other biochemical and physiological processes not specific to the injured brain. The release of brain specific markers has been associated with neuronal degeneration and regeneration, excitotoxicity, oxidative stress, inflammation, cerebral blood flow dysregulation, apoptosis and cell death (Zemlan et al., 1999; Ingebrigtsen and Romner, 2002; Papa et al. 2008; Mondello et al., 2011). In this study, we aimed to evaluate a panel of biomarkers related to neuronal injury, astrocytosis and neuroinflammation.

Axonal NF-H, one of the four subunits of axonal neurofilaments (Marszalek et al., 1996; Shaw et al., 1998), undergoes phosphorylation of the serine residues after neurofilament compaction, a component in the pathology of TAI (Strong et al., 2001) that is unique to axonal NF-H. In contrast, dendritic and perikaryal forms of NF-H are not normally phosphorylated (Sternberger et al. 1993). The distinctive form of NF-H after axonal injury suggests that this biomarker may be a good indicator of axonal injury and degeneration (Shaw et al., 2005; Anderson et al., 2008). Siman et al. (2009) found that pNF-H rises significantly in both CSF and serum of TBI patients. Zurek et al. (2011) showed that patients showing TBI in initial CT scans had significantly higher levels of pNF-H in serum compared to those without TBI. Furthermore, patients who died within 6-month follow up showed significantly higher levels of pNF-H at admission than those who survived. Serum pNF-H also showed correlation with complete and incomplete sensorimotor loss in spinal cord injury (Hayakawa et al., 2012). More recently, Gatson et

al. (2014) reported that pNF-H levels in serum significantly increase up to 3 days in mTBI patients compared to non-injured controls.

In TBI, β -APP accumulates in injured axons due to TBI-induced disruption of axonal transport (Pierce et al., 1996). Post-injury enzymatic cleavage of APP can generate A β peptides, a hallmark finding in Alzheimer's disease (Price et al., 1995; Masters et al., 2006). In a rotational acceleration DAI model in miniature swine, A β accumulation in injured axons were observed (Smith et al., 1999; Chen et al., 2004). In autopsy studies, Roberts et al. (1994) reported that A β plaques were found in as many as 30% of TBI victims (including children). Remarkably, these A β deposits may occur less than 1 d after TBI (Ikonovic et al., 2004). It has also been reported that interstitial fluid A β concentrations correlated with neurological function in TBI patients, with A β accumulating as an indicator of neurological function improvement in the days after TBI (Brody et al., 2008).

GFAP is an intermediate filament protein found specifically in astroglia, which participate early in the cascade of cellular responses triggered by TBI (Honda et al., 2010). Metting et al. (2012) demonstrated that serum GFAP levels increased in mTBI patients with abnormal CT findings, compared to those with normal CT. They also found that serum GFAP level was elevated in patients who were diagnosed with TAI by MRI at three months post-injury. Similarly, Papa et al. (2012) found serum GFAP was significantly higher in mTBI patients with intracranial lesions on CT, compared to those with normal CT. McMahon et al. (2014) showed that serum GFAP had very good predictive ability (AUC= 0.87), and demonstrated significant discrimination of brain injury severity. More important, GFAP levels were not significantly affected by the

presence of fractures in TBI patients (Papa et al., 2014). Although GFAP expression has been correlated to outcome and imaging result in TBI patients, this biomarker on its own cannot predict individual patient outcome (Nylen et al., 2006; Vos et al. 2004; Metting et al. 2012). However, GFAP may be particularly useful clinically, especially in combination with other markers, because extracranial contribution to GFAP is minimal, even in multiple trauma cases (Pelinka et al. 2004). In addition to brain specific markers, central nerve system (CNS) immune cell production of chemokines and cytokines also provide useful information (Petrova et al., 2000).

IL-6 is one such proinflammatory cytokine produced by activated microglia after TBI (Petrova et al., 2000; Wang et al., 2002). In the CNS, neurons, astrocytes, microglia and endothelial cells are the essential sources of IL-6. The level of IL-6 is low under normal conditions, but upon certain stimuli such as TBI, significant amounts of IL-6 will be secreted. In human peripheral blood, monocytes are the main source of IL-6 (Aarden et al., 1987). Endothelial cells, fibroblasts and T cells can also produce IL-6 in response to a wide range of stimuli including endotoxins, viruses and cytokines (Sironi et al., 1989). Although IL-6 is not exclusively expressed in the CNS, it does exhibit a significant upregulation following TBI (Winter et al., 2004; Dash et al., 2010). It has also been suggested that IL-6 is a neuroprotective cytokine (Winter et al., 2004). Hergenroeder et al. (2010) observed significant increase of serum IL-6 levels in TBI patients within the first 24 h of injury. More recently, Ferreira et al. (2014) indicated that IL-10, -8 and -6 levels were elevated significantly in non-surviving TBI patients compared to the survivors in the first sample (study entry) and in the subsequent sample

(24 h later). Andruszkow et al. (2014) also found that increased serum IL-6 levels during hospital admission were associated with injury severity in 59 traumatized children.

In the current study the levels of pNF-H, A β , GFAP and IL-6 were quantified in both CSF and serum at 24 hrs after impact. Previous studies showed that the levels of these biomarkers were significantly elevated at this time point. In a rat CCI model, Anderson et al. (2008) detected a rise in serum pNF-H 6 h after impact, peaking at 24–48 h before gradually decreasing to baseline. The rise was significantly higher in more severe injuries, and correlated with injury levels determined by volumetric analysis of spared cortical tissue. This pattern has also been recorded following blast TBI (Gyorgy et al., 2011). Woertgen et al. (2002) showed that GFAP serum levels were significantly elevated up to 24 h after trauma compared to the control group using a rat CCI model. In a mouse CCI model, David et al. (2009) showed that TBI resulted in accumulation of endogenous mouse A β peptide in the ipsilateral cortex within 24 hrs, and A β levels increased by almost 120% at 3 d after injury before normalizing by 7 d. Similarly, using a mouse CCI model, Washington et al. (2014) showed that TBI resulted in rapidly increased levels of both soluble and insoluble A β 40 and A β 42 in the injured cortex at 1 day post injury. Using the Marmarou model, Hans et al. (1999) showed that the expression of IL-6 increased at 1 h and remained elevated through the first 24 h, returning to normal afterwards.

The goal of this study is to determine if the panel of biomarkers described above is correlated to the measured mechanical inputs during impact and to the quantified TAI, and therefore to screen for reliable biomarkers in helping to determine TBI injury severity.

7.2 METHODS

7.2.1 Animal handling and preparation

Twenty-four anesthetized male Sprague-Dawley rats (395 ± 15 grams) were used. All rats were administered Buprenex (0.3 mg/kg) subcutaneously 20 minutes prior to impact. Fifteen minutes prior to impact, rats were placed in a sealed acrylic chamber. Anesthesia was induced and maintained by a mixture of isoflurane (3%) and oxygen (0.6 L/min). The skull was then exposed by a midline dorsal incision of the skin and a round stainless steel disk (helmet) of 10 mm in diameter and 3 mm in thickness was positioned midline between bregma and lambda and affixed to the skull vault using cyanoacrylate (Elmer's Products, Columbus, OH). All animal surgical procedures were approved by the Wayne State University Animal Care and Use Committee.

7.2.2 Instrumentation and experimental preparation

The modified weight drop device previously described by Li et al. (2011) and Zhang et al. (2012) was developed to study the kinematics of the rat, and as described in detail in Chapter 6. Briefly, TBI was induced by dropping a custom-made 450 gram impactor from a height of 1.25 m ($n = 8$), 1.75 m ($n=8$) and 2.25 m ($n = 8$), respectively, to induce TBI of three different impact severities. Linear and angular responses of the rat head were measured with an accelerometer (Endevco 7269) along the local anatomical z axis (vertical) and an angular rate sensor (DTS AR12k) about the local anatomical y axis (lateral) glued to the skull approximately 10 mm anterior to the helmet using cyanoacrylate. The entire impact event was captured at 10,000 frames per second by a high-speed video camera (MotionXtra HG-100K) placed 0.5 m away from the animal.

Signals from all of the transducers were acquired at a sampling rate of 50,000 samples per second using the TDAS1R4 data acquisition system (Diversified Technical Systems, Inc, Seal Beach, CA). The automatic weight release system, the data acquisition system and the camera system were synchronized through a trigger switch during the experiment.

Table 7-1: Experiment matrix

Test	Impact Height (m)	
	1.25	2.25
Group 1	8	
Group 2		8
Sham		8
Total		24

7.2.3 Induction of traumatic brain injury

The instrumented animals were placed prone on an open-cell flexible polyurethane foam bed (12x12x43 cm, Foam to Size Inc., Ashland, VA) in a Plexiglas box under a 2.5 m long and 57 mm diameter Plexiglas tube, with the helmet centered directly under the lower end of the tube. A laser beam was used to guide the positioning of the helmeted head to ensure that the impactor hit the center of the stainless steel disc (helmet) (Fig. 4E). Rats were taken off anesthesia just prior to the impact, and then were subjected to TBI by dropping the impactor from a height of 1.25 m, 1.75 m or 2.25 m. Immediately after the impact, the Plexiglas box was manually removed to avoid a second impact to the rat head. After the removal of the stainless steel helmet and the transducers, the skull was examined for fractures and then the skin was closed by staples.

7.2.4 Head impact data processing and analysis

Head biomechanical responses were obtained from the head-mounted accelerometers and angular rate sensor as previously described in chapter 6. Briefly, peak linear acceleration (a_{\max}) and average linear acceleration (a_{avg}) of the head were determined from the acceleration-time curve. Peak angular velocity (ω_{\max}) and average angular velocity (ω_{avg}) were determined from the angular velocity-time history curves. The angular velocity-time curve recorded from the angular rate sensor was filtered with Society for Automotive Engineers (SAE) Channel Frequency Class 1,000 Hz (SAE J211) and angular acceleration was obtained from the derivative of the angular velocity with respect to time. Peak angular acceleration (α_{\max}) and average angular acceleration (α_{avg}) were then determined from the angular acceleration curve. Power was also determined for each impact and is proportional to the rate of change of kinetic energy of the head in this study. In the equation below the mass term, which is considered constant, is removed and the equation reflects the rate of change of translational kinetic energy: $\text{Power} = \Delta V^2 / \Delta T$, where ΔT is the time duration of effective acceleration, and ΔT is the change of velocity of the head in this period. Power provides the basis for a hypothesis that head injury severity correlates to the magnitude of the rate of change of kinetic energy that the head undergoes during an impact (DiLorenzo, 1976; Newman et al., 2000).

Time to surface right (SR) is the time taken by an animal to regain a normal ventral position after being placed on its back after impact. It has been used as an indicator of duration of unconsciousness of rats (Adams, 1986; Li et al., 2011a).

7.2.5 TAI quantification

After TBI, rats were allowed to recover and monitored for at least 6 hours. Rats with skull fracture or those exhibiting signs of severe distress were euthanized and were not used in this analysis. After a 24 h survival period, each rat was euthanized with an overdose of sodium pentobarbital (120 mg/kg, intra peritoneal) and exsanguinated. Rats were then transcardially perfused with heparinized (500 units/ml) normal saline followed by cold 4% paraformaldehyde in phosphate buffered saline (0.1 M PBS, pH 7.45). The brain was then carefully removed and post fixed (4% paraformaldehyde in 30% sucrose), after which the cerebral hemispheres were cut into 40 μm thick frozen sections in CC and Py and subjected to β -APP immunostaining as described in Chapter 6.

The total number of β -APP reactive axonal swellings and retraction balls (considered as total TAI counts) in CC or Py from all stained sections from each injured animal were quantified. The total TAI in CC or Py for each rat was the sum of TAI from panoramic images of all selected stained sections. In CC, 7 sections (Bregma 0.36, -0.12, -0.60, -1.08, -1.56, -2.52), which covers most TAI according to previous study (Fig. 6-7), were selected to count total TAI for each rat. In Py, a set of 7 sagittal sections, comprising midline (0 μm), ± 200 μm , ± 600 μm , ± 1000 μm , were selected.

7.2.6 Biomarker quantification

24 h after impact, the CSF was collected from cistern magna using a published method (Liu and Duff 2008). Prior to CSF collection, the rats were anesthetized by ketamine (50mg/kg) and xylazine (20mg/kg), administered intraperitoneally. The skin of the neck was shaved, and the head was flexed so that the external occipital protuberance

in the neck was prominent. Then a dorsal midline incision was made over the cervical vertebrae and occiput. Under the dissection microscope, the subcutaneous tissue and muscles was separated by blunt dissection with forceps, and the atlanto-occipital membrane was exposed. Then, a 25G needle attached to 1 cc syringe was carefully lowered into the cisterna magna (Fig. 7-2) and approximately 0.1–0.15 mL of CSF was collected from each rat. Then 1 mL of blood was collected from heart just before perfusion by 4% paraformaldehyde. Both the CSF and serum were stored at -70°C until further processing for various biomarkers. CSF and serum expression of $\text{A}\beta_{1-42}$ (Invitrogen, KMB3441), NF-H (EnCor Biotechnology Inc, RPCA-NF-H), GFAP (EMD Millipore, NS830), and IL-6 (Invitrogen, KRC0061) were assessed by ELISA as per the manufacturer's instructions.



(Adapted from Liu and Duff, 2008)

Figure 7-2: CSF collection from Cisterma Magna

7.2.7 Statistical analysis:

Comparisons for significant differences in biomarker levels between impact groups, or between impact group and control group were assessed using t-tests. Pearson's correlation analysis was used to evaluate the correlation between biomechanical parameters and biomarker levels using SPSS 13 software (SPSS Inc. Chicago, Illinois).

In this study, a logistic regression analysis was conducted to determine potential biomarker for severe TAI. Similar to what described in chapter 6, the 2.25 m drop height produced the highest levels of TAI and the longest time for surface righting. Therefore the critical value of severe TAI was determined as the lower limit (LL) of 95% confidence interval of normalized total TAI count in 2.25 m impact group, defined as:

$$\text{Lower limit} = \text{Mean} - t(\alpha, N - 1) * s / \sqrt{N} \quad (4)$$

where $t()$ is the test statistic, N is the sample size, α is the desired significance level, which is 95% in our case and s is the sample standard deviation. All rats with TAI number higher than the LL were grouped into category 1. All rats with TAI number lower than the LL were grouped into category 0.

The independent variables tested were biomarker level of NF-H, GFAP, A β 1-42 and IL-6 in serum and CSF. Various univariate and multivariate models were assessed to find a single biomarker variable, or a combination of the variables, which best explained the data. To determine whether relationships between outcome and the biomarker variables were statistically significant, -2Log Likelihood ratio, Wald Chi-Squared and H-L test were performed.

Receiver operating characteristic curve (ROC) analysis and area under ROC were also used to assess and compare the outcome performance between single and paired combinations. The optimal threshold (specificity and sensitivity) for each individual and paired biomarker was determined, which was defined as the point closest to the left upper corner of the ROC curve. The Logistic analysis and ROC analysis were performed using SPSS 13 (SPSS Inc. Chicago, Illinois).

7.3. RESULTS

7.3.1 Head kinematics

The mechanical responses and post-injury behavior from 1.25 m, 1.75 m and 2.25 m impacts are summarized in Table 7.1. The biomechanical and behavioral responses were significantly different between the 2.25 m and 1.75 m groups ($p < 0.05$), except peak angular velocity. The peak angular velocity was significantly different between 1.75 m and 1.25 m impacts, but all other parameters were not statistically different between these two impact groups.

Table 7-2 Mechanical and behavioral responses of rat head in weight-drop experiments.

Height	Head Linear Responses, <i>mean</i> \pm <i>SEM</i>						Head Angular Responses, <i>mean</i> \pm <i>SEM</i>				Behavior
	Peak Linear Acc. (g)	ΔV (m/s)	ΔT (ms)	Average Linear Acc. (g)	Power (m^2/sec^3)	HIC	Peak Ang. Vel. (rad/sec)	Average Ang. Vel. (rad/sec)	Peak Ang. Acc. (krad/sec ²)	Average Ang. Acc. (krad/sec ²)	Time to Surface Righting (min)
2.25 m (n=8)	730 \pm 33	5.28 \pm 0.18	1.82 \pm 0.10	300 \pm 13	15.55 \pm 0.85	2823 \pm 209	153 \pm 12	108 \pm 9	187 \pm 14	80 \pm 7	15 \pm 4
1.75 m (n=8)	466 \pm 56	4.38 \pm 0.28	2.19 \pm 0.33	223 \pm 19	9.35 \pm 0.69	1468 \pm 154	164 \pm 6	67 \pm 11	151 \pm 14	69 \pm 7	4 \pm 1
1.25 m (n=8)	422 \pm 48	4.63 \pm 0.16	2.80 \pm 0.20	178 \pm 19	8.23 \pm 1.08	1186 \pm 216	111 \pm 14	81 \pm 9	146 \pm 10	51 \pm 8	5 \pm 2

7.3.2 TAI quantification in CC and Py

The total TAI counts per rat in CC were 314 \pm 95 for 2.25 m group, 31 \pm 4 for 1.75 m group and 17 \pm 3 for 1.25 m group, respectively. The total TAI count at the 2.25 m group was significantly higher than that at the 1.75 m group ($p < 0.02$), while TAI count at the 1.75 m group was significantly higher than that at the 1.25m group ($p < 0.05$) (Fig. 7-3A).

In Py, The total TAI counts per rat were 6451 \pm 1569 for 2.25 m group, 544 \pm 124 for 1.75 m group and 634 \pm 247 for 1.25 m group, respectively. The total TAI count

at the 2.25 m group was significantly higher than that at the 1.75 m group ($p < 0.01$), however TAI count had no statistically difference between 1.75 m and 1.25 m groups ($p > 0.05$) (Fig. 7-3B).

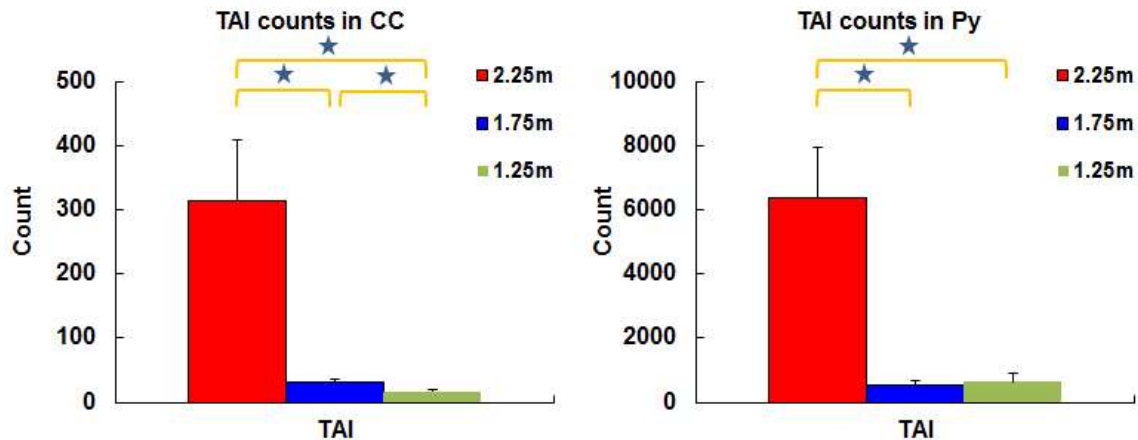


Figure 7-3: TAI counts in CC (A) and Py (B).

7.3.3 Biomarker assessment in CSF and serum

Changes in the expression of potential biomarkers targeting axonal injury (NF-H and A β), astrocytic activation (GFAP) and neuroinflammation (IL-6) were studied. Compared to control, significantly higher CSF and serum NF-H levels were observed in all the impact groups, except with no statistical significance between 1.25 m and control in serum. Furthermore, CSF and serum NF-H levels at 2.25 m were significantly higher than 1.75 m & 1.25 m impact groups and CSF and serum NF-H levels of 1.75 m group were significantly higher than that of 1.25 m group (Fig. 7-4 A, B). GFAP levels were significantly higher at 2.25 m compared to other heights and control in both CSF and serum. Although there was no significant difference between 1.75 m and 1.25 m groups, CSF and serum GFAP levels in these groups were significantly higher than control (Fig. 7-4 C, D). TBI rats also showed significantly higher levels of IL-6 versus control in both

CSF and serum. Although dramatically high CSF IL-6 levels were observed in 5 of 14 rats in the 2.25 m impact group, no significant differences were observed between each impact group (Fig. 7-4 E, F). Levels of A β , a breakdown product of β -Amyloid precursor protein (β -APP), were not significantly different between groups (Fig. 7-4 G, H).

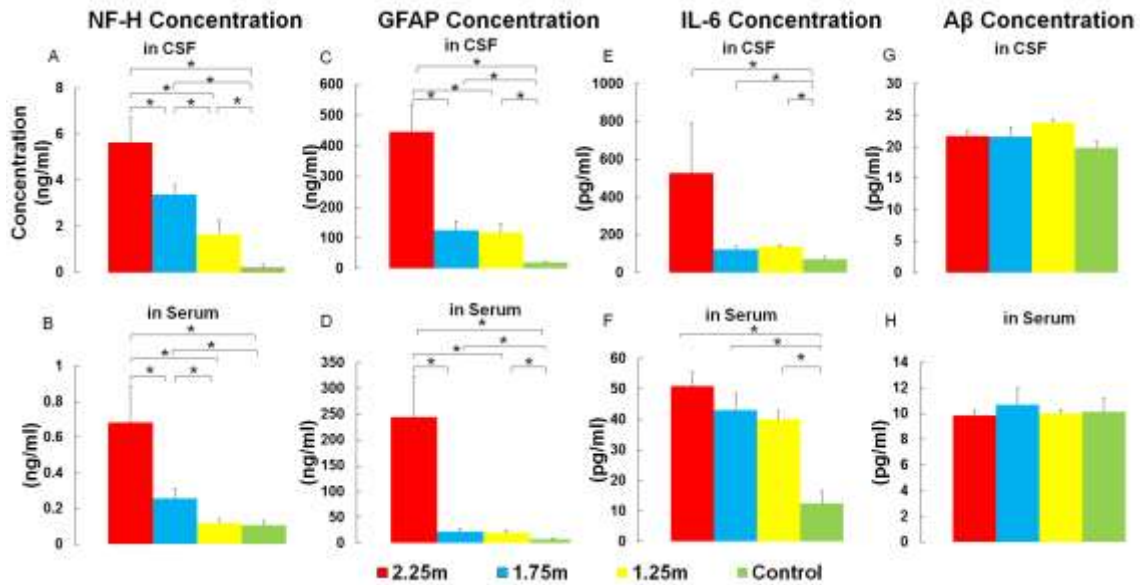


Figure 7-4: Comparisons of biomarker levels between different impact heights in CSF and Serum. * indicates significant differences between groups.

7.3.4 Comparison of CSF and serum biomarker levels

The concentration of all four biomarkers was higher in the CSF compared to the serum. There were positive correlation between the CSF and serum NF-H levels ($p < 0.01$) based on Pearson's correlation analysis. The concentrations of GFAP, A β or IL-6 were not correlated between matched CSF and serum samples (Fig. 7-5).

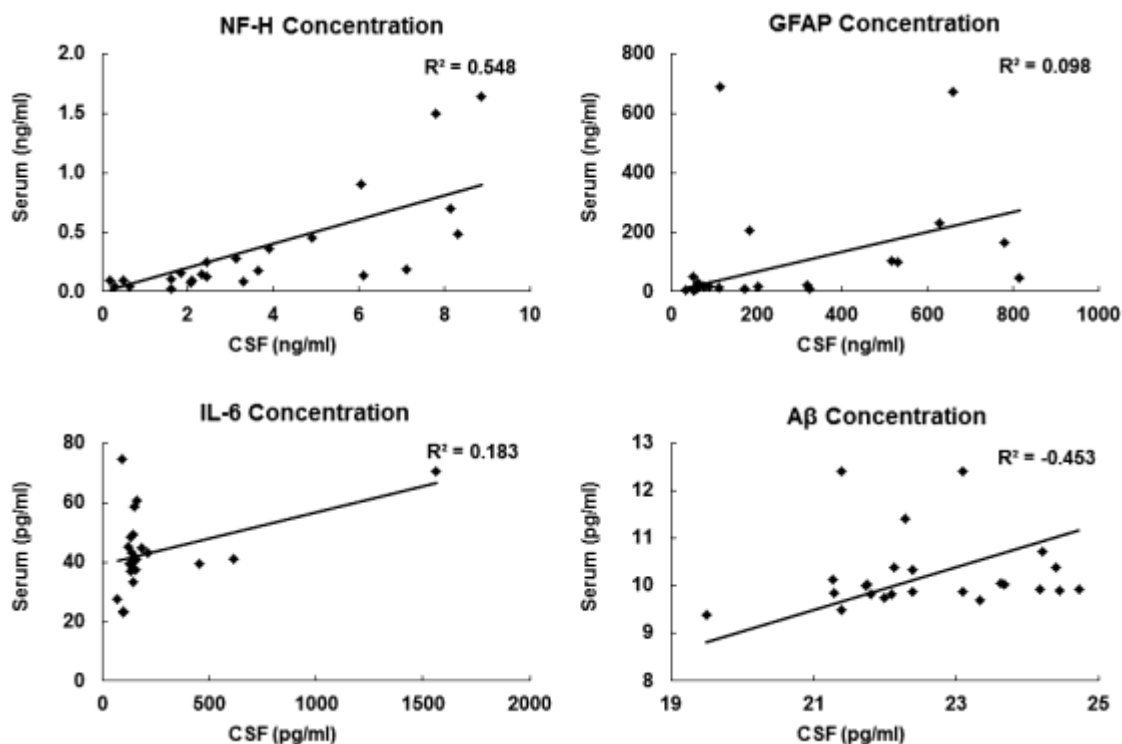


Figure 7-5: Correlation of biomarker levels in CSF and Serum. Pearson's correlation showed NF-H concentration in CSF had good correlation with that in Serum.

7.3.5 Biomarker for severe TAI

A potential biomarker for severe TAI in brain regions can be determined by defining the dependent variable as "1" in logistic model if severe injury occurred in either CC or Py. Single and paired biomarkers were tested in serum and CSF, respectively. NF-H and GFAP in CSF and serum have been identified as potential biomarkers for severe TAI (Appendix A-4). CSF biomarkers showed better predict ability than serum biomarkers.

Among CSF biomarkers tested, GFAP was the best single biomarker with an area under the ROC curve of 0.946 (Fig. 7-6), followed by NF-H with an area under the ROC

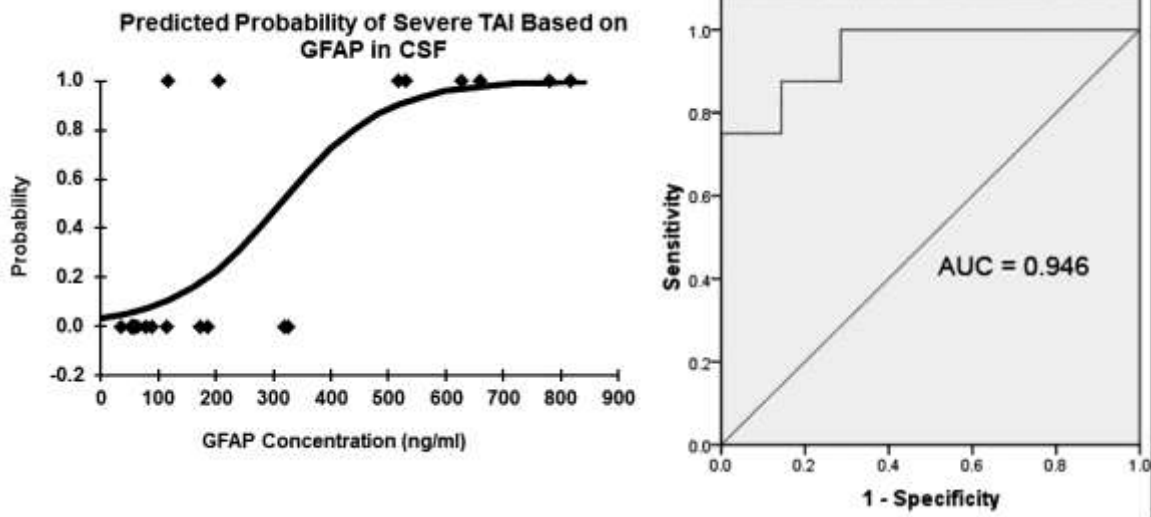


Figure 7-6: CSF GFAP to predict severe TAI

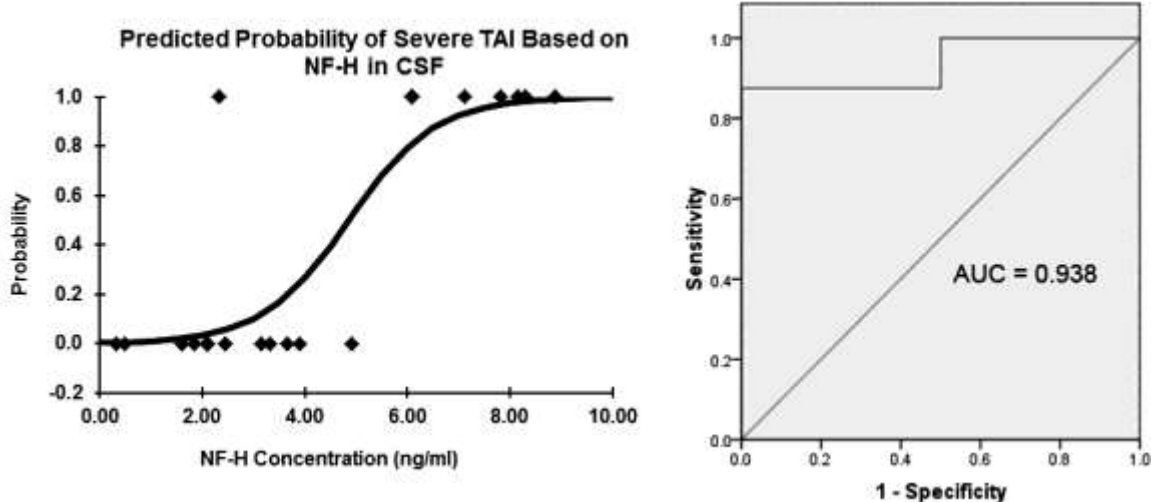


Figure 7-7: CSF NF-H to predict severe TAI

curve of 0.938 (Fig. 7-7). In serum biomarkers tested, GFAP also had better predict ability than the others, with an area under the ROC curve of 0.920 (Fig. 7-8). NF-H in serum was also a potential biomarker with an area under the ROC curve of 0.857 (Fig. 7-9). However, combined multiple biomarkers didn't show better prediction values than single biomarker in current study.

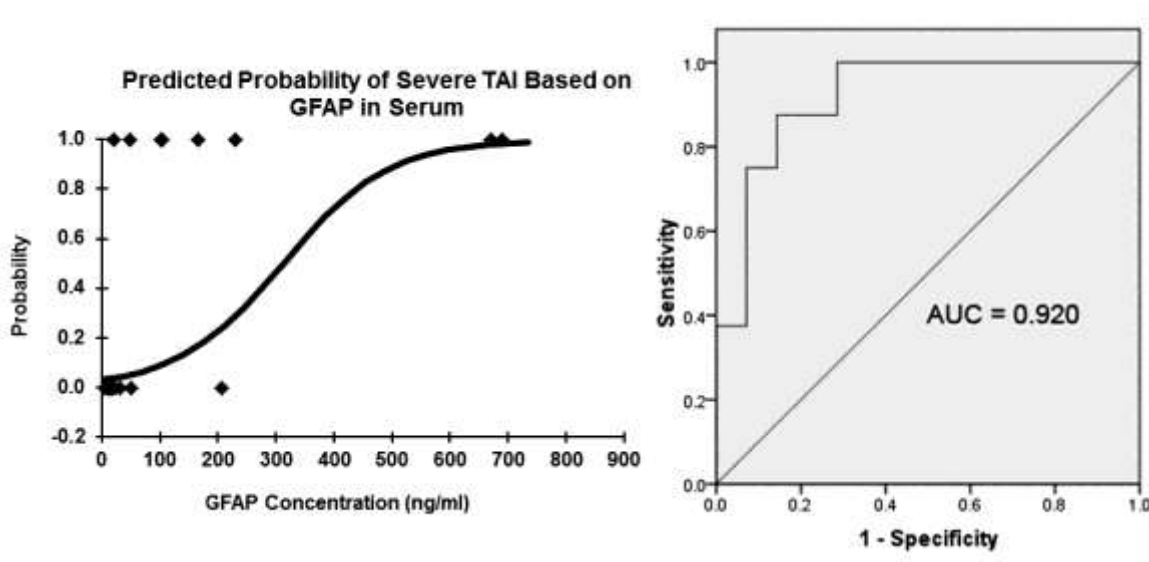


Figure 7-8: Serum GFAP to predict severe TAI

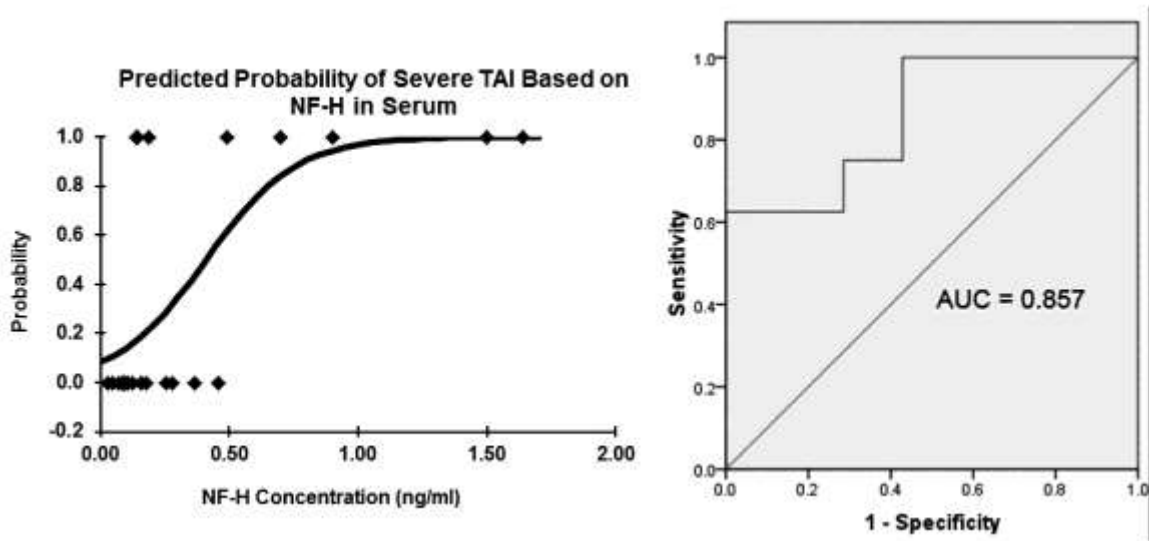


Figure 7-9: Serum NF-H to predict severe TAI

7.3.6 Correlation between biomarker levels and mechanical response

Pearson's correlation analysis showed that NF-H and GFAP levels in CSF had positive correlation with power ($p < 0.001$), followed by correlations with average linear acceleration ($p < 0.01$) and surface righting ($p < 0.01$), which are good biomarkers for TAI

according to histologic assessment in our previous study (Li et al., 2011a, 2011b). NF-H and GFAP levels in serum also showed good correlation with power, average linear acceleration, and surface righting ($p < 0.01$) (Fig. 7-10).

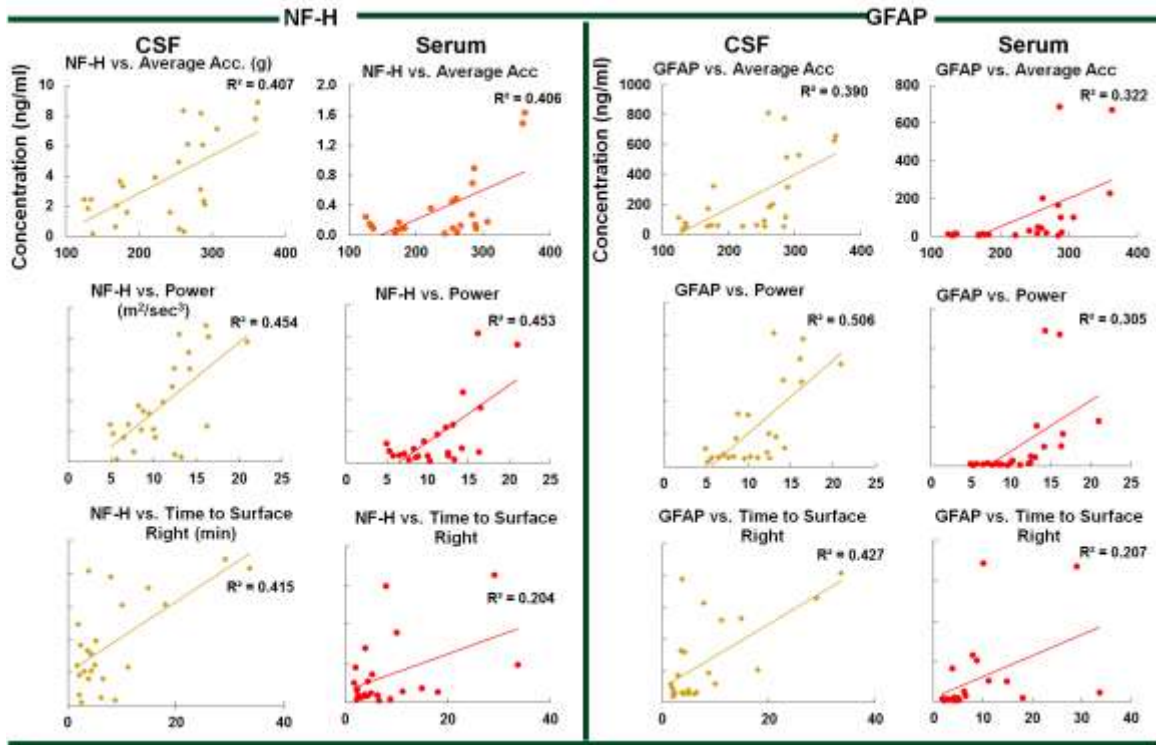


Figure 7-10: Correlation between biomarkers and biomechanics. Pearson's correlation showed NF-H and GFAP had good correlation with power, average linear acceleration and surface righting.

7.4 DISCUSSION

One of the limitations of clinical biomarker studies has been that the population being studied has experienced TBI with varying mechanisms and severities which are not documented nor measured. Other characteristics, including age, gender, and possible genetic factors also vary. In fact levels of various biomarkers and outcomes following TBI may also be influenced by acute and chronic nontraumatic neurologic insults such as posttraumatic seizures or hypoxemia, chronic nontraumatic neurologic insults such as

previous strokes, or noncranial injuries from impact such as bone fractures (Berger et al., 2006; Pelinka et al., 2005; Dash et al. 2010). The presence of polytrauma in other body regions can give rise to biomarker expression related to the injured tissues. In this regard, the modified impact acceleration model used in a controlled experimental setting offers benefits over human clinical studies. First, the model enables close monitoring of various mechanical parameters that produce the injury and secondly the animal model enables evaluation of biomarker levels at precise time periods following TBI and also avoids most polytrauma.

Although much information and data is available regarding biomarkers and how they relate to TBI, there are many discrepancies which have been attributed to lack of model reproducibility and reliability (Cernak 2005), leading to difficulty in comparing the outcomes of different studies. We previously showed that TAI severity is directly related to the combination of linear and angular acceleration during the brain injury event (Li et al., 2011b). By incorporating the mechanical input into the investigation of the biomarkers as studied, we are able to determine the induced injury severity as well. Measuring the mechanical input can also link different studies and give investigators the ability to compare results between studies based on quantified differences or similarities in the mechanical severity of the impacts.

Currently, the Glasgow Coma Scale (GCS) is the primary selection criterion in most TBI clinical trials (Teasdale and Jennett, 1974, 1976; Teasdale and Murray, 2000; Laureys et al., 2002) and is also used to assess TBI severity. However, it does not capture the full spectrum of injury severity, especially for the milder forms of injury (Ross et al., 1998; Fisher et al., 2001). Saatman et al (2008) proposed a multidimensional

classification system based on the injury mechanism with an assumption that brain injuries with similar injury mechanism are likely to share common injury pathophysiology. This classification may be useful in understanding the role of specific biomechanical loading and injury severity. Since the magnitude of loading can be measured and graded, this approach could help identify biomarkers that reflect a continuous rather than categorical injury severity. The present study examined a panel of biomarkers associated with axonal injury (pNF-H and A β), astrocytic activation (GFAP) and neuroinflammation (IL-6) and correlated to the mechanical severity of the head impact.

In the present study, a positive correlation between serum and CSF concentrations of pNF-H was found, but no such correlation was found between serum and CSF concentrations of GFAP, A β and IL-6. Phosphorylated pNF-H has been found to be resistant to breakdown by calpain and caspases (Shaw et al., 2005) and thus may readily reach the serum and hence offer a more reliable representation of the extent of neuronal damage. The serum GFAP levels of 1.75 m and 1.25 m impact decreased while levels in CSF remained high. The high CSF GFAP levels may be related to an intact or somewhat less affected BBB following moderate to mild TBI compared to severe impact (Zetterberg et al., 2006; Blennow et al., 2011). Serum IL-6 levels in all three impact groups were high, and increased independently of CSF IL-6 levels. These elevated levels may be related to a systemic inflammatory response following TBI (Pape et al., 2002; Dash et al., 2010). Furthermore, a lack of correlation between serum and CSF expression of these biomarkers may also be related to the time dependency of their release in the CSF compared to the serum, and warrants additional studies using more time points.

Clinically, it is faster and safer to collect serum than CSF. The findings from the current study show that in the current study pNF-H shows potential as a blood-based biomarker for TBI that may accurately depict the magnitude of axonal injury.

pNF-H presents as a unique biomarker for traumatic axonal injury for mainly two reasons. It is easy to detect because its many serine residues are most commonly phosphorylated. pNF-H expression has been studied in rats using a controlled cortical impact (CCI) model and has been found to increase with impact depth from 1.5 mm to 2 mm in both serum and CSF (Anderson et al., 2008; Shaw et al., 2005). In the present study, CSF and serum pNF-H expression was also found to be significantly higher in all impact groups, except between 1.25 m and control in serum. Furthermore, pNF-H expression was also determined to be positively correlated with mechanical responses of the head; power, average linear acceleration and surface righting. These have all been found to be good biomarkers of TAI (Li et al., 2011a, 2011b). These results suggest that pNF-H not only tracks the level of TAI severity (mild, moderate, severe), but also correlates well with impact severity.

Astroglial cells are found in the CNS to support and provide nourishment for the surrounding cells. When these cells in either the brain or spinal cord are injured, they release the intermediate filament GFAP. Due to GFAP's specified location and release after injury, it presents itself as a viable TBI biomarker (Pelinka et al., 2004). GFAP has also been considered as a reliable marker of injury outcome in clinical and experimental TBI studies. GFAP release after TBI was shown to be time-dependent reaching peak levels at 6 h after CCI injury in rats (Woertgen et al., 2002). Clinically, elevated serum GFAP levels have been considered as a valid biomarker of TBI (Pelinka et al., 2004;

Lumpkins et al., 2008). Ahmed et al. (2012) studied GFAP expression in a swine blast model and found that GFAP concentrations increased significantly 6h post injury. In the present study serum and CSF GFAP levels were significantly higher in the 2.25 m group compared to other heights and control. However, compared to NF-H, GFAP level was elevated in the 1.25 m group in both CSF and serum, making it potentially a more sensitive biomarker for mild injury. Similar to pNF-H, GFAP levels also showed a positive correlation with power, average linear acceleration and time to surface right, which further support that GFAP may be used to grade injury severity.

IL-6 is a proinflammatory cytokine that is found in the CNS and activated as part of the acute inflammatory response after injury. This biomarker may be especially useful due to the independency between patient age and concentrations of IL-6 in serum (Bell et al., 1997). Pediatric clinical studies have found IL-6 to be indicative of poor clinical outcome and indicative of head injury severity (Chiaretti et al., 2005). Although clinically there is evidence for IL-6 as a potential biomarker for determining patient outcome and injury severity, Zhu et al (2004) showed different results in rat studies of severe and mild CCI with increased plasma IL-6 levels compared to controls but no significant difference in plasma IL-6 between the severe and mild injury groups. Results from our study support usefulness of IL-6 in determining the presence or absence of TBI but do not support any relationship between its expression and injury severity. Due to the discrepancy between the clinical outcomes and animal models, further studies are needed required to determine whether IL-6 levels are useful for grading injury severity.

A β , a breakdown product of β -APP important in the formation of amyloid plaques is associated with an increased risk of onset of Alzheimer's disease (Roberts et al., 1994;

Dekosky et al., 2007). Although serum and CSF A β levels can be measured (Tian et al., 2011; Yu et al., 2012; Abrahamson et al., 2006) the change in the amount of serum and CSF A β in the present study was insignificant 24 hrs after TBI. Olsson et al. (2004) found A β in CSF increased significantly on day 3 vs. day 0-1 (573%), on day 4 vs. day 0-1 (855%), on day 5-6 vs. day 0-1 (1173%) in TBI patients. The use of A β as a biomarker for TBI immediately after injury is limited by the possible time delay between β -APP release and the subsequent A β breakdown product expression in the serum and CSF.

One limitation about this study is the possibility of spinal injury produced by the impact acceleration model. Kallakuri et al. (2003) observed epidural hemorrhages at the base of the skull and spinal cord down to C3–C4 levels in 1.5- and 2.0-m drops with the Marmarou model. These injuries may be caused by the stretch of the neck when the dropped weight pushes the head and neck into the foam pad. In this phase, deformations of the neck may lead to epidural injury. Viano et al. (2012) also indicated that even without skull fracture, the head-neck motion during compression into the foam and rebound can cause skull deformation, which would contribute to loading of the brain and then the brain pushing on the spinal cord. The possibility of producing spinal cord injury is another potential confounding effect of the Marmarou drop-weight technique, and could affect the accuracy of biomarker to evaluate TBI.

CHAPTER 8

CONCLUSIONS

The objective of this dissertation was 1) to investigate the relationship of impact mechanics and TAI, and 2) to identify potential biomarker to predict TAI. To achieve these goals, a modified impact-acceleration model of TAI has been developed to monitor the consistency, reproducibility and reliability of mechanical trauma imparted to the animals from impact acceleration injury. The new design incorporating real time measurements and analysis of head kinematics that allow determination of head linear acceleration, head angular velocity and impact force as a result of each impact. These technical renovations will help advance the standardization of this model between different research groups, and assist in interpretation of severities of TAI.

Based on the results of the rat head kinematics and quantified TAI severities, the following conclusions can be drawn:

1. TAI in different brain regions may result from different mechanical input.
2. Different impact sites, the magnitude and direction and of linear acceleration and the magnitude and axis of head rotational acceleration may result in different TAI distributions and injury types.
3. Power, a function of the rate change of kinetic energy to the impacted rat head, was the best single predictor for severe TAI in CC and Py combined.
4. Combined linear and angular responses may produce higher levels of TAI than linear or angular acceleration alone.

The model in this thesis also showed promise in elucidating the relationship between biomarker levels and severity of the mechanical trauma to the brain, which cannot be determined in clinical trials. The results indicated:

1. Both NF-H and GFAP levels in CSF and serum were good biomarkers for severe TBI.
2. The Levels of NF-H and GFAP had positive correlation with the following biomechanical responses: average linear acceleration and power.
3. CSF NF-H, CSF and serum GFAP had potential to be good biomarkers for mild TBI.
4. Combined multiple biomarkers did not show better predictive ability for TAI than single biomarkers in the current study.

CHAPTER 9

FUTURE STUDIES

9.1 SCALING: ANIMAL TO HUMAN

The mechanical data measured in this study can be converted to levels in humans using scaling laws. A common technique is equal stress / equal velocity (Gutierrez et al., 2001, Margulies et al., 1985, Viano et al., 2009). For application to the current study, a characteristic length ratio ($\lambda = r_h / r_r$) is determined, where r_h is the radius of the human brain and r_r is the radius of the rat brain. In our FE studies, the average radius of the rat brain was 7 mm and the radius of the human brain was 80 mm (Zhang et al., 2001; Zhang et al., 2010). This gives $\lambda = 11.4$. Equal stress and velocity method was then applied to obtain the scaled mechanical data for human. Twelve rats with severe TAI (category 1 in logistic regression) were used in this analysis. The scaled peak head accelerations of 76 ± 47 g (mean \pm SD) is lower than 103 ± 30 g (Zhang et al., 2004) and 98 ± 28 g (Pellman et al., 2003) from reconstructed NFL game impacts of injury cases. The scaled peak angular velocity of 11 ± 5 rad/sec is lower than 35 ± 15 rad/sec reported by Pellman et al. (2003) from reconstructed NFL game impacts, and also lower than the proposed TAI threshold by Margulies et al. (1992), which is 46.5 rad/sec for human. Therefore, more research is necessary to evaluate the contribution of linear and angular head mechanical response to TAI and in scaling animal data to human. Limitations in current scaling methods include the differences of brain structure and geometry between human and rat, which may lead to different response during impact. In addition, the rat is lissencephalic with only a fraction of the white matter compared to a human. Thus their tolerance to

injury might be at different level (Viano et al., 2009). Although the rodent model is widely used in laboratory studies of TBI, the low mass of the rat brain requires very high angular accelerations to produce closed head injuries. Larger animals with similar geometry and mass to human are better models for scaling animal data to human. Primates (Gennarelli et al., 1982), swine (Meaney et al., 1995; Smith et al., 1997, 2000), sheep (Anderson et al., 1997), and rabbits (Gutierrez et al., 2001) have been used for rotational acceleration studies of the head in the different planes. In the future, how to similarly reproduce results in rodent model in higher species more closely related to human, such as the pig and the sheep, will be the next step.

9.2 COMBINED BIOMECHANICAL AND COMPUTATIONAL APPROACH

Despite recent efforts to understand biomechanics on TAI, there are still no widely accepted injury criteria for humans. Animal studies as in this thesis have resulted in important advances in the understanding of brain injury due to different levels of dynamic loads. However, the applicability of animal brain injury results to humans remains uncertain as described in section 9.1.

Finite element (FE) model is a promising method to address issues related to biofidelity and to scaling between human and animal. Many studies have used it to study the local level of injury criterion of brain tissue (Zhang et al., 2004; Ruan et al., 1994; Zhou et al., 1995). The computer model can be built in highly detailed anatomical structures of brain and can measure the parameters that are difficult to inquire from experiment. In order to transfer the information obtained in the current animal study, , an anatomically based, high resolution FE model of rat head was developed (Zhang et al.,

2011, 2012). This high resolution model will permit a direct correlation between the detailed experimental injury map and response map at the level of the finite element (Fig. 9-1), thereby result in establishment of tissue level thresholds associated with TAI. Knowing the mechanical behavior of neural tissue does not vary significantly from one species to another; these tissue level thresholds can be directly translated to human head models and therefore will enhance the capability of the human head model in predicting brain injury. In addition, such an improved human head model can assist in the diagnosis of DAI by predicting microscopic injury which is invisible to conventional imaging techniques.

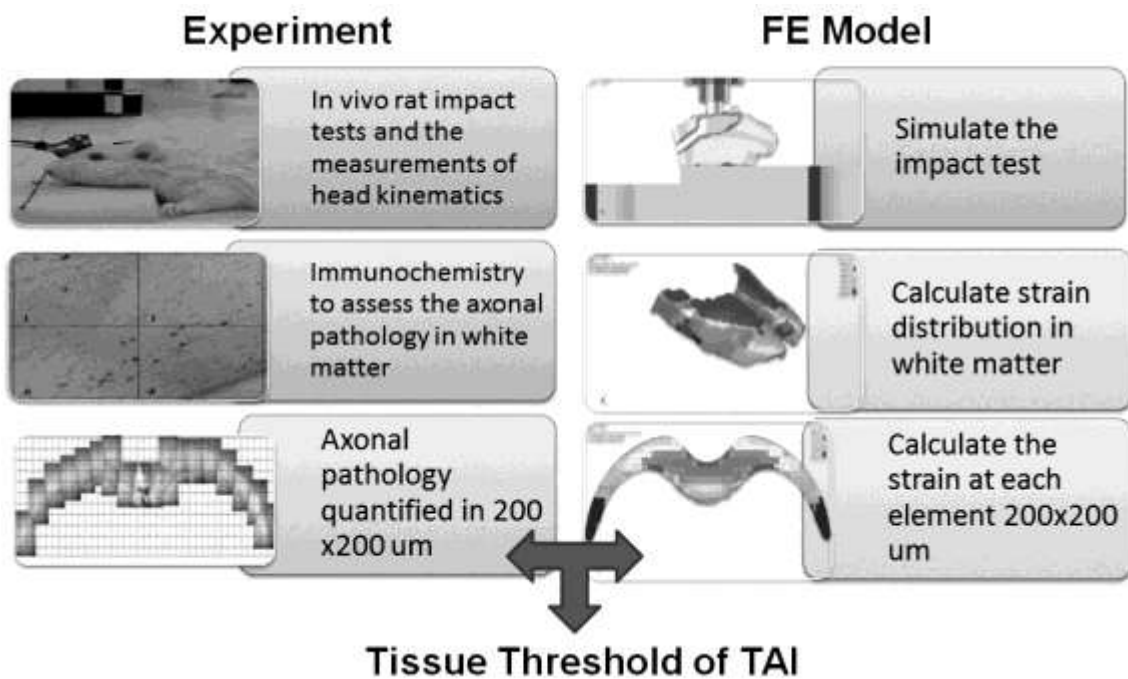


Figure 9-1: Frame work of combined biomechanical and computational approach

9.3 TEMPORAL CHANGES OF BIOMARKER LEVELS

In this thesis, an animal model was developed which can precisely measure mechanical response in mild to severe TBI and facilitate the development of reliable

biomarkers before clinical trials. However, one limitation was the biomarkers has only been tested at one time point (24hrs). Little was know about time course of these biomarkers, of which the peak concentration in CSF and serum may occur at an earlier or later time point. In order to accurately evaluate a biomarker, investigating the time profile of the biomarker is of great importance.

Temporal changes in serum concentrations of A β , phosphorylated NF-H (pNF-H), cleaved tau (c-tau), SBDPs, UCH-L1 and interleukin-6 (IL-6) have been studied mainly in the rat controlled cortical impact (CCI) model. Abrahamson et al. (2006) reported that the brain tissue level of A β 1-42 peaked 3 h after CCI, remained high for 6 to 12 h and showed a slow secondary increase between 12 and 72 h. Shaw et al. (2005) showed increased levels of serum pNF-H after TBI with a peak at 2 days post-injury. Another study by Anderson et al. (2008) detected the presence of pNF-H in serum as early as 6 h post-injury and the levels peaked at 24-48 h. Also, serum c-tau levels were significantly increased 6 h after TBI but not at later time points (Gabbita et al., 2005). Significant elevation of SBDP levels in CSF was measured within 24-72 h following CCI (Pike et al., 2001). Liu et al. (2011) reported that CSF UCH-L1 levels were significantly higher than their counterparts in the sham group at 2 h and 6 h for CCI at 1.0 mm and at 2h, 6h and 24h for CCI at 1.6 mm. Stover et al. (2000) found IL-6 in CSF peaked at 24 h in the rat CCI model. However, data on CSF and serum levels of biomarkers and related histology changes in the closed head impact acceleration model are lacking. Based on these studies, we recommend biomarker and histology analyses at 6, 24, and 72h after impact in future study.

APPENDIX

Table A-1: Significance test for univariate and multivariate logistic regression models of biomechanical response to predict TAI in CC

Predictor	d.f.	Likelihood Ratio Test		Wald Statistic Test		H-L Test	
		Statistic	P	Statistic	P	Statistic	P
Peak Linear Acc.	1	4.865	0.027	2.818	0.093	5.893	0.659
Avg. Linear Acc.	1	15.934	<0.001	6.327	0.012	4.420	0.817
Power	1	18.078	<0.001	4.561	0.033	1.866	0.985
Peak Angular Vel.	1	0.525	0.469	0.509	0.476	4.659	0.702
Avg. Angular Vel.	1	0.654	0.419	0.631	0.467	7.536	0.480
Peak Angular Acc.	1	2.782	0.095	2.381	0.123	1.143	0.980
Avg. Angular Acc.	1	2.163	0.141	2.017	0.156	13.398	0.099
Surface Righting	1	8.844	0.003	5.319	0.021	13.108	0.108
Avg. LinearAcc	2	21.930	<0.001	4.736	0.030	3.934	0.863
+Surface Righting				3.767	0.052		
Power + Surface	2	21.254	<0.001	2.279	0.131	4.381	0.821
Righting				1.950	0.163		

Table A-2: Significance test for univariate and multivariate logistic regression models of biomechanical response to predict TAI in Py

Predictor	d.f.	Likelihood Ratio Test		Wald Statistic Test		H-L Test	
		Statistic	P	Statistic	P	Statistic	P
Peak Linear Acc.	1	0.070	0.791	0.066	0.797	10.210	0.251
Avg.Linear Acc.	1	1.893	0.169	1.754	0.185	18.583	0.017
Power	1	6.011	0.014	3.482	0.062	7.185	0.517
Peak Angular Vel.	1	10.467	0.001	6.368	0.012	7.256	0.403
Avg. Angular Vel.	1	11.037	0.001	5.698	0.017	14.260	0.047
Peak Angular Acc.	1	0.248	0.619	0.240	0.624	2.779	0.836
Avg. Angular Acc.	1	1.504	0.220	1.434	0.231	8.215	0.314
Surface Righting	1	8.810	0.003	5.231	0.022	6.793	0.559
Peak Angular Vel + Surface Righting	2	12.184	0.002	3.928	0.047	6.245	0.511
Avg. Angular Vel +Surface Righting	2	12.632	0.002	4.048	0.044	10.954	0.141
				5.829	0.016		
				5.833	0.016		

Table A-3: Significance test for univariate and multivariate logistic regression models of biomechanical response to predict to predict TAI in combined CC and Py region

Predictor	d.f.	Likelihood Ratio Test		Wald Statistic Test		H-L Test	
		Statistic	P	Statistic	P	Statistic	P
Peak Linear Acc.	1	1.820	0.177	1.435	0.231	6.800	0.558
Avg. Linear Acc.	1	10.265	0.001	4.938	0.026	14.239	0.076
Power	1	20.497	<0.001	7.337	0.007	8.069	0.427
Peak Angular Vel.	1	4.857	0.028	4.039	0.044	11.871	0.105
Avg. Angular Vel.	1	5.223	0.022	4.200	0.040	10.499	0.122
Peak Angular Acc.	1	0.193	0.661	0.187	0.665	1.688	0.946
Avg. Angular Acc.	1	6.033	0.014	4.900	0.027	13.704	0.057
Surface Righting	1	12.417	<0.001	6.622	0.010	6.389	0.604
Avg. Linear Acc. + Surface Righting	2	18.882	<0.001	3.554	0.059	6.569	0.584
Power + Surface Righting	2	23.816	<0.001	4.590	0.032	3.050	0.931
Peak Angular Vel. + Surface Righting	2	10.027	0.007	1.065	0.302	4.795	0.685
Avg. Angular Vel. + Surface Righting	2	10.096	0.006	1.120	0.290	5.877	0.554
Avg. Angular Acc. + Surface Righting	2	23.584	<0.001	3.415	0.065	2.921	0.939
Avg. Linear Acc. + Peak Angular Vel.	2	18.128	<0.001	4.175	0.041	2.944	0.890
Avg. Linear Acc. + Avg. Angular Vel.	2	18.706	<0.001	5.002	0.025	4.180	0.759
Avg. Linear Acc. + Avg. Angular Acc.	2	12.302	0.002	3.507	0.061	3.232	0.863
				3.575	0.059		

Table A-4: Significance test for univariate and multivariate logistic regression models for biomarkers to predict TAI.

Predictor	d.f.	Likelihood Ratio Test		Wald Statistic Test		H-L Test	
		Statistic	p-value	Statistic	p-value	Statistic	p-value
NF-H CSF	1	10.708	0.001	6.231	0.013	12.027	0.150
NF-H Serum	1	18.882	0.002	6.145	0.012	9.062	0.337
GFAP CSF	1	13.075	0.001	7.420	0.006	5.381	0.716
GFAP Serum	1	18.633	0.001	6.291	0.012	8.409	0.395
IL-6 CSF	1	20.434	0.004	2.163	0.141	5.786	0.671
IL-6 Serum	1	28.772	0.792	0.349	0.554	12.290	0.139
A β CSF	1	27.515	0.250	1.072	0.300	7.444	0.490
A β Serum	1	24.868	0.056	1.793	0.181	6.859	0.552
NF-H + GFAP	2	8.135	0.097	3.254	0.121	3.486	0.423
				3.412	0.132		
NF-H + IL-6	2	12.427	0.102	3.014	0.152	8.425	0.324
				2.943	0.168		

REFERENCES

- Aarden, L. A., De Groot, E. R., Schaap, O.L. and Lansdorp, P. M. (1987). Production of hybridomas growth factor by human monocytes. *Eur J Immunol* 17, 1411-1416.
- Abrahamson, E. E., Ikonovic, M. D., Ciallella, J. R., Hope, C. E., Paljug, W. R., Isanski, B. A, Flood, D. G., 2006. Caspase inhibition therapy abolishes brain trauma-induced increases in Abeta peptide: implications for clinical outcome. *Experimental neurology*, 197(2), 437-450.
- Adams, J. (1986). Methods in behavioral teratology, in *Handbook of Behavioral Teratology*, Riley, E.P. and Vorhees, C.V., Eds, Plenum Press, New York, p.67.
- Adams, J.H., Graham, D.I., Murray, L.S., and Scott, G. (1982). Diffuse axonal injury due to nonmissile head injury in humans: an analysis of 45 cases. *Ann Neurol.* 12, 557-563.
- Adams, J., Doyle, D., Graham, D., Lawrence, A., McLellan, D. (1984). Diffuse axonal injury in head injuries caused by a fall. *Lancet* 2:1420–1422.
- Adelson, P.D., Dixon, C.E., and Kochanek, P.M. (2000). Long-term dysfunction following diffuse traumatic brain injury in the immature rat. *J. Neurotrauma* 17, 273-282.
- Adelson, P.D., Dixon, C.E., Robichaud, P., and Kochanek, P.M. (1997). Motor and cognitive functional deficits following diffuse traumatic brain injury in the immature rat. *J. Neurotrauma* 14, 99-108.
- Adelson, P.D., Jenkins, L.D., and Hamilton, R.L. (2001). Histopathologic response of the immature rat to diffuse traumatic brain injury. *J. Neurotrauma* 18, 967-976.

- Ahmed, F., Gyorgy, A., Kamnaksh, A., Ling, G., Tong, L., Parks, S., Agoston, D., 2012. Time-dependent changes of protein biomarker levels in the cerebrospinal fluid after blast traumatic brain injury. *Electrophoresis*, 33, 3705-3711.
- Anderson, K. J., Scheff, S. W., Miller, K. M., Roberts, K. N., Gilmer, L. K., Yang, C., Shaw, G., 2008. The phosphorylated axonal form of the neurofilament subunit NF-H (pNF-H) as a blood biomarker of traumatic brain injury. *J.Neurotrauma*, 25(9), 1079-1085.
- Anderson, R.W.G., Brown, C.J., Scott, G., et al., (1997). Biomechanics of a sheep model of axonal injury, in: *Proceedings of the International IRCOBI Conference on the Biomechanics of Impact*, pps. 181–192.
- Anderson, R.W.G., Brown, C.J., Blumbergs, P.C., McLean, A.J., and Jones, N.R. (2003). Impact mechanics and axonal injury in a sheep model. *J. Neurotrauma*. 20, 961-974.
- Andruszkow, H., Fischer, J., Sasse, M. et al. (2014). Interleukin-6 as inflammatory marker referring to multiple organ dysfunction syndrome in severely injured children. *Scand J Trauma Resusc Emerg Med* 22, 16.
- Arslanoglu, A., Bonekamp, D., Barker, P.B., Horska A. (2004). Quantitative proton MR spectroscopic imaging of the mesial temporal lobe. *J Magn Reson Imaging* 20:772-778.
- Ashwal, S., Holshouser, B.A., Tong, K.A. (2006). Use of advanced neuroimaging techniques in the evaluation of pediatric traumatic brain injury. *Dev Neurosci* 28:309–26.

- Bain, A.C., Raghupathi, R., and Meaney, D.F. (2001). Dynamic stretch correlates to both morphological abnormalities and electrophysiological impairment in a model of traumatic axonal injury. *J. Neurotrauma* 18, 499-511.
- Baker, E.H., Basso, G., Barker, P.B., Smith, M.A., Bonekamp, D., Horska A. (2008). Regional apparent metabolite concentrations in young adult brain measured by (1)H MR spectroscopy at 3 Tesla. *J Magn Reson Imaging* 27:489-499.
- Bandak, F.A., and Eppinger, R.H. (1994). A three-dimensional finite element analysis of the human brain under combined rotational and translational accelerations. 37th Stapp Car Crash Conference, SAE 942215.
- Beaumont, A., Marmarou, A., Czigner, A., Yamamoto, M., Demetriadou, K., and Shirovani, T. (1999). The impact-acceleration model of head injury: injury severity predicts motor and cognitive performance after trauma. *Neurol. Res.* 21, 742-754.
- Beck, J.R., and Shultz, E.K. (1986). The use of relative operating characteristic (ROC) curves in test performance evaluation. *Arch. Pathol. Lab Med.* 110(1), 13-20.
- Bell, M. J., Kochanek, P. M., Doughty, L. A., Carcillo, J. A., Adelson, P. D., Clark, R. S. B., Wisniewski, S. R., 1997. Interleukin-6 and interleukin-10 in cerebrospinal fluid after traumatic brain injury in children. *J. Neurotrauma*, 14, 451-457.
- Berger, R. P., 2006. The use of serum biomarkers to predict outcome after traumatic brain injury in adults and children. *J. Head Trauma Rehabilitation*, 21(4), 315-333.
- Berger, R. P., Beers, S. R., Richichi, R., Wiesman, D., Adelson, P. D., 2007. Serum biomarker concentrations and outcome after pediatric traumatic brain injury. *J. Neurotrauma*, 24(12), 1793-1801.

- Berger, R. P., Ta'asan, S., Rand, A., Lokshin, A., Kochanek, P., 2008. Multiplex assessment of serum biomarker concentrations in well-appearing children with inflicted traumatic brain injury. *Pediatr. Res.*, 65, 97–102.
- Berger, R. P., Adelson, P. D., Pierce, M. C., Dulani, T., Cassidy, L. D., Kochanek, P. M., 2005. Serum neuron-specific enolase, S100B, and myelin basic protein concentrations after inflicted and noninflicted traumatic brain injury in children. *J. Neurosurg.*, 103, 61–68.
- Bigler, E.D., Ryser, D.K., Gandhi, P. et al., (2006). Day-of injury computerized tomography, rehabilitation status, and development of cerebral atrophy in persons with traumatic brain injury. *Am J Phys Med Rehabil* 85:793–806.
- Bland, M. (2000). *An introduction to medical statistics*. 3rd edition. Oxford university press, Oxford, UK.
- Blennow, K., Jonsson, M., Andreasen, N., Rosengren, L., Wallin, A., Hellstrom, P. A., and Zetterberg, A. 2011. No neurochemical evidence of brain injury after blast overpressure by repeated explosions or firing heavy weapons. *Acta Neurol. Scand.* 123, 245–251.
- Blumbergs, P.C. (1997). Pathology, in Reilly P and Bullock R (ed): *Head Injury*. London: Chapman & Hill, pps 39-70.
- Bradley, W.G. (1993). MR appearance of hemorrhage in the brain. *Radiology* 189:15–26.
- Brody, D. L., Magnoni, S., Schwetye, K. E., Spinner, M. L., Esparza, T. J., Stocchetti, N., Zipfel, G. J. and Holtzman, D. M. (2008). Amyloid-beta dynamics correlate with neurological status in the injured human brain. *Science*. 321(5893), 1221-1224

- Büki, A., Povlishock, J. T., 2006. All roads lead to disconnection? Traumatic axonal injury revisited. *Actaneurochirurgica*, 148(2), 181-93; discussion 193-194.
- Carré E., Cantais, E., Darbin, O., Terrier, J.P., Lonjon, M., Palmier, B., and Risso, J.J. (2004). Technical aspects of an impact acceleration traumatic brain injury rat model with potential suitability for both microdialysis and PtiO₂ monitoring. *J. Neurosci. Methods* 30, 23-28.
- Cenci, M.A., Whishaw, I.Q., Schallert, T. (2002). Animal models of neurological deficits: how relevant is the rat? *Nat Rev Neurosci* 3: 574–579.
- Centers for Disease Control and Prevention (2011). Nonfatal Traumatic Brain Injuries Related to Sports and Recreation Activities Among Persons Aged ≤19 Years — United States, 2001 – 2009. *MMWR* 2011; 60(39):1337 – 1342.
- Cernak, I. (2005). Animal models of head trauma. *NeuroRx*. 2, 410-422.
- Cernak, I., Chapman, S.M., Harnlin, G.P., and Vink, P. (2002). Temporal characterization of pro- and anti-apoptotic mechanisms following diffuse traumatic brain injury in rats. *J. Clin. Neurosci.* 9, 565-572.
- Cernak, I. Noble-Haeusslein, L. J. (2010). Traumatic brain injury: an overview of pathobiology with emphasis on military populations. *J. Cereb. Blood Flow Metab.* 30:255–266.
- Cernak I, Vink R, Zapple DN, Cruz MI, Ahmed F, Chang T. (2004). The pathobiology of moderate diffuse traumatic brain injury as identified using a new experimental model of injury in rats. *Neurobiol. Dis.* 17:29-43.

- Chen, X. H., Siman, R., Iwata, A., Meaney, D. F., Trojanowski, J. Q., Smith, D. H., 2004. Long-term accumulation of amyloid-beta, beta-secretase, presenilin-1, and caspase-3 in damaged axons following brain trauma. *Am. J. Pathol.*, 165, 357–371.
- Chiaretti, A., Genovese, O., Aloe, L., Antonelli, A., Piastra, M., Polidori, G., Di Rocco, C., 2005. Interleukin 1beta and interleukin 6 relationship with paediatric head trauma severity and outcome. *Childs Nerv.Syst.*, 21(3), 185-93; discussion 194.
- Czeiter, E., Pal, J., Kovesdi, E., Bukovics, P., Luckl, J., Doczi, T., and Buki, A. (2008). Traumatic axonal injury in the spinal cord evoked by traumatic brain injury. *J. Neurotrauma* 25, 205-213.
- Dash, P. K., Zhao, J., Hergenroeder, G., Moore, A. N., 2010. Biomarkers for the diagnosis, prognosis, and evaluation of treatment efficacy for traumatic brain injury. *Neurotherapeutics*, 7(1), 100-114.
- Deck, C., and Willinger, R. (2008). Improved head injury criteria based on head model. *Int J. Crashworthiness* 13, 667-678.
- DeKosky, S. T., Abrahamson, E. E., Ciallella, J. R., Paljug, W. R., Wisniewski, S. R., Clark, R. S., Ikonovic, M. D., 2007. Association of increased cortical soluble abeta42 levels with diffuse plaques after severe brain injury in humans. *Arch. Neurol.*, 64, 541–544.
- Dieterich, D.C., Bockers T.M., and Gundelfinger E.D. (2002). Screening for differentially expressed genes in the rat inner retina and optic nerve after optic nerve crush. *Neurosci. Lett.* 317, 29-32.
- Dilorenzo, F.A. (1976). Power and bodily injury. Automotive engineering congress and exposition, SAE paper, No.760014.

- DiLeonardi, A.M., Huh, J.W., and Raghupathi, R. (2009). Impaired axonal transport and neurofilament compaction occur in separate populations of injured axons following diffuse brain injury in the immature rat. *Brain Res.* 1263, 174-182.
- Dixon, C.E., Clifton, G.L., Lighthall, J.W., Yaghmai, A.A., and Hayes, R.L. (1991). A controlled cortical impact model of traumatic brain injury in the rat. *J. Neurosci. Methods* 39, 253-262.
- Dixon, C.E., Lyeth, B.G., Povlishock, J.T., Findling, R.L., Hamm, R.J., and Marmarou A. (1987). A fluid percussion model of experimental brain injury in the rat. *J. Neurosurg.* 67, 110-119
- Ducreux, D., Huynh, I., Fillard, P. et al., (2005). Brain MR diffusion tensor imaging and fibre tracking to differentiate between two diffuse axonal injuries. *Neuroradiology* 47:604–8.
- Duma, S.M., Manoogian, S.J., Bussone, W.R., Broinson, P.G., Goforth, M.W., Donnenwerth, J.J., Greenwald, R.M., Chu, J.J., and Crisco, J.J. (2005). Analysis of real-time head accelerations in collegiate football players. *Clin. J. Sport Med.* 15, 3-8.
- Erta, M., Quintana, A. and Hidalgo, J (2012). Interleukin-6, a major cytokine in the central nervous system. *Int J Biol Sci* 8(9), 1254-1266.
- Faul, M., Xu, L., Wald, M.M., Coronado, V.G. (2010). Traumatic brain injury in the United States: emergency department visits, hospitalizations, and deaths. Atlanta (GA): Centers for Disease Control and Prevention, National Center for Injury Prevention and Control.

- Fei., Z., Zhang, X., and Bai, H.M. (2006). Metabotropic glutamate receptor antagonists and agonists: potential neuroprotectors in diffuse brain injury. *J. Clin. Neurosci.* 13, 1023-1027.
- Fei., Z., Zhang, X., Bai, H.M., Jiang, X.F., Li, X., Zhang, W., and Hu, W. (2007). Posttraumatic secondary brain insults exacerbates neuronal injury by altering metabotropic glutamate receptors. *BMC Neurosci.* 17, 96.
- Ferreira, L. C., Regner, A., Miotto, K. D. et al. (2014). Increased levels of interleukin-6, -8 and -10 are associated with fatal outcome following severe traumatic brain injury. *Brain Inj.* 28, 1311–1316.
- Fijalkowski, R.J., Stemper, B.D., Pintar, F.A., Yoganandan, N., Crowe, M.J., and Gennarelli T.A. (2007). New rat model for diffuse brain injury using coronal plane angular acceleration. *J. Neurotrauma* 24, 1387-1398.
- Fischer, J., Mathieson, C. (2001). The History of the Glasgow Coma Scale: Implications for Practice. *Crit. Care Nurs. Q.*, 23, 52-58.
- Foda, M.A., and Marmarou, A. (1994). A new model of diffuse brain injury in rats, Part II: morphological characterization. *J. Neurosurg.* 80, 301-313.
- Franklyn, M., Fildes, B., Zhang, L., Yang, K.H., and Sparke, L. (2005). Analysis of finite element models for head injury investigation: Reconstruction of four real-world impacts. *Stapp Car Crash J.* 49, 1-32.
- Finkelstein, E., Corso, P., and Miller, T. (2006). The incidence and economic burden of injuries in the United States. New York: Oxford University Press.
- Gadd, C.W. (1966). Use of weighted-impulse criterion for establishing injury hazard. 10th stapp car crash conference proceedings, 164.

- Galbraith, J.A., Thibault, L.E., and Matteson, D.R. (1993). Mechanical and electrical responses of the squid giant axon to simple elongation. *J. Biomech. Eng.* 115, 13-22.
- Garman, R. H. (2011). Blast exposure in rats with body shielding is characterized primarily by diffuse axonal injury. *J. Neurotrauma* 28:947–959.
- Gatson, J. W., Barillas, J., Hynan, L. S., Diaz-Arrastia, R., Wolf, S. E., and Minei, J. P. (2014). Detection of neurofilament-H in serum as a diagnostic tool to predict injury severity in patients who have suffered mild traumatic brain injury. *J. Neurosurg.* 121, 1232–1238.
- Geeraerts, T., Ract, C., Tardieu, M., Fourcade, O., Mazoit, J.X., Benhamou, D., Duranteau, J., and Vigué B. (2006). Changes in cerebral energy metabolites induced by impact-acceleration brain trauma and hypoxic-hypotensive injury in rats. *J. Neurotrauma* 23, 1059-1071.
- Gennarelli, T.A., Adams, J.H., and Graham, D.I. (1981). Acceleration induced head injury in the monkey.I. The model, its mechanical and physiological correlates. *Acta Neuropathol. Suppl. (Berl)* 7, 23-25.
- Gennarelli, T.A., Pintar, F.A., and Yognandan, N. (2003). Biomechanical tolerances for diffuse brain injury and a hypothesis for genotypic variability in response to trauma. *Annual Proc Assoc Adv Automotive Med.* 47, 624-628.
- Gennarelli, T.A., Thibault, L.E., Adams, J.H., Graham, D.I., Thompson, C.J., and Marcincin, R.P. (1982). Diffuse axonal injury and traumatic coma in the primate. *Ann Neurol.* 12, 564-574.
- Gennarelli, T.A., Thibault, L.E., and Graham, D.I. (1998). Diffuse axonal injury: An important form of traumatic brain damage. *Neuroscientist* 4, 202-215.

- Gennarelli, T.A., Thibault, L.E., and Tipperman, R. (1989). Axonal injury in the optic nerve: a model simulating diffuse axonal injury in the brain. *J. Neurosurg.* 71, 244-253.
- Gentleman SM, Roberts GW, Gennarelli TA, Maxwell WL, Adams JH, Kerr S, Graham DI (1995). Axonal injury: a universal consequence of fatal closed head injury. *ActaNeuropathol* 89:537–543.
- Gilchrist, M.D. (2004). Experimental device for simulating traumatic brain injury resulting from linear accelerations. *Strain* 40, 180-192.
- Goldsmith, W., and Ommaya, A.K. (1984). Head and neck injury criteria and tolerance levels, in: *The Biomechanics of Impact Trauma*. B. Aldman and A. Chapon (eds), Elsevier: Amsterdam, pps. 149–187.
- Gutierrez, E., Huang, Y., Haglid, K., Bao, F., Hansson, H.A., Hamberger, A., and Viano, D. (2001). A new model for diffuse brain injury by rotational acceleration : I model, gross appearance, and astrogliosis. *J. Neurotrauma* 18, 247-257.
- Gyorgy, A., Ling, G., Wingo, D., et al. (2011). Time-dependent changes in serum biomarker levels after blast traumatic brain injury. *J. Neurotrauma* 28, 1121–1126.
- Hans, V., Kossmann, T., Lenzlinger, P. M. et al. (1999). . Experimental axonal injury triggers interleukin-6 mRNA, protein synthesis and release into cerebrospinal fluid. *Journal of Cerebral Blood Flow & Metabolism* 19, 184–194.
- Hayakawa, K., Okazaki, R., Ishii, K., Ueno, T., Izawa, N., Tanaka, Y., et al. (2012). Phosphorylated neurofilament subunit NF-H as a biomarker for evaluating the severity of spinal cord injury patients, a pilot study. *Spinal Cord* 50, 493–496.

- Heath, D.L., and Vink, R. (1999). Improved motor outcome in response to magnesium therapy received up to 24 hours after traumatic diffuse axonal brain injury in rats. *J. Neurosurg.* 90, 504-509.
- Hergenroeder G. W., Moore, A. N. McCoy, J. P. et al. (2010). Serum IL-6: a candidate biomarker for intracranial pressure elevation following isolated traumatic brain injury. *Journal of Neuroinflammation* 7, 19.
- Honda M., Tsuruta R., Kaneko T. (2010). Serum glial fibrillary acidic protein is a highly specific biomarker for traumatic brain injury in humans compared with S-100B and neuron-specific enolase. *J. Trauma*, 69(1), 104–109.
- Huisman, T.A. (2003). Diffusion-weighted imaging: basic concepts and application in cerebral stroke and head trauma. *Eur Radiol* 13:2283–97.
- Ikonomovic, M. D., Uryu, K., Abrahamson, E. E., Ciallella, J. R., Trojanowski, J. Q., Lee, V. M., Clark, R. S., Marion, D. W., Wisniewski, S. R. and DeKosky, S. T. (2004). Alzheimer's pathology in human temporal cortex surgically excised after severe brain injury. *Exp Neurol.* 190(1), 192-203.
- Ingebrigtsen, T., Romner, B. (2002). Biochemical serum markers of traumatic brain injury. *J. Trauma*, 52, 798–808.
- Kallakuri, S., Cavanaugh, J. M., Ozaktay, A. C. and Takebayashi, T. (2003). The effect of varying impact energy on diffuse axonal injury in the rat brain: a preliminary study. *Exp. Brain Res.* 148, 419–424.
- Kallakuri, S., Kreipke, C.W., Rossi, N., Rafols, J.A., and Petrov, T. (2007). Spatial alterations in endothelin receptor expression are temporally associated with the altered microcirculation after brain trauma. *Neurol. Res.* 29, 362-368.

- Kelley, B.J., Farkas, O., Lifshitz, J., and Povlishock, J.T. (2006). Traumatic axonal injury in the perisomatic domain triggers ultrarapid secondary axotomy and Wallerian degeneration. *Exp. Neurol.* 198, 350-360.
- King, A.I. (2000). Fundamentals of impact biomechanics: biomechanics of the head, neck and thorax. *Annu. Rev. Biomed. Eng.* 2, 55-81.
- King, A.I., Ruan, J.S., Zhou, C., Hardy, W.N., Khalil, T.B. (1995). Recent advances in biomechanics of brain injury research. *J. Neurotrauma* 12, 651-658.
- King, A.I., Yang, K.Y., Zhang, L., Hardy, W.N., and Viano, D.C. (2003). Is head injury caused by linear or angular acceleration? Bertil Aldman Lecture, International IRCOBI Conference on the Biomechanics of Impact.
- Kleiven, S. (2007). Predictors for traumatic brain injuries evaluated through accident reconstructions. *Stapp car crash J.* 51, 81-114.
- Kleiven S. (2013). Why most traumatic brain injuries are not caused by linear acceleration but skull fractures are. *Front. Bioeng. Biotechnol.* 1:15.
- Kuehn, R. (2011). Rodent model of direct cranial blast injury. *J. Neurotrauma* 28:2155–2169.
- Kvesdi, E., Lückl, J., Bukovics, P. et al. (2010). Update on protein biomarkers in traumatic brain injury with emphasis on clinical use in adults and pediatrics. *Acta Neurochir (Wien)*. 152(1):1-17.
- Laureys, S., Majerus, S., Moonen, G., 2002. Assessing Consciousness in Critically Ill Patients. in: 2002 Yearbook of Intensive Care and Emergency Medicine. VINCENT J. L. (ed.). Berlin, Springer, pp 715-727.

- Li, Y., Zhang, L., Kallakuri, S., Zhou, R., Cavanaugh, J. M., 2011a. Quantitative relationship between axonal injury and mechanical response in a rodent head impact acceleration model. *Journal of neurotrauma*, 28(9), 1767-1782.
- Li, Y., Zhang, L.Y., Kallakuri, S., Zhou, R., Cavanaugh, J.M., 2011b. Injury predictors for traumatic axonal injury in a rodent impact acceleration model. *Stapp Car Crash Journal*, 55, 25-47.
- Lighthall, J.W. (1988). Controlled cortical impact: a new experimental brain injury model. *J. Neurotrauma* 5, 1-15.
- Linda, P., Salvatore, S., Gretchen, B., et al. (2014). GFAP out-performs S100 β in detecting traumatic intracranial lesions on computed tomography in trauma patients with mild traumatic brain injury and those with extracranial lesions. *Journal of Neurotrauma*. November 15, 2014, 31(22): 1815-1822.
- Lissner, H.R., Lebow, M., and Evans, G. (1960). Experimental studies on the relation between acceleration and intracranial pressure changes in man. *Surg. Gynec. Obst. U.S.A.* 111, 329-338.
- Liu, L., Duff, K., 2008. A technique for serial collection of cerebrospinal fluid from the cisterna magna in mouse. *J. Vis. Exp.*, 10, 21.
- Lo, T. Y., Jones, P. A., Minns, R. A., 2009. Pediatric brain trauma outcome prediction using paired serum levels of inflammatory mediators and brain specific proteins. *J. Neurotrauma*, 26, 1479–1487.
- Loane, D. J., Pocivavsek, A., Moussa, C. E., et al. (2009). Amyloid precursor protein secretases as therapeutic targets for traumatic brain injury. *Nat Med.* 15(4), 377–379.

- Lumpkins, K. M., Bochicchio, G. O., Keledjian, K., Simard, J. M., Mccunn, M., Scalea, T., 2008. Glial Fibrillary Acidic Protein is Highly Correlated With Brain Injury. *J. Trauma*, 65(4), 778-782; discussion 782-784.
- Margulies, S.S., and Thibault, L.E. (1992). A proposed tolerance criterion for diffuse axonal injury in man. *J. Biomech.* 25, 917-923
- Margulies, S.S., Thibault, L.E., and Gennarelli, T.A. (1985). A study of scaling and head injury criteria using physical model experiments. Proceedings of the IRCOB/AAAM conference, 13-15.
- Marmarou, A., Foda, M.A., Brink, W.V., Campbell, J., Kita, H., and Demetriadou, K. (1994). A new model of diffuse brain injury in rats. Part I: Pathophysiology and biomechanics. *J. Neurosurg.* 80, 291–300.
- Marmarou, A., Signoretti, S., Aygok, G., Fatouros, P., and Portella, G. (2006). Traumatic brain edema in diffuse and focal injury: cellular or vasogenic? *Acta Neurochir. Suppl.* 96, 24-29.
- Marmarou, C.R., and Povlishock, J.T. (2006). Administration of the immunophilin ligand FK506 differentially attenuates neurofilament compaction and impaired axonal transport in injured axons following diffuse traumatic brain injury. *Exp. Neurol.* 197, 353-362.
- Marmarou, C.R., Walker, S.A., Davis, C.L., and Povlishock, J.T. (2005). Quantitative analysis of the relationship between intra- axonal neurofilament compaction and impaired axonal transport following diffuse traumatic brain injury. *J. Neurotrauma* 22, 1066-1080.

- Marszalek, J. R., Williamson, T. L., Lee, M. K. Xu, Z., Hoffman, P.N. et al., 1996. Neurofilament subunit NF-H modulates axonal diameter by selectively slowing neurofilament transport. *J. Cell Biology*, 135(3), 711-724.
- Masters, C. L., Cappai, R., Barnham, K. J., Vilmagne, V. L., 2006. Molecular mechanisms for Alzheimer's disease: implications for neuroimaging and therapeutics. *J. Neurochem.*, 97, 1700–1725.
- Maxwell, W.L., and Graham, D.I. (1997). Loss of axonal microtubules and neurofilaments after stretch-injury to guinea pig optic nerve fibers. *J. Neurotrauma* 14, 603-614.
- Maxwell, W.L., Kansagra, A.M., Graham, D.I., Adams, J.H., Gennarelli, TA. (1988). Freeze-fracture studies of reactive myelinated nerve fibres after diffuse axonal injury. *Acta Neuropathol. (Berl)* 76, 395-406.
- Maxwell, W. L., Watt, C., Graham, D. I., and Gennarelli, T. A. (1993). Ultrastructural evidence of axonal shearing as a result of lateral acceleration of the head in non-human primates. *Acta Neuropathol.* 86, 136–144.
- McCracken, E., Hunter, A., Patel, S., Graham, D., De-war, D. (1999). Calpain activation and cytoskeletal protein breakdown in the corpus callosum of head-injured patients. *J Neurotrauma.*16:749–761.
- McElhaney, J.H., Roberts, V.L., Hilyard, J.F. (1976). *Handbook of Human Tolerance.* Ibaraki, Japan: Automob. Res. Inst. 289pp.
- McGowan, J., McCormack, T., Grossman, R. (1999). Diffuse axonal pathology detected with magnetiza- tion transfer imaging following brain injury in the pig. *Magn Reson Med.*41:727–733.

- McIntosh, T. K., Noble, L., Andrews, B. Faden, A. I. (1987). Traumatic brain injury in the rat: characterization of a midline fluid-percussion model. *Cent. Nerv. Syst. Trauma* 4, 119–134.
- McIntosh, A.D., Kallieris, D., Mattern, R., and Miltner, E. (1989). Traumatic brain injury in the rat: Characterization of a lateral fluid-percussion model. *Neuroscience* 28, 233-244.
- Mclean, A.J. (1995). Brain injury without head impact? *J. Neurotrauma* 12, 621-625.
- McMahon, P. J., Panczykowski, D., Yue, J. K., et al., (2014). Measurement of the GFAP-BDP biomarker for the detection of traumatic brain injury compared to CT and MRI. *J Neurotrauma*. [Epub ahead of print].
- Meaney, D.F., Smith, D.H., Ross, D.T., and Gennarelli, T.A. (1993). Diffuse axonal injury in miniature pig: Biomechanical development and injury threshold. *Cashworthiness and Occupant Protection in Transportation Systems, ASME*. 169, 169-175.
- Meaney, D.F., Smith, D.H., Shreiber, D.I., Brain, A.C., Miller, R.T., Ross, D.T., and Gennarelli, T.A. (1995). Biomechanical analysis of experimental diffuse axonal injury. *J. Neurotrauma* 12, 689-694.
- Metting, Z., Wilczak, N., Rodiger, L. A., Schaaf, J. M. and van der Naalt, J. (2012). GFAP and S100B in the acute phase of mild traumatic brain injury. *Neurology* 78, 1428–1433.
- Meythaler, J. M., Peduzzi, J. D., Eleftheriou, E., Novack, T. A., 2001. Current concepts: Diffuse axonal injury associated traumatic brain injury. *Archives of Physical Medicine and Rehabilitation*, 82(10), 1461-1471.

- Mondello, S., Muller, U., Wang, W. W., 2011. Blood-based diagnostics of traumatic brain injuries. *Expert Rev. Mol. Diagn.*, 11(1), 65-78.
- Morales, D.M., Marklund, N., Lebold, D., et al. (2005). Experimental models of traumatic brain injury : do we really need to build a better mousetrap? *Neuroscience* 136, 971-989.
- Murai, H., Detre, J., McIntosh, T., Smith, D. (1996). Detection of acute pathologic changes following experimental traumatic brain injury using diffusion- weighted magnetic resonance imaging. *J Neuro- trauma* 13:515–521.
- Naganawa, S., Sato, C., Ishihira, S. et al., (2004). Serial evaluation of diffusion tensor brain fiber tracking in a patient with severe diffuse axonal injury. *Am J Neuroradiol* 25:1553–6.
- Newman, J.A. (1998). Kinematics of head injury – an overview. *Frontiers of head and neck trauma: clinical and biomechanical*, IOS press Inc., Burke, Virginia, 200-214.
- Newman, J.A., Beusenbergh, M.C., Shewchenko, N., Withnall, C., and Fournier, E. (2005). Verification of biomechanical methods employed in a comprehensive study of mild traumatic brain injury and the effectiveness of American football helmets. *J. Biomech.* 38, 1469-1481.
- Newman, J. A., Shewchenko, N., Welbourne, E. (2000). A new biomechanical head injury assessment function: the maximum power index. In: *Proc. 44th STAPP Car Crash Conf.*
- Nishimoto, T., and Murakami, S. (1998). Relation between diffuse axonal injury and internal head structures on blunt impact. *J. Biomech. Eng.* 120, 140-147.

- Nylen, K., 2006. Increased serum-GFAP in patients with severe traumatic brain injury is related to outcome. *J.Neurol.Sciences*, 240, 85-91.
- Olsson, A., Csajbok, L., Ost, M., Höglund, K., Nylén, K., Rosengren, L., Nellgård, B., Blennow, K. (2004). Marked increase of beta-amyloid(1-42) and amyloid precursor protein in ventricular cerebrospinal fluid after severe traumatic brain injury. *J Neurol.*, 251(7), 870-876.
- Ommaya, A.K., Faas, F., Yarnell, P. (1968). *J. Am. med. Ass.* 204: 285-289.
- Papa, L., Lewis, L. M., Falk, J. L., et al. (2012). Elevated levels of serum glial fibrillary acidic protein breakdown products in mild and moderate traumatic brain injury are associated with intracranial lesions and neurosurgical intervention. *Ann. Emerg. Med.* 59, 471–483.
- Papa, L., Ramia, M.M., Kelly, J.M. et al. (2013). Systematic review of clinical research on biomarkers for pediatric traumatic brain injury. *J Neurotrauma.* 30(5):324-38.
- Papa, L., Robinson, G., Oli, M. W., 2008. Use of biomarkers for diagnosis and management of traumatic brain injury patients. *Expert Opin. Med. Diagn.*, 2, 937–945.
- Pape, H.C., Giannoudis, P., Krettek, C. (2002). The timing of fracture treatment in polytrauma patients: relevance of damage control orthopedic surgery. *Am. J. Surg.* 183, 622-629.
- Park, C.O., and Yi, H.G. (2001). Apoptotic change and NOS activity in the experimental animal diffuse axonal injury model. *Yosei Med. J.* 42, 518-526.
- Pascual, J.M., Solivera, J., Prieto, R., Barrios, L., López-Larrubia, P., Cerdán, S., and Roda, J.M. (2007). Time course of early metabolic changes following diffuse

- traumatic brain injury in rats as detected by (1)H NMR spectroscopy. *J. Neurotrauma* 24, 944-959.
- Paxinos, G., and Watson, C. (2007). *The Rat Brain in Stereotaxic Coordinates*. 6th ed. Sydney, Academic Press.
- Peduzzi, P., Concato, J., Kemper, E., Holford, T.R., and Feinstein, A.R. (1996). A simulation study of the number of events per variable in logistic regression analysis. *J. Clinical Epidemiology* 49, 1373-1379.
- Pelinka, L. E., Kroepfl, A., Leixnering, M., Buchinger, W., Raabe, A., Redl, H., 2004. GFAP versus S100B in serum after traumatic brain injury: relationship to brain damage and outcome. *J. neurotrauma*, 21(11), 1553-1561.
- Pelinka, L.E., Hertz, H., Mauritz, W., Harada, N., Jafarmadar, M., Albrecht, M., Redl, H., Bahrami, S. 2005. Nonspecific increase of systemic neuron-specific enolase after trauma: clinical and experimental findings. *Shock*, 24, 119–123.
- Petrova, T.V., 2000. Modulation of glial activation by astrocyte-derived protein S100B: differential responses of astrocyte and microglial cultures. *Brain research*, 853, 74-80.
- Pettus, E.H., and Povlishock, J.T. (1996). Characterization of a distinct set of intra-axonal ultrastructural changes associated with traumatically induced alteration in axolemmal permeability. *Brain Res.* 722, 1-11.
- Petzold, A. (2007). CSF biomarkers for improved prognostic accuracy in acute CNS disease. *Neurol Res.* 29(7), 691-708.
- Pierce, J. E., Trojanowski, J. Q., Graham, D. I., Smith, D. H., McIntosh, T. K., 1996. Immunohistochemical characterization of alterations in the distribution of amyloid

precursor proteins and beta-amyloid peptide after experimental brain injury in the rat. *J. Neurosci.*, 16, 1083–1090.

Pike, B.R., Zhao, X., Newcomb, J.K., Posmantur, R.M., Wang, K.K., Hayes, R.L. (1998).

Regional calpain and caspase-3 proteolysis of alpha-spectrin after traumatic brain injury. *Neuroreport*. 9(11):2437-42.

Pincemaille, Y., Trosseille, X., Mack, P. (1989). Some new data related to human

tolerance obtained from volunteer boxers, in: *Stapp Car Crash Conference*. pps. 177–190.

Pineda, J. A., Wang, K. K., Hayes, R. L., 2004. Biomarkers of Proteolytic Damage

Following Traumatic Brain Injury. *Brain Pathol.*, 14, 202-209.

Piper, I.R., Thomson, D., and Miller, J.D. (1996). Monitoring weight drop velocity and

foam stiffness as an aid to quality control of a rodent model of impact acceleration neurotrauma. *J. Neurosci. Methods* 69, 171-174.

Povlishock, J.T. (1993). Pathobiology of traumatically induced axonal injury in animals

and man. *Ann Emerg. Med.* 22, 980-986.

Povlishock, J.T. (1986). Traumatically induced axonal damage without concomitant

change in focally related neuronal somata and dendrites. *Acta Neuropathol. (Berl)* 70, 53-59.

Povlishock, J.T. (1992). Traumatically induced axonal injury: pathogenesis and

pathobiological implications. *Brain Pathol.* 2, 1-12.

Povlishock, J.T., and Becker, D.P. (1985). Fate of reactive axonal swellings induced by

head injury. *Lab Invest.* 52, 540-552.

- Povlishock, J.T., Becker, D.P., Cheng, C.L., and Vaughan, G.W. (1983). Axonal change in minor head injury. *J. Neuropathol. Exp. Neurol.* 42, 225-242.
- Povlishock, J.T., and Christman, C.W. (1995). The pathobiology of traumatically induced axonal injury in animals and humans: a review of current thoughts. *J. Neurotrauma* 12, 555-564.
- Povlishock, J.T., and Pettus, E.H. (1996). Traumatically induced axonal damage: evidence for enduring changes in axolemmal permeability with associated cytoskeletal change. *Acta Neurochir. Suppl.* 66, 81-86.
- Prange, M.T., Coats, B., Duhaime, A.C., and Margulies, S.S. (2003). Anthropomorphic simulations of falls, shakes, and inflicted impacts in infants. *J. Neurosurg.* 99, 143-150.
- Prasad, P., and Mertz, H.J. (1985). The position of the United States Delegation to the ISO working group 6 on the use of HIC in the automotive environment. SAE, Paper No. 851246.
- Price, D. L., Sisodia, S. S., Gandy, S. E., 1995. Amyloid beta amyloidosis in Alzheimer's disease. *Curr. Opin. Neurol.*, 8, 268–274.
- Rafols, J.A., Morgan, R., Kallakuri, S., Kreipke, C.W. (2007). Extent of nerve cell injury in Marmarou's model compared to other brain trauma models. *Neurol. Res.* 29, 348-355.
- Rhodes, J.K., Andrews, P.J., Holmes, M.C., and Seckl, J.R. (2002). Expression of interleukin-6 messenger RNA in a rat model of diffuse axonal injury. *Neurosci. Lett.* 335, 1-4.

- Riddle, A., Maire, J., Gong, X., Chen, K., Kroenke, C., Hohimer, A., Back, S. (2012). Differential susceptibility to axonopathy in necrotic and non-necrotic perinatal white matter injury. *Stroke* 43(1):178-84.
- Roberts, G.W., Gentleman, S.M., Lynch, A., Murray, L., Landon, M., Graham, D.I., 1994. Beta amyloid protein deposition in the brain after severe head injury: implications for the pathogenesis of Alzheimer's disease. *J. Neurol. Neurosurg. Psychiatry*, 57, 419–425.
- Ross, S., E., Leipold, C., Terregino, C., O., Malley, K., 1998. Efficacy of the Motor Component of the Glasgow Coma Scale in Trauma. *J. Trauma*, 45, 42-44.
- Ross, D.T., Meaney, D.F., Sabol, M.K., Smith, D.H., and Gennarelli, T.A. (1994). Distribution of forebrain diffuse axonal injury following inertial closed head injury in miniature swine. *Exp. Neurol.* 126, 291-299.
- Ruan, J.S., Khalil, T.B., and King, A.I. (1993). Finite element modeling of direct head impact. 37th stapp car crash conference proceedings, No.933114.
- Saatman, K. E., Duhaime, A. C., Bullock, R., Maas A. I. R., Valadka, A., Manley, G. T., 2008. Classification of traumatic brain injury for targeted therapies. *J. Neurotrauma*, 25, 719–738.
- Sandler, S. J. I., Figaji, A. A., Adelson, P. D., 2010. Clinical applications of biomarkers in pediatric traumatic brain injury. *Child's nervous system*, 26(2), 205-213.
- Sawauchi, S., Marmarou, A., Beaumont, A., Signoretti, S., and Fukui, S. (2004). Acute subdural hematoma associated with diffuse brain injury and hypoxemia in the rat: effect of surgical evacuation of the hematoma. *J. Neurotrauma* 21, 563-573.

- Sengul, G., Takci, E., Malcok, U.A., Akar, A., Erdogan, F., Kadioglu, H.H., and Aydin, I.H. (2008). A preliminary histopathological study of the effect of agmatine on diffuse brain injury in rats. *J. Clin. Neurosci.* 15, 1125-1129.
- Schmidt, R.H., Scholten, K.J., and Maughan, P.H. (2000). Cognitive impairment and synaptosomal choline uptake in rats following impact acceleration injury. *J. Neurotrauma* 17, 1129-1139.
- Shafieian, M., Darvish, K.K., and Stone, J.R. (2009). Changes to the viscoelastic properties of brain tissue after traumatic axonal injury. *J. Biomech.* 42, 2136-2142.
- Shaw, G., 1998. Neurofilaments. Springer-Verlag: New York.
- Shaw, G., Yang, C., Ellis, R., Anderson, K., Parker Mickle, J., Scheff, S., Pike, B., 2005. Hyperphosphorylated neurofilament NF-H is a serum biomarker of axonal injury. *Biochemical and biophysical research communications*, 336(4), 1268-1277.
- Shaw, G., Yang, C., Zhang, L., Cook, P., Pike, B. R., Hill, W. D., 2007. Characterization of the bovine neurofilament NF-M protein and cDNA sequence and identification of in vitro and in vivo calpain cleavage sites. *Biochem. Biophys. Res. Commun.*, 325, 619–625.
- Shenton, M.E., Hamoda, J.S., Schneiderman, J.S. et al., (2012). A review of magnetic resonance imaging and diffusion tensor imaging findings in mild traumatic brain injury. *Brain Imaging and Behavior* 6:137–192.
- Shreiber, D.I., Bain, A.C., Ross, T.D., Smith, D.H., Gennarelli, T.A., and McIntosh, T.D. (1999) Experimental investigation of cerebral contusion: histopathological and immunohistochemical evaluation of dynamic cortical deformation. *J Neuropathol Exp Neurol* 58: 153–164.

- Siman, R., McIntosh, T. K., Soltesz, K. M., Chen, Z., Neumar, R.W., Roberts, V. L., 2004. Proteins released from degenerating neurons are surrogate markers for acute brain damage. *Neurobiol. Dis.*, 16(2), 311-320.
- Siman, R., Toraskar, N., Dang, A., McNeil, E., McGarvey, M., Plaum, J., et al. (2009). A panel of neuron-enriched proteins as markers for traumatic brain injury in humans. *J. Neurotrauma* 26, 1867–1877.
- Singh, A., Lu, Y., Chen, C.Y., Kallakuri, S., and Cavanaugh, J.M. (2006). A new model of traumatic axonal injury to determine the effects of strain and displacement rates. *Stapp car crash J.* 50, 601-623.
- Sironi, M., Breviario, F., Proserpio, P., Biondi, A., Vecchi, V., Van Damme, J., Dejana, E. and Mantovani, A. (1989). IL-1 stimulates IL-6 production in endothelial cells. *J Immunol* 14 (2), 549-553.
- Smith, D. H. (1995). A model of parasagittal controlled cortical impact in the mouse: cognitive and histopathologic effects. *J. Neurotrauma* 12:169–178.
- Smith, M. (2003). Diffuse axonal injury in adults. *Trauma* 5, 227-234.
- Smith, D., Cecil, K., Meaney, D. (1998). Magnetic resonance spectroscopy of diffuse brain trauma in the pig. *J Neurotrauma* 15:665–674.
- Smith, D. H., Chen, X. H., Nonaka, M., Trojanowski, J. Q., Lee, V. M., Saatman, K. E., 1999. Accumulation of amyloid beta and tau and the formation of neurofilament inclusions following diffuse brain injury in the pig. *J. Neuropathol. Exp. Neurol.*, 58, 982–992.

- Smith, D.H., Chen, X.H., Xu, B.N., et al., (1997). Characterization of diffuse axonal pathology and selective hippocampal damage following inertial brain trauma in the pig. *J. Neuropathol. Exp. Neurol.* 56:822–834.
- Smith, D.H., and Meaney, D.F. (2000). Axonal damage in traumatic brain injury. *Neuroscientist* 6, 483-494.
- Sternberger, L.A., Sternberger, N.H., 1983. Monoclonal antibodies distinguish phosphorylated and nonphosphorylated forms of neurofilaments in situ. *Proc. Natl. Acad. Sci. USA*, 80, 6126–6130.
- Stone, J.R., Okonkwo, D.O., Dialo, A.O., Rubin, D.G., Mutlu, L.K., Povlishock, J.T., and Helm G.A. (2004). Impaired axonal transport and altered axolemmal permeability occur in distinct populations of damaged axons following traumatic brain injury. *Exp. Neurol.* 190, 59-69.
- Stone, J.R., Singleton, R.H., and Povlishock, J.T. (2001). Intra-axonal neurofilament compaction does not evoke local axonal swelling in all traumatically injured axons. *Exp. Neurol.* 172, 320-331.
- Strong, M.J., Strong, W.L., Jaffe, H., Traggert, B., Sopper, M.M., Pant, H.C., 2001. Phosphorylation state of the native high-molecular-weight neurofilament subunit protein from cervical spinal cord in sporadic amyotrophic lateral sclerosis. *J. Neurochem.*, 76, 1315–1325.
- Strich, S.J. (1956). Diffuse degeneration of the cerebral white matter in severe dementia following head injury. *J. Neurol. Neurosurg. Psychiatry* 19, 163-185.

- Suehiro, E., Singleton, R.H., Stone, J.R., and Povlishovk, J.T. (2001). The immunophilin ligand FK506 attenuates the axonal damage associated with rapid rewarming following posttraumatic hypothermia. *Exp. Neurol.* 172, 199-210.
- Tang-Schomer, M., Johnson, V., Baas, P., Stewart, W., Smith, D. (2012). Partial interruption of axonal transport due to microtubule breakage accounts for the formation of periodic varicosities after traumatic axonal injury. *Exp Neuro* 233(1):364-72.
- Tashlykov, V., Katz, Y., Gazit, V., Zahar, O., Schreiber, S., and Pick, C.G.. (2007). Apoptotic changes in the cortex and hippocampus following minimal brain trauma in mice. *Brain Res.* 1130, 197-205.
- Tavazzi, B., Signoretti, S., Lazzarino, G., Amorini, A.M., Delfini R., Cimatti, M., Marmarou, A., and Vagnozzi, R. (2005). Cerebral oxidative stress and depression of energy metabolism correlate with severity of diffuse brain injury in rats. *Neurosurgery* 56, 582-589.
- Teasdale, G., Jennett, B., 1974. Assessment of coma and impaired consciousness. A practical scale. *Lancet*, 2, 81-84.
- Teasdale, G., Jennett, B., 1976. Assessment and prognosis of coma after head injury. *Acta Neurochir. (Wien)*, 34, 45-55.
- Teasdale, G., Murray, L., 2000. Revisiting the Glasgow Coma Scale and Coma Score. *Intensive Care Med.*, 26, 153-154.
- Tian, L., Guo, R., Yue, X., Lv, Q., Ye, X., Wang, Z., Chen, Z., 2012. Intranasal administration of nerve growth factor ameliorate β -amyloid deposition after traumatic brain injury in rats. *Brain Research*, 1440, 47-55.

- Thornton, E., Vink, R., and Blumbergs, P.C. (2006). Soluble amyloid precursor protein alpha reduces neuronal injury and improves functional outcome following diffuse traumatic brain injury rats. *Brain Res.* 1094, 38-46.
- Toyama, Y., Kobayashi, T., Nishiyama, Y. et al., (2005). CT for acute stage of closed head injury. *Radiat Med* 23:309–16.
- Ucar, T., Tanriover, G., Gurer, I., Onal, M.Z., and Kazan, S. (2006). Modified experimental mild traumatic brain injury model. *J. Trauma* 60, 558-565.
- Ueda, T., Iwata, A., Komatsu, H., Aihara, N., Yamada, K., Ugawa, S., and Shimada, S. (2001). Diffuse brain injury induces local expression of Na⁺/myo-inositol cotransporter in the rat brain. *Brain Res. Mol. Brain Res.* 86, 63-69.
- Vagnozzi, R., Signoretti, S., Tavazzi, B., Cimatti, M., Amorini, A.M., Donzelli, S., Delfini, R., and Lazzarino, G. (2005). Hypothesis of the postconcussive vulnerable brain: experimental evidence of its metabolic occurrence. *Neurosurgery* 57, 164-171.
- Vagnozzi, R., Tavazzi, B., Signoretti, S., Amorini, A.M., Belli, A., Cimatti, M., Delfini, R., DiPietro, V., Finocchiaro, A., Lazzarino, G. (2007). Temporal window of metabolic brain vulnerability to concussions: mitochondrial-related impairment-part I. *Neurosurgery* 61, 379-388.
- Versace, J. (1971). A review of the severity index. 15th stapp car crash conference proceedings, 771-796.
- Viano, D.C., Casson, I.R., Pellman, E.J., Zhang, L., Yang, K.H., King, A.I. (2005). Concussion in professional football: Brain responses by finite element analysis – Part 9. *Neurosurgery* 57(5), 891-916.

- Viano, D.C., Casson, I.R., Pellman, E.J., Bir, C.A., Zhang, L., Sherman, D.C., and Boitano, M.A. (2005). Concussion in Professional Football: Comparison with Boxing Head Impacts - Part 10. *Neurosurg.* 57, 1154-1172.
- Viano, D.C., Hamberger, A., Bolouri, H., and Saljo, A. (2009). Concussion in professional football: animal model of brain injury. *J. Neurosurg.* 64, 1162-1173.
- Viano, D. C., Hamberger, A. H., Bolouri, H. and Saljo, A. (2012). Evaluation of three animal models for concussion and serious brain injury. *Annals of Biomedical Engineering*, 40 (1), 213–226.
- Vos, P. E., Lamers, K. J., Hendriks, J.C., 2004. Glial and neuronal proteins in serum predict outcome after severe traumatic brain injury. *Neurology*, 62, 1303–1310.
- Walilko, T.J., Viano, D.C., and Bir, C.A. (2005). Biomechanics of the head for Olympic boxer punches to the face. *Br. J. Sports Med.* 39, 710-719.
- Wang, J., Asensio, V. C., Campbell, I. L., 2002. Cytokines and chemokines as mediators of protection and injury in the central nervous system assessed in transgenic mice. *Current Topics in Microbiology and Immunology*, 265, 23-48.
- Wang, H.C., Duan, Z.X., Wu, F.F., Xie, L., Zhang, H., and Ma, Y.B. (2010). A new rat model for diffuse axonal injury using a combination of linear acceleration and angular acceleration. *J. Neurotrauma* 27, 707-719.
- Wang, H.C., Ma, Y.B. (2010). Experimental models of traumatic axonal injury. *J. Clinical Neuroscience* 17, 157-162.
- Wang, K.K., Ottens, A.K., Liu, M.C., Lewis, S.B., Meegan, C., Oli, M.W., Tortella, F.C., Hayes, R.L. (2005). Proteomic identification of biomarkers of traumatic brain injury. *Expert Rev. Proteomics*, 2, 603–614.

- Ward, C. C., Chan, M., and Nahum, A. M. (1980) Intracranial pressure-A brain injury criterion. Proceedings, 24th Stapp Car Crash Conf., SAE Paper No. 801304.
- Washington, P. M., Morffy, N., Parsadonian, M., Zapple, D. N. and Burns, M. P. (2014). Experimental traumatic brain injury induces rapid aggregation and oligomerization of amyloid-beta in an Alzheimer's disease mouse model. *J Neurotrauma* 31(1), 125-34.
- Williams, A. J. (2005). Characterization of a new rat model of penetrating ballistic brain injury. *J. Neurotrauma* 22:313–331.
- Williams, A. J., Ling, G. S. & Tortella, F. C. (2006). Severity level and injury track determine outcome following a penetrating ballistic-like brain injury in the rat. *Neurosci. Lett.* 408, 183–188.
- Williams, A. J., Wei, H. H., Dave, J. R. Tortella, F. C. (2007). Acute and delayed neuroinflammatory response following experimental penetrating ballistic brain injury in the rat. *J. Neuroinflamm.* 4: 17.
- Winter, C. D., Pringle, A. K., Clough, G. F., Church, M. K., 2004. Raised parenchymal interleukin-6 levels correlate with improved outcome after traumatic brain injury. *Brain*, 127(2), 315-320.
- Woertgen, C., 2002. Glial and neuronal serum markers after controlled cortical impact injury in the rat. *Actaneurochirurgica. Supplement* (0065-1419), 81, 205.
- Woertgen, C., Rotherl, R.D., Wiesmann, M., Missler, U. and Brawanski, A. (2002). Glial and neuronal serum markers after controlled cortical impact injury. *Acta neurochir* 81, 205-207.
- Xiong, Y., Mahmood, A., Chopp, M. (2013). Animal models of traumatic brain injury. *Nat Rev Neurosci.* 14(2):128-42.

- Yaghmai, A. and Povlishock, J.T. (1992). Traumatically induced reactive change as visualized through the use of monoclonal antibodies targeted to neurofilament subunits. *J. Neuropathol. Exp. Neurol.* 51, 158-176.
- Yen, K., Weis, J., Kreis, R. et al., (2006). Line-scan diffusion tensor imaging of the posttraumatic brain stem: changes with neuropathologic correlation. *Am J Neuroradiol* 27:70–3.
- Yu, F., Zhang, Y., Chuang, D. M. (2012). Lithium Reduces BACE1 Overexpression, Beta Amyloid Accumulation, and Spatial Learning Deficits in Mice with Traumatic Brain Injury. *J. Neurotrauma*, 10, 1-10.
- Zemlan, F. P., Rosenberg, W. S., Luebke, P. A., Campbell, T. A., Dean, G. E., Weiner, N. E., Cohen, J. A. (1999). Quantification of axonal damage in traumatic brain injury: affinity purification and characterization of cerebrospinal fluid tau proteins. *J. Neurochem.*, 72(2), 741-750.
- Zetterberg, H. et al., (2006). Neurochemical after match of amateur boxing. *Arch. Neurol.* 63, 1277–1280.
- Zetterberg, H., Smith, D.H., Blennow, K. (2013). Biomarkers of mild traumatic brain injury in cerebrospinal fluid and blood. *Nat Rev Neurol.* 9(4):201-10.
- Zhu, T., Yao, Z., Yuan, H. N., Lu, B. G., Yang, S. Y. (2004). Changes of interleukin-1 beta, tumor necrosis factor alpha and interleukin-6 in brain and plasma after brain injury in rats. *Chin. J. Traumatol.* 7, 32–35.
- Zhang, L, Yang, K.H., King, A.I. (2001a). Biomechanics of neurotrauma. *Neurol. Res.* 23, 144-156.

- Zhang, L., Yang, K.H., and King, A.I (2001b). Comparison of brain responses between frontal and lateral impacts by finite element modeling, *J. Neurotrauma* 18 (1), 21-30.
- Zhang, L., Yang, K.H., Dwarampudi, R., Omori, K., Li, T., Chang, K., Hardy, W.N., Khalil, T.B., King, A.I. (2001c). Recent advances in brain injury research: A new human head model development and validation. *Stapp Car Crash J* 45, 369-393.
- Zhang, L, Yang, K.H., King, A.I. (2004). A proposed injury threshold for mild traumatic brain injury. *J. Biomech. Eng.* 126, 226-236.
- Zhang, L., Gurao, M., Yang, K.H., King, A.I. (2005). Material characterization of low density polyurethane foam used for traumatic brain injury modeling. In: *Proceedings of ASME Bioengineering Conference No. 54807*, American Society of Mechanical Engineers.
- Zhang, L.Y., Li, Y., Cavanaugh, J.M. (2010a). A new measuring system to quantify head kinematics in a rodent model of traumatic axonal injury. In: *Proceedings of IBIA 8th World Congress on Brain Injury 2010*, International Brain Injury Association.
- Zhang, L.Y., Zhou, R., Yue, N. (2010b). Biomechanical response of impact acceleration-induced traumatic axonal injury: rat head model development and injury localization. *J. Neurotrauma* 26, A-18.
- Zurek, J., Bartlov ́ L., and Fedora, M. (2011). Hyperphosphorylated neurofilament NF-H as a predictor of mortality after brain injury in children. *Brain Inj.* 25, 221–226.

ABSTRACT**AN INVESTIGATION OF THE RELATIONSHIP BETWEEN
AXONAL INJURY, BIOMARKER EXPRESSION
AND MECHANICAL RESPONSE
IN A RODENT HEAD IMPACT ACCELERATION MODEL**

by

YAN LI**May 2015****Advisor:** Dr. John Cavanaugh**Co-Advisor:** Dr. Liying Zhang**Major:** Biomedical Engineering**Degree:** Doctor of Philosophy

In the United States 1.4 million people sustain traumatic brain injury (TBI) each year, resulting in 235,000 hospitalizations and 50,000 fatalities annually. Traumatic axonal injury (TAI) is a serious outcome of TBI that accounts for 40-50% of hospitalizations due to head injury and one third of the mortality due to TBI, and it is difficult to diagnose and evaluate. The purpose of this dissertation is to determine mechanical injury predictors for TAI and identify potential biomarkers to evaluate TAI.

In this dissertation, a modified Marmarou impact acceleration injury model was developed to allow the monitoring of velocity of the impactor and characterization of head kinematics during impact. The rat head sustained linear acceleration and angular velocity of $918 \pm 281g$ and 116 ± 45 rad/sec, respectively in 2.25m impacts, and $609 \pm 142g$ and 98 ± 31 rad/sec, respectively in 1.25m impacts. The variability in head kinematics resulting from the same drop height suggested that monitoring of mechanical parameters

are critical factors for illustration of the level of closed head injury with this model. Using this modified impact acceleration model, a series studies were performed to investigate correlation between impact mechanics and TAI, as well as correlation between biomarker levels and TAI.

In the first part of this dissertation, thirty-one anesthetized male Sprague-Dawley rats (392 ± 13 grams) were impacted using a modified impact acceleration injury device from 2.25 m and 1.25 m heights. Beta-amyloid precursor protein (β -APP) immunocytochemistry was used to assess and quantify axonal changes in CC and Py. Linear and angular responses of the rat head were monitored and measured in vivo with an attached accelerometer and angular rate sensor, and were correlated to TAI data. Logistic regression analysis suggested that the occurrence of severe TAI in CC was best predicted by average linear acceleration, followed by Power and time to surface righting. The combination of average linear acceleration and time to surface righting showed an improved predictive result. In Py, severe TAI was best predicted by time to surface righting, followed by peak and average angular velocity. When both CC and Py were combined, power was the best predictor, and the combined average linear acceleration and average angular velocity was also found to have good injury predictive ability.

In the second part of this dissertation, twenty-four anesthetized male Sprague-Dawley rats were subjected to a closed head injury from 1.25, 1.75 and 2.25 m drop heights ($n=8$ for each group). 24 h after impact, cerebrospinal fluid (CSF) and serum were collected. CSF and serum levels of neurofilament H (NF-H), glial fibrillary acidic protein (GFAP), interleukin (IL)-6, and amyloid beta ($A\beta$) 1-42 were assessed by enzyme-linked immunosorbent assay (ELISA). Compared to controls, significantly

higher CSF and serum pNF-H levels were observed in all impact groups, except between 1.25 m and control in serum. Furthermore, CSF and serum pNF-H levels were significantly different between the impact groups. For GFAP, both CSF and serum levels were significantly higher at 2.25 m compared to 1.75 m, 1.25 m and controls. There was no significant difference in CSF and serum GFAP levels between 1.75 m and 1.25 m, although both groups were significantly higher than control. TBI rats also showed significantly higher levels of IL-6 versus control in both CSF and serum, but no significant difference was observed between each impact group. Levels of A β were not significantly different between groups. Logistic regression analysis suggested that both pNF-H and GFAP levels in CSF and serum were good biomarkers for severe TBI. Pearson's correlation analysis showed pNF-H and GFAP levels in CSF and serum had positive correlation with power (rate of impact energy), followed by average linear acceleration and surface righting ($p < 0.01$), which were good predictors for traumatic axonal injury (TAI) according to histologic assessment in first part study, suggesting that they are directly related to the injury mechanism.

AUTOBIOGRAPHICAL STATEMENT

YAN LI

EDUCATION

WAYNE STATE UNIVERSITY, Detroit, Michigan PhD in Biomedical Engineering, 2014	01/2007-12/2014
WAYNE STATE UNIVERSITY, Detroit, Michigan MS in Biomedical Engineering, 2007	01/2005-12/2006
UNIVERSITY OF MICHIGAN, Ann Arbor, Michigan Department of Molecular, Cellular & Developmental Biology	08/2002-12/2004
FUDAN UNIVERSITY, Shanghai, China BS in Biology with Honors, 2001	09/1997-06/2001

AWARDS

Student Paper Award, 55th Stapp Car Crash Conference (2011).
University Graduate Research Fellowship (UGRF) Dissertation Award (2011-2012).

PUBLICATIONS AND PRESENTATIONS

- Li, Y.,** Zhang, L.Y., Kallakuri, S., Zhou, R., and Cavanaugh, J.M. (2011). Injury predictors for traumatic axonal injury in an impact acceleration model. *Stapp Car Crash Journal*, 55: 25-47.
- Li, Y.,** Zhang, L.Y., Kallakuri, S., Zhou, R., and Cavanaugh, J.M. (2011). Quantitative relationship between axonal injury and mechanical response in a rodent head impact acceleration model. *J. Neurotrauma*, 28(9): 1767-1782.
- Kallakuri, S., **Li, Y.,** Zhou, R., Bandaru, S., Zakaria, N., Zhang, L.Y., and Cavanaugh, J.M. (2012). Impaired axoplasmic transport is the dominant injury induced by an impact acceleration injury device. *Brain Res.* 1552: 29-38.
- Kallakuri, S., **Li, Y.,** Chen, C. Y., and Cavanaugh J.M. (2012). Innervation of cervical ventral facet joint capsule: Histological evidence. *World J Orthop.* 3(2): 10-14.
- Li, Y.,** Zhang, L.Y., Kallakuri, S., and Cavanaugh, J.M. (2012). Correlating biomechanical insult with biomarker levels: a new model for biomarker evaluation in TBI. Poster presentation in 30th National Neurotrauma Symposium, Phoenix, Arizona, July 22-25, 2012.
- Li, Y.,** Zhang, L.Y., Kallakuri, S., Zhou, R., and Cavanaugh, J.M. (2011). Predicting traumatic axonal injury in corpus callosum and pyramidal tract following impact acceleration induced traumatic brain injury in rodent. Poster presentation in 29th National Neurotrauma Symposium, Hollywood Beach, Florida, July 10-13, 2011.
- Li, Y.,** Zhang, L.Y., Kallakuri, S., and Cavanaugh, J.M. (2010). The relationship between mechanical response and diffuse axonal injury in a rodent impact acceleration model. Podium presentation in 6th World congress on Biomechanics, Singapore. August 1-6, 2010.
- Yaek, J., **Li, Y.,** Lemanski, P., and Cavanaugh, J.M. (2014). Biofidelity assessment of the 6 year old ATDs in side impact. Oral presentation in 10th Injury Biomechanics Symposium, Columbus, Ohio, May 18-20, 2014.
- Zhang, L.Y., **Li, Y.,** and Cavanaugh, J.M. (2010). A new measuring system to quantify head kinematics in a rodent model of traumatic axonal injury. Podium presentation in 8th World Congress on Brain Injury, Washington DC. March 10-14, 2010
- Zhang, L.Y., Zhou, R., **Li, Y.,** Kallakuri, S., and Cavanaugh, J.M. (2011). Local brain strain predicts traumatic axonal pathology in a rodent model of head impact acceleration induced brain injury. Poster presentation in 29th National Neurotrauma Symposium, Hollywood Beach, Florida, July 10-13, 2011.